

This document has been digitized by the Oil Sands Research and Information Network, University of Alberta with permission of Alberta Environment.

A WINTERTIME INVESTIGATION OF THE DEPOSITION OF
POLLUTANTS AROUND AN ISOLATED POWER PLANT IN
NORTHERN ALBERTA

by

L.A. BARRIE and J. KOVALICK
Atmospheric Environment Service

for

ALBERTA OIL SANDS ENVIRONMENTAL
RESEARCH PROGRAM

Project AS 3.2

May 1980

TABLE OF CONTENTS

	Page
DECLARATION	ii
LETTER OF TRANSMITTAL	iii
DESCRIPTIVE SUMMARY	iv
LIST OF TABLES	xi
LIST OF FIGURES	xii
ABSTRACT	xvii
ACKNOWLEDGEMENTS	xviii
1. INTRODUCTION	1
2. SAMPLING PROCEDURE AND ANALYSIS	7
2.1 Sample Collection	7
2.2 Sample Handling and Analysis	8
3. METEOROLOGICAL HISTORY OF THE SNOWPACK	13
4. RESULTS	16
4.1 Concentrations of Soluble Constituents in Snowmelt	16
4.2 Snowpack Loadings of Major Ions	16
4.3 Snowpack Loadings of Non-Alkaline Metals: Insoluble and Soluble	22
5. DISCUSSION	26
5.1 Deposition Patterns and Mass Balances	26
5.2 Major Ions and Snowpack Acidity	31
5.3 Principal Component and Cluster Analysis of the Data	31
6. CONCLUSIONS	41
7. REFERENCES CITED	43
8. APPENDIX	44
8.1 The Spatial Distribution of the Measured Concentration of Soluble Snowmelt Constituents	44
8.2 The Spatial Distribution of Measured Snowpack Loadings of Major Ions	75

TABLE OF CONTENTS (CONCLUDED)

	Page
8.3 The Spatial Distribution of Measured Snowpack Loadings of Insoluble Particulate Mass and of Al, V, Mn, Ti, Fe, and Ni	95
9. LIST OF AOSERP RESEARCH REPORTS	112

LIST OF TABLES

	Page
1. The Elemental Composition of Three Flyash Samples Collected from the Power Plant Emissions Using Electrostatic Precipitation	3
2. Analytical Techniques Used in the Quantitative Determination of Major Ion Concentrations	9
3. Analytical Techniques Used to Analyze Acidified Snowmelt Samples and Filters Containing Insoluble Particulate Matter for Various Metals	11
4. The Detection Limit of Parameters Measured and how it was Determined	12
5. Measured Snowmelt Major Ion Concentrations for Each Site on 26 to 28 January 1978	17
6. Measured Snowpack Depth and Density as well as Soluble Metal Concentrations for Each Site on 26 to 28 January 1978..	18
7. The Intrasite Variability of a Trace Constituent's Concentration in Snowmelt and of the Meltwater Volume	19
8. Snowpack Loadings of Major Ions for Each Site on 26 to 28 January 1978 Calculated from Measured Concentrations, Snowmelt Volume and Area Sampled	21
9. The Intrasite Variability of Major Ion Loadings of the Snowpack	23
10. Snowpack Loadings of Metals for Each Site on 26 to 28 January 1978 Calculated from Measured Concentrations, Snowmelt Volume, and Area Sampled	24
11. The Intrasite Variability of Snowpack Loadings of Insoluble Al, V, Mn and of Soluble Al, V, Fe, Ni	25
12. The Mass Budget of Various Substances Released to the Atmosphere by the GCOS Power Plant and Deposited within 25 km from 17 November 1977 to 26 January 1978	29
13. Results of an Ion Balance Done with Snowmelt Major Ion Concentration for Each Site	33

LIST OF FIGURES

	Page
1. Map of the AOSERP Study Area	2
2. Map of the Study Area	5
3. A Map of the Study Area Close to the Source of Atmospheric Emissions from GCOS	6
4. Air Temperature and Accumulated Fresh Snowfall for the Study Area from November 1977 to January 1978	14
5. Wind Roses Showing the Frequency Distribution of Wind Direction for the Lifetime of the Snowpack Sampled and for the Winters of 1973-74 and 1974-75	15
6. A Comparison of pH Measured in the Field Immediately after Melting Snow with that Measured a Month Later in the Laboratory	20
7. The Spatial Distribution of Snowpack Loading of Sulphate and Nitrate Ions in the Study Area on 26 January 1978	27
8. The Spatial Distribution of Snowpack Loading of Insoluble Aluminum, Vanadium and Manganese in the Study Area on 26 January 1978	28
9. The Spatial Distribution of Snowpack pH in the Study Area on 26 January 1978	32
10. The Contribution of Hydrogen and Calcium Ions to the Total Positive Ion Equivalents in Snowmelt Collected from the Oil Sands Area 26 January 1978 as a Function of pH	34
11. The Spatial Distribution of the Contribution of Hydrogen Ions to the Total Positive Ion Equivalents in Snowmelt Collected from the Oil Sands Area 26 January 1978	35
12. A Three-Dimensional Representation of a Principal Component Analysis of the Snowpack Loading Data Analysis	38

LIST OF FIGURES (CONTINUED)

	Page
13. The Geographical Location of Groups of Sites Identified as Having Similar Snow Chemistry by Cluster Analysis	39
14. Spatial Distribution of Laboratory pH Measurements	45
15. Plotted Laboratory pH Snowmelt at Sampling Sites	46
16. Spatial Distribution of $\text{SO}_4^=$ Measurements	47
17. Plotted Values of $\text{SO}_4^=$ from Snowmelt at Sampling Sites	48
18. Spatial Distribution of Cl^- Measurements	49
19. Plotted Values of Cl^- from Snowmelt at Sampling Sites	50
20. Spatial Distribution of NO_3^- Measurements	51
21. Plotted Values of NO_3^- from Snowmelt at Sampling Sites	52
22. Spatial Distribution of SiO_2 Measurements	53
23. Plotted Values of SiO_2 from Snowmelt at Sampling Sites ...	54
24. Spatial Distribution of NH_4^+ Measurements	55
25. Plotted Values of NH_4^+ from Snowmelt at Sampling Sites	56
26. Spatial Distribution of K^+ Measurements	57
27. Plotted Values of K^+ from Snowmelt at Sampling Sites	58
28. Spatial Distribution of Na^+ Measurements	59
29. Plotted Values of Na^+ from Snowmelt at Sampling Sites	60
30. Spatial Distribution of Mg^{++} Measurements	61
31. Plotted Values of Mg^{++} from Snowmelt at Sampling Sites	62
32. Spatial Distribution of Ca^{++} Measurements	63
33. Plotted Values of Ca^{++} from Snowmelt at Sampling Sites ...	64
34. Spatial Distribution of Alkalinity Measurements	65

LIST OF FIGURES (CONTINUED)

	Page
35. Plotted Values of Alkalinity at Sampling Sites	66
36. Spatial Distribution of Soluble Aluminum Concentration ...	67
37. Plotted Values of Soluble Aluminum Concentrations at Sampling Sites	68
38. Spatial Distribution of Soluble Vanadium Concentration	69
39. Plotted Values of Soluble Vanadium Concentration at Sampling Sites	70
40. Spatial Distribution of Soluble Iron Concentration	71
41. Plotted Values of Soluble Iron Concentrations at Sampling Sites	72
42. Spatial Distribution of Soluble Nickel Concentration	73
43. Plotted Values of Soluble Nickel Concentrations at Sampling Sites	74
44. Spatial Distribution of $\text{SO}_4^{=}$ Snowpack Loading	76
45. Plotted Values of $\text{SO}_4^{=}$ Snowpack Loading at Sampling Sites	77
46. Spatial Distribution of NO_3^- Snowpack Loading	78
47. Plotted Values of NO_3^- Snowpack Loading at Sampling Sites	79
48. Spatial Distribution of Cl^- Snowpack Loading	80
49. Plotted Values of Cl^- Snowpack Loading at Sampling Sites	81
50. Spatial Distribution of Silicate Snowpack Loading	82
51. Plotted Values of Silicate Snowpack Loading at Sampling Sites	83
52. Spatial Distribution of NH_4^+ Snowpack Loading	84

LIST OF FIGURES (CONTINUED)

	Page
53. Plotted Values of NH_4^+ Snowpack Loading at Sampling Sites	85
54. Plotted Values of K^+ Snowpack Loading at Sampling Sites	86
55. Spatial Distribution of Na^+ Snowpack Loading	87
56. Plotted Values of Na^+ Snowpack Loading at Sampling Sites	88
57. Spatial Distribution of Mg^{++} Snowpack Loading	89
58. Plotted Values of Mg^{++} Snowpack Loading at Sampling Sites	90
59. Spatial Distribution of Ca^{++} Snowpack Loading	91
60. Plotted Values of Ca^{++} Snowpack Loading at Sampling Sites	92
61. Spatial Distribution of Total Insoluble Metal Loading	94
62. Plotted Values of Total Insoluble Metal Loading at Sampling Sites	95
63. Spatial Distribution of Insoluble Aluminum Loading	96
64. Plotted Values of Insoluble Aluminum at Sampling Sites	97
65. Spatial Distribution of Insoluble Vanadium Loading	98
66. Plotted Values of Insoluble Vanadium at Sampling Sites	99
67. Spatial Distribution of Insoluble Manganese Loading ...	100
68. Plotted Values of Insoluble Manganese at Sampling Sites	101
69. Spatial Distribution of Insoluble Titanium Loading	102
70. Plotted Values of Insoluble Titanium at Sampling Sites	103

LIST OF FIGURES (CONCLUDED)

	Page
71. Spatial Distribution of Soluble Aluminum Loading	104
72. Plotted Values of Soluble Aluminum Loading at Sampling Sites	105
73. Spatial Distribution of Soluble Vanadium Loading	106
74. Plotted Values of Soluble Vanadium Loading at Sampling Sites	107
75. Spatial Distribution of Soluble Iron Loading	108
76. Plotted Values of Soluble Iron Loading at Sampling Sites	109
77. Spatial Distribution of Soluble Nickel Loading	110
78. Plotted Values of Soluble Nickel Loading at Sampling Sites	111

ABSTRACT

The results of a snowpack chemistry survey conducted in January 1978 in the Athabasca Oil Sands region of northeastern Alberta are presented. Snow collected at 60 sites within 100 km of the Great Canadian Oil Sands extraction plant was melted and analyzed for the major ions: $\text{SO}_4^{=}$, NO_3^- , Cl^- , NH_4^+ , K^+ , H^+ , Na^+ , Mg^{++} , Ca^{++} ; as well as for insoluble (Al, V, Mn, Ti) and soluble (Al, V, Fe, Ni) constituents. Snowpack loadings and deposition patterns are reported. Relationships are discussed between the snowpack chemistry, chemical composition of the power plant emissions and site location as revealed by multivariate analysis of the data. The fraction of total emissions that was transported out of the area was estimated from a mass balance. At least 98% of the acidic oxides of sulphur and nitrogen released by the power plant was transported beyond 25 km while less than 50% of the flyash constituents Al, V, and Mn escaped from the region.

ACKNOWLEDGEMENTS

This research project AS 3.2 was funded by the Alberta Oil Sands Environmental Research Program, a joint Alberta-Canada research program established to fund, direct, and co-ordinate environmental research in the Athabasca Oil Sands area of north-eastern Alberta.

The authors thank D. Wheipdale for editing the report and K. Puckett and E. Finegan for their helpful editing and for doing the multivariate analysis of the data.

1. INTRODUCTION

Pollutant emissions from oil extraction plants in the Athabasca Oil Sands region of Alberta have received the attention of atmospheric scientists since 1975. Because of low background pollutant levels in that part of the continent, the change in air quality effected by even a single mining operation is striking. In an effort to assess more objectively the impact of present and future emissions, several investigations were undertaken to determine the ambient concentrations and deposition rates of atmospheric trace constituents in the area. They were carried out within the framework of the Alberta Oil Sands Environmental Research Program (AOSERP) (see Figure 1 for map of AOSERP study area).

Deposition studies were centred on the Great Canadian Oil Sands (GCOS)¹ extraction plant. In operation since 1969, it was the major source of atmospheric pollutants until summer 1978 when Syncrude began production. The major source of emissions from GCOS is a coke-burning power plant whose 107 m stack releases approximately 200 t of sulphur dioxide and 27 t of particulates daily. For the studies mentioned in this report, no particulate control devices such as electrostatic precipitators were installed. A second, minor source of sulphur dioxide was a 107 m incinerator stack which releases between 5 and 20 t per day. The elemental composition of three flyash samples collected from the power house stack (Shelfentook 1978) are shown in Table 1.

Summertime deposition studies that were conducted include an event precipitation-chemistry network of about 15 sites operated every year since 1976 (Barrie et al. 1978) and the determination of particulate dry deposition patterns around the source in June 1977 using a network of artificial collectors (Barrie 1979a). Wintertime measurements have taken advantage of the snowpack's ability

¹GCOS amalgamated with Sun Oil Company in August 1979, after the writing of this report was completed, to become Suncor, Inc.

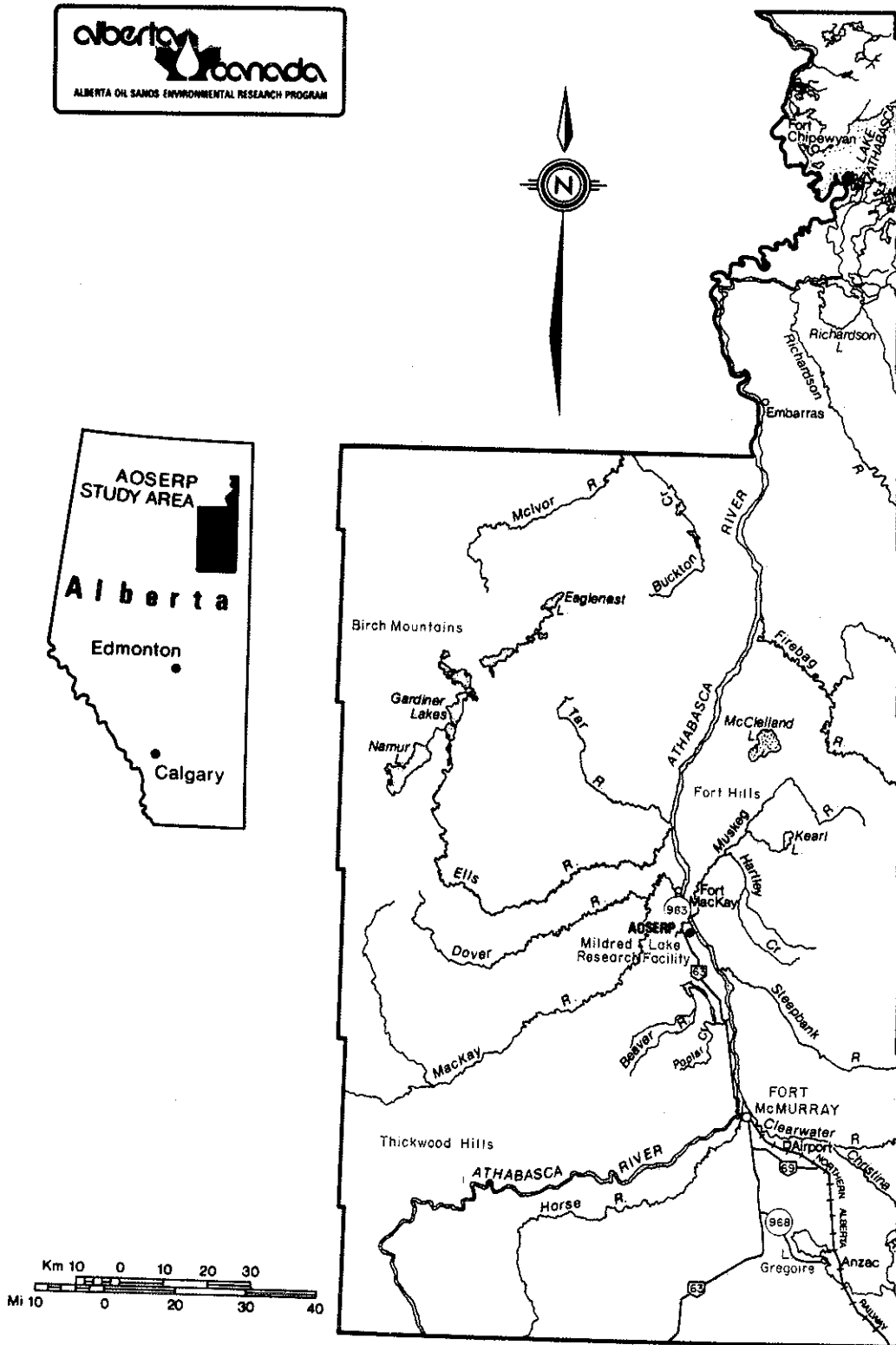


Figure 1. Map of the AOSERP study area.

Table 1. The elemental composition of three flyash samples collected from the power plant emissions using electrostatic precipitation (Shelfentook 1978).

	WEIGHT FRACTION OF SAMPLE (%)		
	1	2	3
Silica (SiO ₂)	34.6	36.3	31.9
C	11.3	10.3	20.7
Al	11.2	11.4	12.3
Fe	4.6	4.5	4.8
V	2.4	2.8	2.4
Ca	2.2	2.2	1.4
Ti	1.9	1.9	1.4
S	1.5	1.6	1.6
Ni	0.99	1.1	0.94
Mg	0.84	0.85	0.71
Mo	0.24	0.25	0.21
Mn	0.090	0.084	0.095

to collect total (wet plus dry) deposition in order to determine deposition patterns. In March 1976, a snow chemistry survey at 55 sites yielded the spatial distribution of sulphur and hydrogen in deposition (Barrie and Whelpdale 1978). Sulphur deposition rates determined in the study were used to calculate the deposition velocity of sulphur dioxide to snow (Barrie and Walmsley 1979). In January 1978, a second snow chemistry survey was conducted at 60 sites shown in Figures 2 and 3. Chemical analysis was extended to include not only sulphate and hydrogen ions but also major ions and trace metals. Furthermore, a larger area was covered than in March 1976. In this report, the data collection and analysis techniques, the results, and the conclusions of the 1978 snow chemistry survey are presented.

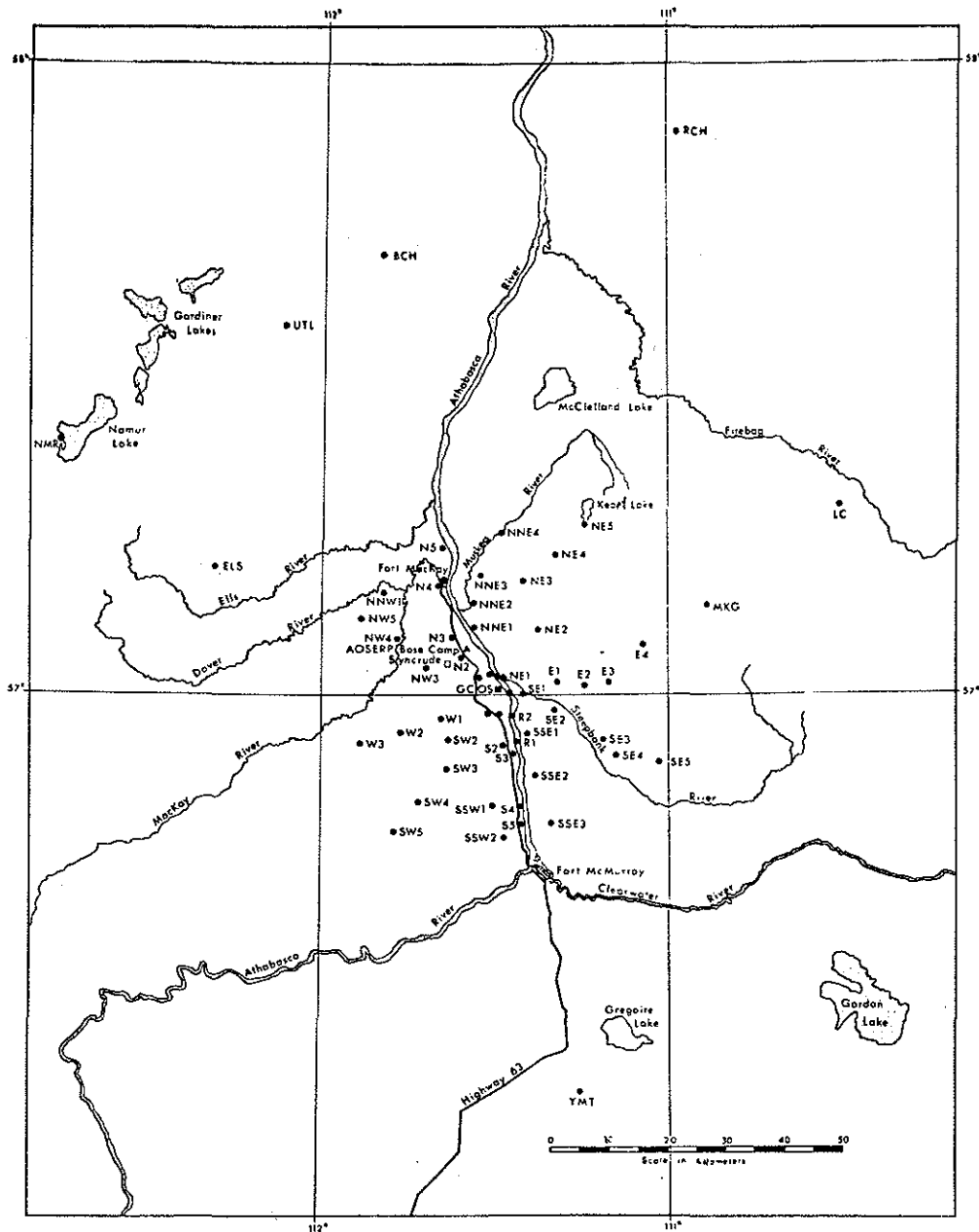


Figure 2. Map of the study area. Black dots mark the locations at which snow was sampled. The GCOS extraction plant is marked with a black square.

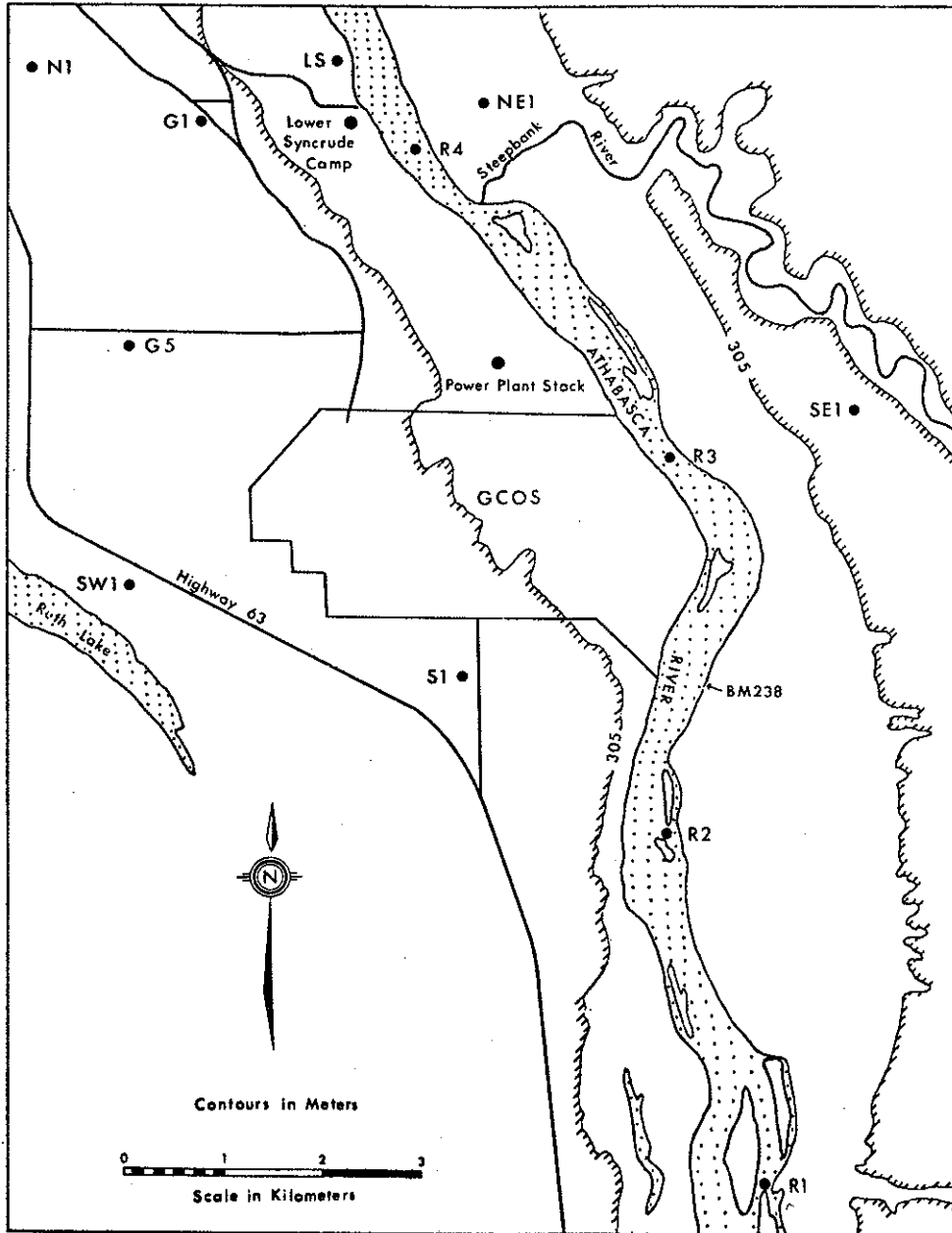


Figure 3. A map of the study area close to the source of atmospheric emissions from GCOS. Black dots mark the locations at which snow was sampled.

2. SAMPLING PROCEDURE AND ANALYSIS

2.1 SAMPLE COLLECTION

Snow was collected at 60 sites within 100 km of GCOS (Figures 2 and 3) between 25 and 28 January 1978; 55 sites were visited in the first three days. All sites were reached by helicopter except those on the river and along Highway 63 which were accessible by snowmobile and automobile, respectively.

At each site, two samples were collected in plastic bags; one for trace metal analysis, and one for major ion analysis. Each sample contained three snow cores taken with a device similar to that used in March 1976 (Barrie and Whelpdale 1978). The snow corer was a half-cylindrical tube, 1 m long, whose flat side was removable. An aluminum sampler was used for major ions (100 cm² cross-section) and an acrylic sampler for metals (87.2 cm² cross-section). The plastic one proved to be so rugged that in future it will be the only corer used.

To obtain a snow core, the procedure was as follows:

1. Measure snow depth;
2. Clean snow corer by inserting and removing it from the snowpack several times;
3. Insert sampler vertically to the bottom of the snowpack;
4. Clear snow from the plane face of the sampler;
5. Insert a shovel made of the same material as the corer and having the same cross-section under the lower end of the sampler;
6. Tilt the sampler until horizontal;
7. Remove the flat-faced side to expose the snow core;
8. Measure core length and crust positions; and
9. Use the scoop to remove snow containing ground debris and slide the core into a plastic bag.

At four of the 60 sites, five snow cores were bagged individually using both acrylic and aluminum samplers. The cores were analyzed separately to determine how much of the intersite (between site) variability of snowpack loading is due to intrasite (within site) variability.

2.2 SAMPLE HANDLING AND ANALYSIS

Snow samples were kept frozen in plastic bags until immediately before initial processing and analysis were performed in the field laboratory. Melting was done in a warm room at 30°C and generally took 6 to 12 h. Samples collected for major ion analysis with the aluminum sampler were treated as follows:

1. Measure meltwater volume with a 1 L polyethylene volumetric cylinder;
2. Measure pH with an Orion digital pH meter and combination electrode; and
3. Place a 250 mL aliquot in a polyethylene bottle that had been cleaned with a mild detergent and rinsed thoroughly with distilled water.

Samples were transported to the main laboratory, stored refrigerated at 4°C, and analyzed for major ions within a month. The chemical techniques used for the quantitative analysis of major ions are listed in Table 2.

Samples collected for metal analysis with the acrylic corer were handled in the following way:

1. Measure meltwater volume with a 1 L polyethylene volumetric cylinder;
2. Filter the meltwater through a 0.45 µm Sartorius cellulose acetate filter (SM-1106);
3. Fold the filter so that particulate matter is on the inner face; store in a polyethylene 'whirl-pack' bag;
4. Acidify approximately 280 mL of the filtered liquid to pH 1.5 with ultrapure concentrated nitric acid (BDH Aristar 45004); and

Table 2. Analytical techniques used in the quantitative determination of major ion concentrations.

	METHOD
pH	electrode
$\text{SO}_4^{=}$	methyl-thymol blue (colorimetric) and isotope dilution
Cl^-	mercury-thiocyanate (colorimetric)
NO_3^-	cadmium reduction (colorimetric)
Sol. Silica (SiO_2)	molybdate-oxalic acid (colorimetric)
NH_4^+	alk. phenol (colorimetric)
K^+	flame photometric
Na^+	flame photometric
Mg^{++}	atomic absorption
Ca^{++}	atomic absorption
alkalinity	titration to pH 4 then back to 5.6 under N_2

5. Fill 25 and 250 mL linear polyethylene bottles with the acidified samples (the bottles had been prepared by soaking 24 h in concentrated nitric acid and then rinsing thoroughly with distilled water).

The acidified meltwater and filters were transported to the main laboratory where they were analyzed for metals using the techniques listed in Table 3. Filters were first weighed with a microbalance to determine the mass of insoluble particles in the snow core.

Field blanks of distilled water in plastic snow sampling bags were processed and analyzed together with actual samples. Blank concentrations of some chemical constituents were above the detection limit of the analytical technique (Table 4). In such a case, the detection limit of the measurement was defined as being three times the standard deviation of several field blank concentrations. For instance, if a set of blanks had an average concentration and standard deviation of \bar{X} and σ , respectively, the detection limit was defined as 3σ . Any sample having a concentration \bar{X} greater than $\bar{X} + 3 \sigma$ was corrected by subtracting \bar{X} . If blanks were low, the detection limit was determined by the sensitivity of the technique used for quantitative analysis. Table 4 lists those parameters measured in the snow chemistry survey. It also gives detection limits for meltwater concentrations and snowpack loadings as well as how those detection limits were obtained.

Table 3. Analytical techniques used to analyze acidified snowmelt samples and filters containing insoluble particulate matter for various metals.

	METHOD
Soluble	
Al	solvent extraction, atomic absorption
Fe	solvent extraction, atomic absorption
Ni	solvent extraction, atomic absorption
V	neutron activation
Insoluble	
Al	neutron activation
V	neutron activation
Mn	neutron activation
Ti	neutron activation

Table 4. The detection limit of parameters measured and how it was determined (FB-from field blanks, At-from the detection limit of the analytical technique).

	Detection Concentration	Limit of Loading (10^{-3}gm^{-2})	Determined by
MAJOR IONS			
SO_4^- -S	0.01 ($\text{mg}\cdot\text{L}^{-1}$)	0.4	AT
Cl^-	0.06 ($\text{mg}\cdot\text{L}^{-1}$)	2.4	FB
NO_3^- -N	0.005($\text{mg}\cdot\text{L}^{-1}$)	0.2	AT
sol silica (SiO_2)	0.002($\text{mg}\cdot\text{L}^{-1}$)	0.08	FB
NH_4^+ -N	0.001($\text{mg}\cdot\text{L}^{-1}$)	0.04	AT
K^+	0.06 ($\text{mg}\cdot\text{L}^{-1}$)	2.4	FB
Na^+	0.02 ($\text{mg}\cdot\text{L}^{-1}$)	0.8	AT
Mg^{++}	0.01 ($\text{mg}\cdot\text{L}^{-1}$)	0.4	AT
Ca^{++}	0.05 ($\text{mg}\cdot\text{L}^{-1}$)	2.0	AT
TOTAL INSOLUBLE MASS		3800	FB
METALS			
Soluble			
Al	1.0 ($\mu\text{g}\cdot\text{L}^{-1}$)	0.05	AT
V	1.2 ($\mu\text{g}\cdot\text{L}^{-1}$)	0.06	FB
Fe	2.0 ($\mu\text{g}\cdot\text{L}^{-1}$)	0.10	FB
Ni	2.0 ($\mu\text{g}\cdot\text{L}^{-1}$)	0.10	FB
Insoluble			
Al		3.4 ^a	FB
V		0.1 ^a	FB
Mn		0.1 ^a	FB
Ti		7.0 ^a	FB

^aFor sites ELS, RHS, NMR, SMT, LC, UT these values are divided by 3.

3. METEOROLOGICAL HISTORY OF THE SNOWPACK

A snowlayer will retain all of the non-volatile substances deposited onto it, provided substantial melting does not occur. Once liquid water trickles through the snowpack, pollutants are leached out rapidly. The first 10% of meltwater can remove 30 to 40% of the pollutant load (Johannessen and Henriksen 1978). During late November, December and January 1977-78, meteorological conditions in northeastern Alberta were ideal for a deposition study. Air temperatures never exceeded -5°C from 18 November, when snow began to accumulate permanently, until the end of January, when the snow chemistry survey was conducted (Figure 4). During this 70 d period, a total of 58 cm of fresh snow fell. The depth of the snowpack at the time of sampling was 30 to 40 cm.

The frequency distribution of surface wind direction at Mildred Lake (near site N2 in Figure 2), 10 km north-northwest of the source during the 70 d deposition period, is shown in Figure 5. For purposes of comparison, the frequency distributions for the winters of 1974 and 1975 are included since they are similar to the long-term average distribution.

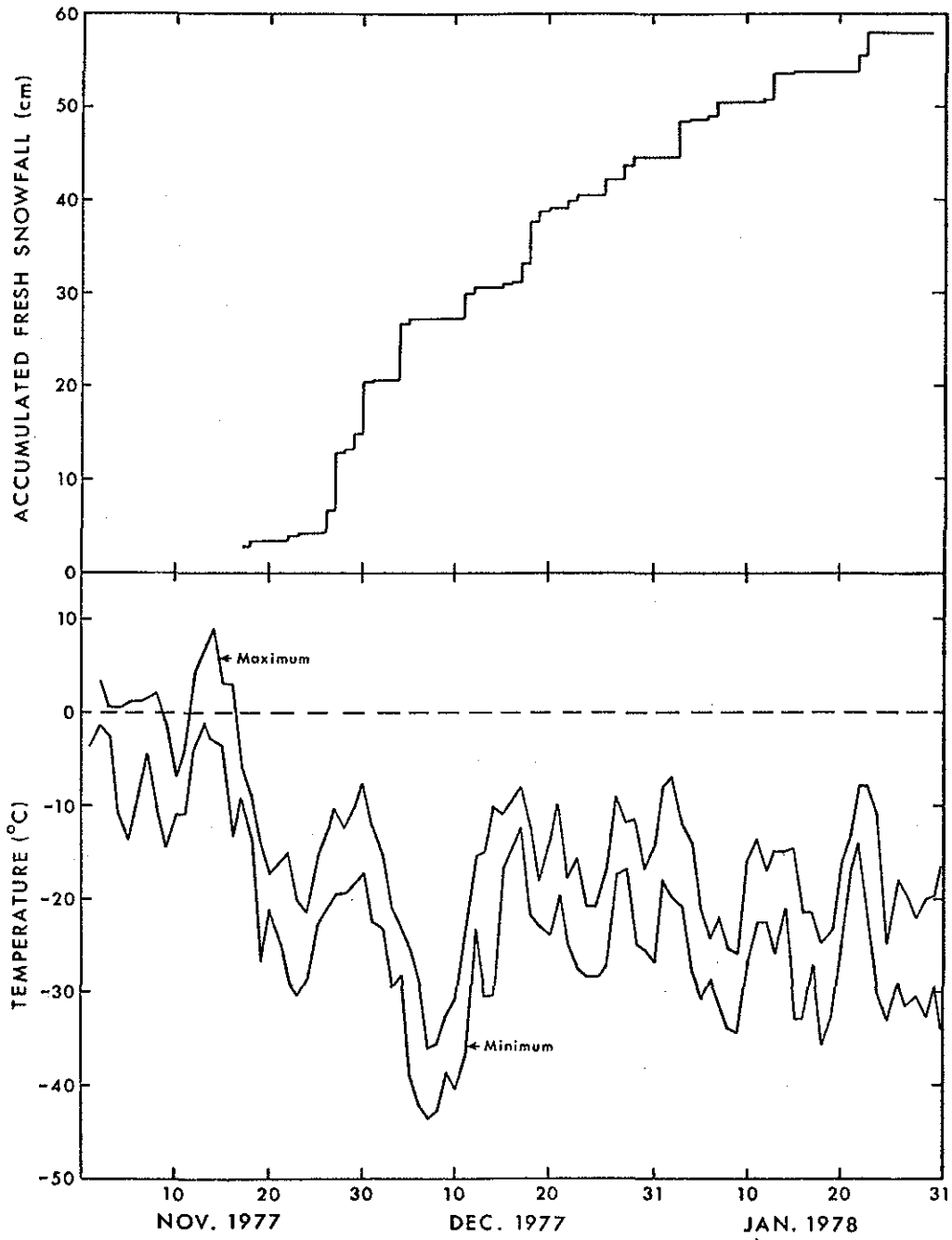


Figure 4. Air temperature and accumulated fresh snowfall for the study area from November 1977 to January 1978.

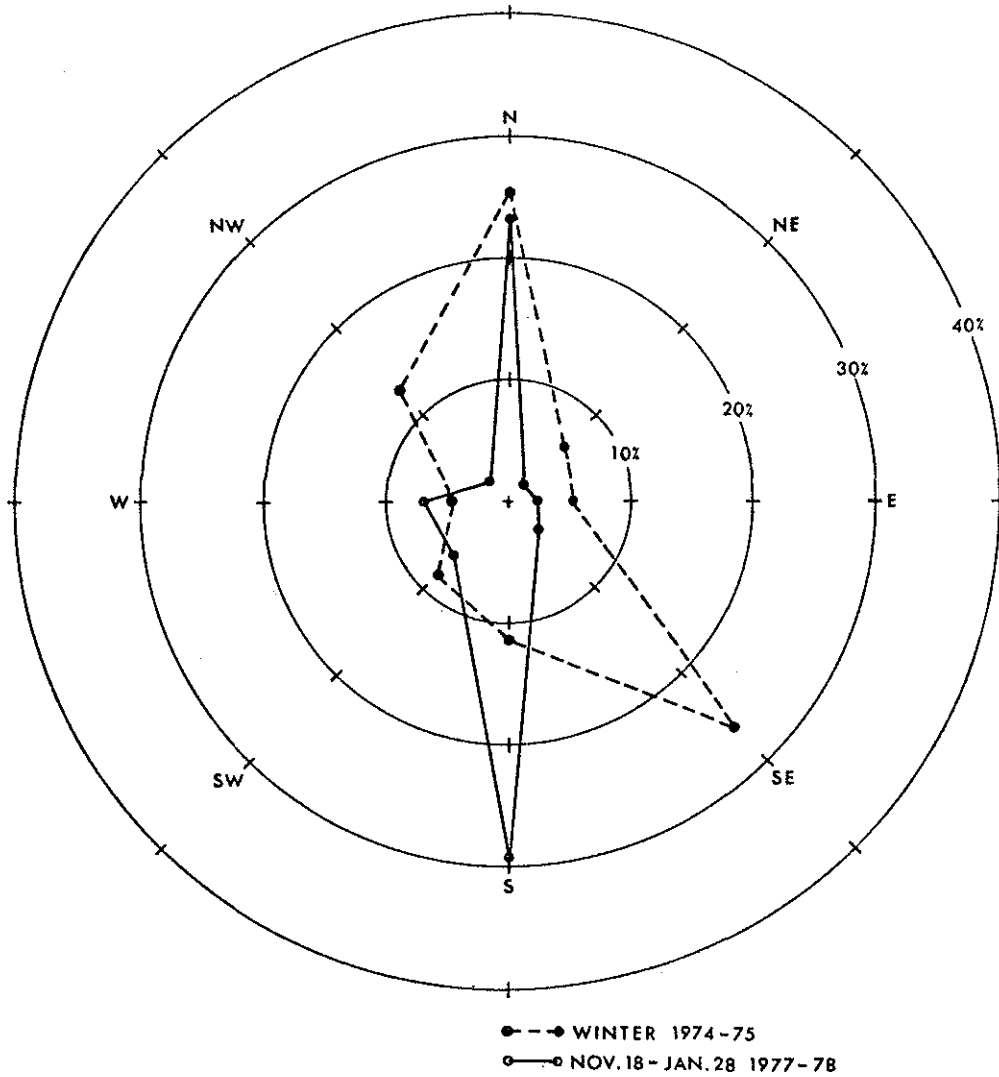


Figure 5. Wind roses showing the frequency distribution of wind direction for the lifetime of the snowpack sampled (solid line) and for the winters of 1973-74 and 1974-75 (dashed lines). Winds were calm (less than 1.5 m/s) for 25% of the time.

4. RESULTS

4.1 CONCENTRATIONS OF SOLUBLE CONSTITUENTS IN SNOWMELT

The measured concentrations of major ions and dissolved Al, Fe, V and Ni in snowmelt are listed for each site in Tables 5 and 6, respectively. The average volume of a melted snow core, snow depth, and density also are given. The composition of five individual samples (labelled A to E) was obtained for sites M, SW5, R4 and N1. From these data, the intrasite variation of a concentration measurement expressed as per cent standard deviation of the mean was estimated (Table 7). The average standard deviation of a concentration measurement was less than 20% for $\text{SO}_4^{=}$, Cl^- , NO_3^- and the soluble metals Al, V, Fe, Ni, and less than 36% for the other constituents.

A comparison of pH measured in the field and later in the laboratory (Figure 6) shows that, in meltwater with initial pH above 5, the latter is higher than the former and that the difference increases with increasing pH. Between pH 6 and 7, laboratory pH is about 0.5 units higher than field pH. This difference possibly is due to the presence of calcium and magnesium oxides that slowly dissolve during the period between sampling and analysis. It would require that only $0.014 \text{ mg}\cdot\text{L}^{-1}$ of the 0.5 to $1 \text{ mg}\cdot\text{L}^{-1}$ of Ca^{++} found in snowmelt of pH 6 to 7 dissolve to explain a pH change from 6 to 6.5. Thus, even though pH is altered significantly, the concentration of soluble calcium is not. Below pH 5, where hydrogen ions become important in the ion balance of a solution, no significant difference between field and laboratory pH was observed. The spatial distribution of pH and major ion concentrations in the snowpack is shown in Appendix 8.1. The map used encompasses about 55 of the 60 sites sampled and extends to about 40 km from the source.

4.2 SNOWPACK LOADINGS OF MAJOR IONS

Snowpack loading, defined as the amount of a substance in the snowpack per square metre, was calculated for major ions (Table 8) from their snowmelt concentrations, snowmelt volume, and

Table 5. Measured snowmelt major ion concentrations for each site on
26 to 28 January 1978 (see Figures 2 and 3 for site locations).

SITE NAME	SNOWMELT MAJOR ION VOLUME	pH FIELD	pH LAB	MAJOR ION CONCENTRATIONS										ALKALINITY ($10^{-6} \text{ eq l}^{-1}$)
				SO_4^{2-} S	Cl^-	NO_3^- N	SULFATE SILICATE (SiO_2)	NH_4^+ -N	K^+	Na^+	Mg^{++}	Ca^{++}		
	(ml)						(10^{-3} g l^{-1})							
NNE1	467	4.7	4.9	0.36	D.L.	0.173	0.025	0.060	D.L.	0.03	0.04	0.30	-3.2	
NNE2	427	4.7	4.7	0.40	D.L.	0.176	0.032	0.059	0.09	0.08	D.L.	0.22	-10.6	
NNE3	547	4.8	5.0	0.21	D.L.	0.118	0.014	0.035	D.L.	0.03	0.02	0.12	-5.2	
NNE4	476	5.0	5.0	0.20	D.L.	0.120	0.023	0.017	D.L.	0.03	0.02	0.14	-4.4	
NE1	490	5.7	6.0	0.43	D.L.	0.154	0.040	0.135	0.12	0.13	0.09	0.65	13.2	
NE2	385	5.4	5.0	0.19	D.L.	0.102	0.013	0.033	D.L.	0.04	D.L.	0.08	-0.6	
NE3	625	4.8	4.9	0.20	D.L.	0.113	0.007	0.015	D.L.	0.03	D.L.	0.08	-4.8	
NE4	499	5.0	5.0	0.20	D.L.	0.095	D.L.	0.012	D.L.	0.03	D.L.	0.06	1.4	
NE5	700	6.1	6.6	0.30	D.L.	0.109	0.044	0.020	D.L.	0.05	0.27	0.75	62.4	
E1	618	5.0	5.1	0.46	D.L.	0.157	0.011	0.020	0.42	0.38	0.02	0.14	0.1	
E2	493	4.9	5.0	0.17	D.L.	0.119	0.006	0.021	0.09	0.10	D.L.	0.10	2.3	
E3	460	5.0	5.0	0.16	D.L.	0.104	0.004	0.013	D.L.	D.L.	D.L.	0.06	3.8	
E4	498	5.1	5.0	0.20	D.L.	0.097	D.L.	0.021	D.L.	D.L.	D.L.	D.L.	-4.2	
EA	266	5.0	5.2	0.12	0.08	0.088	D.L.	0.019	D.L.	D.L.	0.02	D.L.	5.0	
EB	220	5.0	5.0	M	0.07	0.101	D.L.	0.014	D.L.	D.L.	D.L.	D.L.	2.8	
EC	271	5.2	5.0	0.14	D.L.	0.142	D.L.	0.010	D.L.	D.L.	D.L.	D.L.	3.0	
ED	265	5.1	5.0	0.13	D.L.	0.121	D.L.	0.017	D.L.	D.L.	D.L.	D.L.	-0.8	
EE	190	5.0	5.0	0.16	0.08	0.139	D.L.	0.013	D.L.	D.L.	D.L.	D.L.	-1.2	
SE1	561	5.2	5.4	0.36	D.L.	0.122	0.015	0.068	D.L.	0.06	0.05	0.34	7.6	
SE2	674	5.2	5.1	0.20	D.L.	0.090	0.007	0.025	D.L.	0.03	D.L.	0.12	5.0	
SE3	532	5.9	6.2	0.14	D.L.	0.082	0.007	0.021	D.L.	0.05	0.15	0.30	23.0	
SE4	547	5.2	5.4	0.23	D.L.	0.088	D.L.	0.137	D.L.	D.L.	D.L.	0.08	8.4	
SE5	542	6.2	6.6	0.26	D.L.	0.048	0.020	0.022	D.L.	0.05	0.11	0.70	45.0	
SSE1	591	5.0	5.0	0.26	D.L.	0.108	0.008	0.045	D.L.	D.L.	D.L.	0.10	-1.8	
SSE2	527	6.5	6.8	0.33	D.L.	0.092	0.164	0.017	D.L.	0.13	0.21	1.30	66.8	
SSE3	403	5.5	5.9	M	D.L.	0.052	0.007	0.017	D.L.	D.L.	0.05	0.18	19.8	
S1	533	5.6	6.1	0.95	0.11	0.204	0.078	0.145	0.07	0.12	0.19	1.10	4.0	
S2	645	5.4	5.4	0.50	0.22	0.176	0.035	0.052	D.L.	0.20	0.10	0.50	14.8	
S3	734	4.8	4.9	0.43	0.33	0.025	0.174	0.043	0.11	0.36	0.03	0.20	-4.6	
S4	677	6.3	6.6	0.36	0.14	0.045	0.138	0.024	D.L.	0.12	0.18	0.80	47.6	
S5	547	6.5	7.1	0.44	0.37	0.154	0.085	0.005	0.09	1.08	0.67	1.50	136.6	
SSW1	593	5.4	5.4	0.27	D.L.	0.132	0.018	0.095	D.L.	0.09	0.05	0.20	8.2	
SSW2	530	5.0	5.1	0.30	D.L.	0.123	0.014	0.046	D.L.	0.09	0.02	0.12	-3.0	
SW1	553	6.0	6.6	0.43	0.22	0.210	0.031	0.057	0.03	0.16	0.35	0.80	43.2	
SW2	517	6.9	M	0.33	0.11	0.130	0.147	0.011	M	M	M	M	M	
SW3	557	6.1	6.4	0.14	0.07	0.114	0.039	0.012	D.L.	0.34	0.09	0.35	29.6	
SW4	714	5.1	5.2	0.23	D.L.	0.116	D.L.	0.075	D.L.	D.L.	0.02	0.08	4.2	
SW5A	530	5.1	5.4	0.16	D.L.	0.120	D.L.	0.023	D.L.	0.05	0.06	0.15	10.0	
SW5B	520	5.2	5.3	M	D.L.	0.188	D.L.	0.026	D.L.	0.04	0.05	0.15	9.2	
SW5C	510	5.0	5.1	0.16	D.L.	0.124	D.L.	0.027	D.L.	0.03	0.02	0.08	4.6	
SW5D	500	5.0	5.1	0.16	D.L.	0.124	D.L.	0.025	D.L.	0.03	0.03	0.10	1.2	
SW5E	520	5.7	5.3	0.14	D.L.	0.112	D.L.	0.024	D.L.	0.05	0.09	0.30	14.2	
W1	629	4.9	5.0	0.17	0.09	0.115	D.L.	0.023	D.L.	0.05	D.L.	0.06	-0.2	
W2	307	6.9	7.3	0.19	0.09	0.117	0.399	0.034	0.30	2.91	0.97	1.10	220.0	
W3	527	5.0	5.0	M	D.L.	0.105	0.004	0.011	D.L.	0.03	0.02	D.L.	-6.0	
NW3	499	5.1	4.9	0.16	D.L.	0.120	0.003	0.018	D.L.	0.05	D.L.	0.08	-6.6	
NW4	527	5.1	5.1	0.14	D.L.	0.119	0.006	0.013	D.L.	0.04	D.L.	0.10	2.0	
NW5	467	9.1	7.7	0.43	D.L.	0.112	0.148	0.062	0.43	6.97	3.40	1.50	564.0	
NW1	523	5.0	5.3	0.14	D.L.	0.105	M	0.015	D.L.	0.05	0.04	0.10	7.0	
N1A	465	5.6	6.0	0.36	0.07	0.160	0.022	0.042	D.L.	0.10	0.13	0.55	19.8	
N1B	483	5.3	5.8	0.34	0.07	0.163	0.025	0.063	D.L.	0.12	0.12	0.40	11.2	
N1C	482	5.6	5.7	0.36	0.07	0.160	0.031	0.042	D.L.	0.10	0.10	0.44	13.4	
N1D	480	5.6	6.2	0.32	0.07	0.156	0.023	0.043	0.13	0.20	0.15	0.70	20.0	
N1E	500	5.6	6.1	0.35	0.06	0.151	0.024	0.033	D.L.	0.10	0.15	0.65	5.0	
R2	494	6.2	6.9	0.33	0.08	0.174	0.491	0.015	D.L.	0.06	0.33	2.10	116.8	
R3	535	6.4	6.7	0.26	D.L.	0.145	0.035	0.011	D.L.	0.04	0.25	1.00	53.6	
R4	558	5.1	5.1	0.20	D.L.	0.136	0.009	0.011	D.L.	0.08	0.03	0.20	1.8	
R5	571	5.0	5.1	0.20	D.L.	0.128	0.006	0.021	0.07	0.09	D.L.	0.16	-0.8	
R6	340	5.1	5.1	0.20	D.L.	0.050	D.L.	0.020	D.L.	0.05	D.L.	0.06	-2.4	
G1	598	5.6	6.1	0.41	0.10	0.192	0.042	0.060	D.L.	0.07	0.17	0.75	26.0	
G5	507	6.1	6.9	0.77	0.11	0.195	0.061	0.653	D.L.	0.14	0.45	2.10	145.4	
R1	350	6.0	6.7	0.52	0.13	0.219	0.153	0.059	0.19	1.05	0.35	1.20	60.4	
R2	453	6.0	6.2	0.43	0.15	0.237	0.036	0.133	D.L.	0.10	0.12	0.70	27.0	
R3	440	5.6	5.6	0.53	0.17	0.157	0.035	0.114	D.L.	0.04	0.09	0.50	8.2	
R4A	440	6.1	6.7	0.57	0.12	0.205	0.113	0.290	0.12	0.30	0.29	1.40	61.8	
R4B	480	5.9	6.4	0.49	D.L.	0.142	0.071	0.150	D.L.	0.10	0.18	1.00	37.0	
R4C	500	5.7	6.5	0.53	0.07	0.161	0.077	0.149	0.07	0.12	0.17	0.90	36.6	
R4D	520	5.7	6.5	0.56	0.07	0.163	0.069	0.155	0.09	0.14	0.19	0.95	40.2	
R4E	540	5.9	6.5	0.60	0.08	0.168	0.072	0.134	0.07	0.16	0.20	0.95	39.6	
ELS	M	4.8	M	0.14	M	M	M	0.022	D.L.	D.L.	D.L.	D.L.	-5.4	
RCH	M	4.8	4.9	M	D.L.	0.130	D.L.	0.012	D.L.	D.L.	D.L.	D.L.	-5.4	
NMR	M	4.9	4.8	0.14	D.L.	0.078	D.L.	0.013	D.L.	D.L.	D.L.	D.L.	-2.2	
SMT	M	4.7	4.8	0.26	D.L.	0.088	D.L.	0.051	D.L.	0.03	D.L.	D.L.	-8.0	
LC	M	4.8	4.9	M	D.L.	0.095	D.L.	0.023	D.L.	0.04	D.L.	D.L.	-4.8	
UT	M	4.9	4.9	M	D.L.	0.095	D.L.	0.024	D.L.	0.04	D.L.	D.L.	-2.4	
LS	548	5.8	6.3	0.76	0.90	0.355	0.079	0.259	0.21	0.09	0.18	1.37	63.4	

Table 6. Measured snowpack depth and density as well as soluble metal concentrations for each site on 26 to 28 January 1978 (see Figures 2 and 3 for site locations).

SITE NAME	SNOWPACK		SNOWMELT METAL VOLUME	SOLUBLE METAL CONCENTRATIONS			
	DEPTH (cm)	DENSITY (g cm^{-3})		ALUMINUM Al	VANADIUM V	IRON Fe	NICKEL Ni
			(ml)	$(10^{-6} \text{g l}^{-1})$			
NNE1	33	0.14	407	10.0	30.4	23.0	4.0
NNE2	30	0.16	444	14.0	23.4	10.0	D.L.
NNE3	31	0.14	461	9.0	12.4	6.0	D.L.
NNE4	30	0.16	475	6.0	9.3	5.0	D.L.
NE1	31	0.15	427	4.0	52.4	9.0	7.0
NE2	25	0.14	331	12.0	D.L.	9.0	D.L.
NE3	30	0.19	491	7.0	11.4	3.0	D.L.
NE4	32	0.15	437	6.0	6.0	6.0	D.L.
NE5	30	0.22	533	4.0	5.3	2.5	D.L.
E1	33	0.16	543	5.0	15.4	10.0	D.L.
E2	31	0.16	447	3.0	12.4	4.5	D.L.
E3	30	0.16	407	5.0	3.5	4.0	D.L.
E4	33	0.15	609	8.0	4.4	4.5	D.L.
EA	39	0.18	567	2.0	3.5	2.0	D.L.
EB	41	0.19	777	D.L.	2.2	D.L.	D.L.
EC	40	0.19	619	5.5	2.5	4.0	D.L.
ED	38	0.19	540	3.0	3.4	D.L.	D.L.
EE	35	0.17	543	2.0	3.8	2.5	D.L.
SE1	35	0.16	473	13.0	50.6	D.L.	7.0
SE2	40	0.17	593	8.0	20.6	9.0	D.L.
SE3	32	0.16	422	3.0	6.7	3.5	D.L.
SE4	30	0.17	400	3.0	6.2	3.0	D.L.
SE5	31	0.14	393	2.0	2.5	D.L.	D.L.
SSE1	38	0.16	562	9.0	13.4	11.0	D.L.
SSE2	33	0.16	439	3.0	12.4	4.0	D.L.
SSE3	40	0.16	567	5.0	4.6	D.L.	D.L.
S1	36	0.16	577	3.0	91.4	6.0	10.0
S2	37	0.18	593	5.0	42.4	13.5	4.0
S3	38	0.17	585	5.0	24.4	17.5	D.L.
S4	39	0.16	560	5.0	9.4	11.5	D.L.
S5	38	0.13	350	4.0	10.4	D.L.	D.L.
SSW1	35	0.17	497	16.0	38.4	17.0	3.0
SSW2	30	0.17	440	11.0	22.4	17.0	D.L.
SW1	33	0.16	467	D.L.	35.4	D.L.	D.L.
SW2	33	0.14	450	D.L.	7.9	D.L.	D.L.
SW3	34	0.16	470	D.L.	7.6	8.0	D.L.
SW4	41	0.17	592	D.L.	5.1	3.5	D.L.
SW5A	28	0.19	450	D.L.	3.3	D.L.	D.L.
SW5B	28	0.18	460	D.L.	1.8	D.L.	D.L.
SW5C	28	0.18	430	2.0	2.4	D.L.	D.L.
SW5D	28	0.18	470	2.0	1.5	D.L.	D.L.
SW5E	28	0.19	480	2.0	2.9	D.L.	D.L.
W1	39	0.18	627	5.0	3.2	4.0	D.L.
W2	22	0.14	257	D.L.	7.2	4.0	D.L.
W3	33	0.16	450	3.0	M	3.0	D.L.
NW3	31	0.16	417	7.0	7.7	7.0	D.L.
NW4	32	0.16	473	4.0	4.5	2.5	D.L.
NW5	29	0.16	390	2.0	3.3	3.0	D.L.
NNW1	32	0.16	M	M	M	M	M
N1A	30	0.15	430	7.0	35.4	9.0	3.0
N1B	30	0.17	483	M	38.4	M	M
N1C	30	0.16	482	5.0	34.4	10.0	4.0
N1D	30	0.16	480	6.0	32.4	12.0	4.5
N1E	30	0.16	500	6.0	35.4	11.0	4.0
N2	30	0.16	420	3.0	25.4	2.5	3.5
N3	35	0.16	584	4.0	13.4	D.L.	D.L.
N4	32	0.16	558	D.L.	10.4	10.0	D.L.
N5	34	0.16	571	8.0	12.4	11.0	D.L.
BM	19	0.18	283	3.0	D.L.	D.L.	D.L.
G1	35	0.15	387	3.0	120.0	3.5	6.6
G5	31	0.16	420	4.0	35.4	D.L.	D.L.
R1	22	0.16	344	7.0	39.4	8.0	3.5
R2	27	0.16	389	4.0	35.4	5.5	2.5
R3	27	0.16	377	2.0	83.4	13.0	10.0
R4A	27	0.18	480	3.0	55.4	D.L.	6.0
R4B	27	0.19	470	3.0	55.4	D.L.	7.0
R4C	27	0.19	460	4.0	54.4	D.L.	7.0
R4D	28	0.19	470	4.0	60.4	3.0	6.5
R4E	28	0.20	480	5.0	61.4	2.5	6.0
ELS	34	0.21	M	2.0	1.9	D.L.	D.L.
RCH	38	0.18	M	2.0	D.L.	D.L.	D.L.
NMR	32	0.14	M	2.0	D.L.	D.L.	D.L.
SMT	47	0.19	M	5.0	2.4	2.5	D.L.
LC	33	0.20	M	3.0	1.8	D.L.	D.L.
UT	39	0.18	M	2.0	D.L.	D.L.	D.L.
LS	33	0.16	420	5.0	58.1	2.8	5.0

Table 7. The intrasite variability of a trace constituent's concentration in snowmelt and the meltwater volume (represented by the average percent standard deviation about the mean of five samples taken at each of the following sites: M, SW5, R4, N1).

PARAMETER	INTRASITE VARIABILITY (%)
MELTWATER VOLUME OF:	
Major ions	7
Metals	7
CONCENTRATION OF:	
H ⁺	30
SO ₄ ⁼	8
Cl ⁻	7
NO ₃ ⁻	15
Sol. Silica	23
NH ₄ ⁺	24
Na ⁺	36
Mg ⁺⁺	31
Ca ⁺⁺	33
Soluble-	
Al	18
V	16
Fe	12
Ni	12

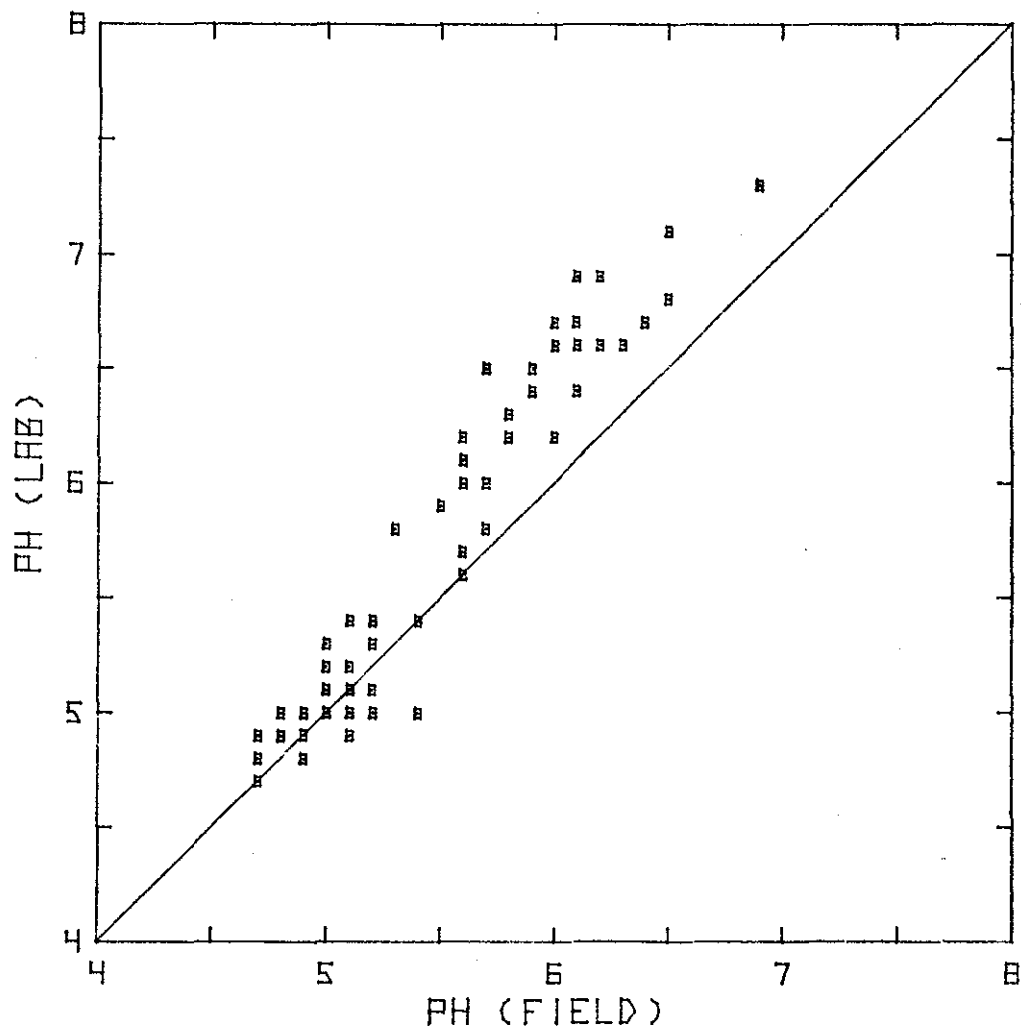


Figure 6. A comparison of pH measured in the field immediately after melting snow with that measured a month later in the laboratory.

Table 8. Snowpack loadings of major ions for each site on 26 to 28 January 1978 calculated from measured concentrations, snowmelt volume, and area sampled (see Figures 2 and 3 for site locations).

SITE NAME	MAJOR ION LOADINGS (mg/m ²)									
	H ⁺	SO ₄ ^{=-S}	Cl ⁻	NO ₃ ^{-N}	SOLUBLE SILICATE (SiO ₂)	NH ₄ ^{+-N}	K ⁺	Na ⁺	Mg ⁺⁺	Ca ⁺⁺
NNE1	0.588	16.8	D.L.	8.08	1.17	2.80	D.L.	1.40	1.07	14.0
NNE2	0.852	17.1	D.L.	7.26	1.37	2.52	3.84	3.42	D.L.	9.4
NNE3	0.547	11.5	D.L.	6.45	0.77	1.91	D.L.	1.64	1.69	6.6
NNE4	0.476	9.5	D.L.	5.71	1.09	0.81	D.L.	1.43	0.95	6.7
NE1	0.048	20.6	D.L.	7.39	1.92	6.62	5.76	6.24	4.32	31.2
NE2	0.385	7.3	D.L.	3.93	0.50	1.27	D.L.	1.54	D.L.	3.1
NE3	0.787	12.5	D.L.	7.06	0.44	0.94	D.L.	1.30	D.L.	5.0
NE4	0.499	10.0	D.L.	4.74	D.L.	0.60	D.L.	1.50	D.L.	3.0
NE5	0.018	21.0	D.L.	7.63	3.08	1.40	D.L.	35.70	18.90	52.5
E1	0.491	28.4	D.L.	9.70	0.68	1.24	25.96	23.48	1.24	8.7
E2	0.493	8.4	D.L.	5.87	0.30	1.04	4.44	4.93	D.L.	4.9
E3	0.460	7.4	D.L.	4.78	0.18	0.33	D.L.	D.L.	D.L.	2.8
E4	0.498	10.0	D.L.	4.83	D.L.	1.05	D.L.	D.L.	D.L.	D.L.
MA	0.168	3.2	D.L.	2.34	D.L.	0.27	D.L.	D.L.	0.53	D.L.
MB	0.220	M	1.54	2.22	D.L.	0.31	D.L.	D.L.	D.L.	D.L.
MC	0.271	3.8	D.L.	3.85	D.L.	0.27	D.L.	D.L.	D.L.	D.L.
MD	0.265	3.4	D.L.	3.21	D.L.	0.45	D.L.	D.L.	D.L.	D.L.
ME	0.190	3.0	1.52	2.64	D.L.	0.29	D.L.	D.L.	D.L.	D.L.
SE1	0.223	20.2	D.L.	6.84	0.84	3.81	D.L.	3.37	2.61	19.1
SE2	0.535	13.5	D.L.	6.07	0.47	1.95	D.L.	2.02	D.L.	8.1
SE3	0.034	7.4	D.L.	4.36	0.37	1.12	D.L.	2.66	7.93	18.0
SE4	0.218	12.6	D.L.	4.81	D.L.	7.49	D.L.	D.L.	D.L.	4.4
SE5	0.014	14.1	D.L.	2.60	1.08	1.19	D.L.	2.71	5.96	37.9
SSE1	0.591	15.4	D.L.	6.36	0.47	2.66	D.L.	D.L.	D.L.	5.9
SSE2	0.008	17.4	D.L.	4.65	8.64	0.90	D.L.	6.85	11.07	60.5
SSE3	0.051	M	D.L.	2.10	0.28	0.69	D.L.	D.L.	2.02	7.3
S1	0.043	51.1	5.92	10.98	4.20	7.80	3.77	6.46	10.22	59.2
S2	0.257	32.3	14.19	11.35	2.26	3.35	D.L.	12.90	6.45	32.3
S3	0.924	31.6	24.22	1.84	12.77	3.16	3.07	26.42	2.20	14.7
S4	0.017	24.4	9.48	3.05	9.34	1.62	D.L.	8.12	12.19	54.2
S5	0.004	24.1	20.24	8.42	4.65	0.27	4.92	59.06	36.65	82.1
SSw1	0.236	16.0	D.L.	7.83	1.07	5.63	D.L.	5.34	2.97	11.9
SSw2	0.421	15.9	D.L.	6.78	0.74	2.44	D.L.	4.77	1.60	6.4
Sw1	0.014	23.8	12.17	11.61	1.71	3.15	4.42	6.55	19.30	44.2
Sw2	M	17.1	5.69	6.72	7.60	0.57	M	M	M	M
Sw3	0.022	7.8	3.90	6.35	2.17	0.67	D.L.	18.94	5.01	19.5
Sw4	0.451	10.4	D.L.	8.28	D.L.	5.36	D.L.	D.L.	1.43	0.7
Sw5A	0.211	8.5	D.L.	6.36	D.L.	1.22	D.L.	2.65	3.13	8.0
Sw5B	0.261	M	D.L.	9.78	D.L.	1.35	D.L.	2.08	2.60	7.8
Sw5C	0.405	8.2	D.L.	6.32	D.L.	1.38	D.L.	1.53	1.02	4.1
Sw5D	0.397	8.0	D.L.	6.20	D.L.	1.25	D.L.	1.50	1.50	5.0
Sw5E	0.082	7.3	D.L.	5.82	D.L.	1.25	D.L.	2.60	4.68	15.6
W1	0.629	10.7	5.66	7.23	D.L.	1.45	D.L.	3.15	D.L.	3.8
W2	0.002	5.8	2.76	3.59	12.25	1.04	9.21	89.34	29.78	33.8
W3	0.527	M	D.L.	5.53	0.21	0.50	D.L.	4.22	1.05	D.L.
Ww3	0.628	8.0	D.L.	5.99	0.15	0.90	D.L.	2.50	D.L.	4.0
Ww4	0.419	7.4	D.L.	6.27	0.32	0.69	D.L.	2.11	D.L.	5.3
Ww5	0.001	20.1	D.L.	5.23	6.91	2.90	20.08	325.50	158.78	70.1
WwW1	0.262	7.3	D.L.	5.49	M	0.78	D.L.	2.62	2.09	5.2
W1A	0.047	16.7	3.26	7.44	1.02	1.95	D.L.	4.65	6.05	25.6
W1B	0.077	16.4	3.38	7.87	1.21	3.28	D.L.	5.80	5.80	19.3
W1C	0.096	17.4	3.37	7.71	1.49	2.02	D.L.	4.82	4.82	21.2
W1D	0.030	15.4	3.36	7.49	1.10	2.06	6.24	9.60	7.20	33.6
W1E	0.040	17.5	3.00	7.55	1.20	1.65	D.L.	5.00	7.50	32.5
W2	0.006	16.3	3.95	8.60	24.26	0.79	D.L.	2.96	16.30	103.7
W3	0.012	15.2	D.L.	8.48	2.05	0.64	D.L.	2.34	14.63	58.5
W4	0.443	11.2	D.L.	7.59	0.50	0.61	D.L.	4.46	1.67	11.2
W5	0.454	11.4	D.L.	7.31	0.34	1.20	4.00	5.14	D.L.	9.1
W6	0.270	6.8	D.L.	1.70	D.L.	0.68	D.L.	1.70	D.L.	2.0
W7	0.048	24.5	5.98	11.48	2.51	3.59	D.L.	4.19	10.17	44.9
W8	0.006	39.0	5.58	9.89	3.09	2.69	D.L.	7.10	22.82	100.5
R1	0.007	18.2	4.55	7.67	5.36	2.07	5.65	37.10	12.25	42.0
R2	0.029	19.5	6.80	10.74	1.63	6.02	D.L.	4.53	5.44	31.7
R3	0.111	23.3	7.48	6.91	1.54	5.02	D.L.	3.52	3.56	22.0
R4A	0.009	25.1	5.28	9.02	4.97	12.76	5.28	13.20	12.76	61.6
R4B	0.019	23.5	D.L.	6.32	3.41	7.20	D.L.	8.30	8.64	48.0
R4C	0.016	26.5	3.50	8.05	3.85	7.45	3.50	6.00	8.50	45.0
R4D	0.016	29.1	3.64	8.48	3.59	8.06	4.68	7.28	9.83	49.4
R4E	0.017	32.4	4.32	9.07	3.89	7.24	3.78	8.64	10.80	51.3
LLS	M	10.0	M	M	M	1.57	D.L.	D.L.	D.L.	D.L.
RCH	0.861	M	D.L.	8.89	D.L.	0.82	D.L.	D.L.	D.L.	D.L.
NMR	0.710	6.3	D.L.	3.49	D.L.	0.81	D.L.	D.L.	D.L.	D.L.
SMT	1.415	23.2	D.L.	7.86	D.L.	4.55	D.L.	2.68	D.L.	D.L.
LC	0.831	M	D.L.	6.27	D.L.	1.52	D.L.	2.64	D.L.	D.L.
UT	0.884	M	D.L.	6.67	D.L.	1.68	D.L.	2.81	D.L.	D.L.
LB	0.027	41.6	49.32	19.45	4.33	14.74	11.51	4.93	9.80	70.1

the area sampled. pH measured in the laboratory was used to calculate hydrogen ion loadings of snow sampled. The intrasite variability of major ion loading (Table 9) was equal to or less than 15% for SO_4^- , NO_3^- , Cl^- , and soluble silica, and less than 36% for the other major ions. Maps showing the spatial distribution of snowpack loading for each major ion are in Appendix 8.2.

4.3 SNOWPACK LOADING OF NON-ALKALINE METALS: INSOLUBLE AND SOLUBLE

The snowpack loadings of non-alkaline metals listed in Table 10 were obtained in the case of insoluble constituents directly from analysis of particulate matter filtered from the snowmelt and in the case of soluble metals from their meltwater concentrations, snow melt volume, and the area sampled. The intersite variability of metal loadings (Table 11) was 14 to 17% for soluble Al, V, Fe and Ni, and 24 to 44% for insoluble Al, V, and Mn. Maps showing the spatial distribution of metal loading around the source are in Appendix 8.3.

Table 9. The intrasite variability of major ion loadings of the snowpack (represented by the average percent standard deviation about the mean of five samples taken at each of the following sites: M, SW5, R4, N1).

LOADING OF	INTRASITE VARIABILITY (%)
H ⁺	36
SO ₄ ⁼	9
Cl ⁻	5
NO ₃ ⁻	15
Soluble Silica	15
NH ₄ ⁺	22
Na ⁺	34
Mg ⁺⁺	30
Ca ⁺⁺	31

Table 10. Snowpack loadings of metals for each site on 26 to 28 January 1978 calculated from measured concentrations, snowmelt volume, and area sampled (see Figures 2 and 3 for site locations).

SITE	TOTAL	INSOLUBLE				SOLUBLE			
		Al	V	Mn	Ti	Al	V	Fe	Ni
NNF1	M	M	M	M	M	0.747	1.792	1.073	0.187
NNE2	D.L.	100	17.2	1.0	19	0.713	1.191	0.509	D.L.
NNE3	D.L.	53	8.7	0.3	D.L.	0.476	0.655	0.317	D.L.
NNE4	D.L.	43	6.8	0.2	D.L.	0.327	0.506	0.272	D.L.
NE1	7200	380	57.3	2.9	50	0.196	2.565	0.441	0.343
NE2	D.L.	45	7.6	0.3	D.L.	0.455	D.L.	0.342	D.L.
NE3	D.L.	44	6.9	0.3	D.L.	0.394	0.642	0.450	D.L.
NE4	D.L.	44	7.1	0.3	D.L.	0.301	0.301	0.301	D.L.
NE5	D.L.	44	5.9	D.L.	12	0.244	0.324	0.153	D.L.
E1	D.L.	130	17.2	0.8	D.L.	0.314	0.968	0.628	D.L.
E2	D.L.	81	12.6	0.6	10	0.410	0.635	0.231	D.L.
E3	D.L.	46	7.2	0.3	D.L.	0.233	0.397	0.187	D.L.
E4	D.L.	49	6.1	0.2	D.L.	0.559	0.307	0.314	D.L.
EA	D.L.	7	0.9	D.L.	D.L.	0.130	0.228	0.130	D.L.
EB	D.L.	6	0.8	D.L.	D.L.	D.L.	0.196	D.L.	D.L.
EC	D.L.	9	0.9	D.L.	D.L.	0.390	0.177	0.284	D.L.
ED	D.L.	9	1.0	D.L.	D.L.	0.186	0.211	D.L.	D.L.
EE	D.L.	7	0.8	D.L.	D.L.	0.126	0.239	0.157	D.L.
SE1	4700	370	57.3	2.4	44	0.712	2.773	D.L.	0.384
SE2	D.L.	240	33.2	1.1	20	0.544	1.401	0.612	D.L.
SE3	D.L.	44	5.6	0.3	D.L.	0.145	0.324	0.169	D.L.
SE4	D.L.	30	4.2	0.2	D.L.	0.138	0.284	0.138	D.L.
SE5	D.L.	26	3.7	0.1	D.L.	0.090	0.113	D.L.	D.L.
SSE1	D.L.	110	17.2	0.8	22	0.580	1.186	0.709	D.L.
SSE2	D.L.	60	3.3	D.L.	13	0.151	0.624	0.201	D.L.
SSE3	D.L.	48	6.3	0.3	D.L.	0.325	0.299	D.L.	D.L.
S1	15100	1000	149.0	8.4	120	0.198	6.047	0.197	0.682
S2	8500	460	66.5	3.6	57	0.343	2.907	1.268	0.274
S3	D.L.	140	21.8	1.1	26	0.335	1.637	1.174	D.L.
S4	D.L.	130	18.3	0.9	9	0.321	0.604	0.738	D.L.
S5	4500	110	12.6	0.8	D.L.	0.161	0.417	D.L.	D.L.
SSW1	D.L.	210	33.2	1.5	23	0.912	2.188	0.959	0.171
SSW2	D.L.	100	17.2	0.7	22	0.555	1.130	0.858	D.L.
SW1	11700	640	56.2	3.8	60	D.L.	1.895	D.L.	D.L.
SW2	D.L.	92	9.7	0.9	11	D.L.	0.408	D.L.	D.L.
SW3	D.L.	80	10.8	0.6	D.L.	D.L.	0.410	0.431	D.L.
SW4	D.L.	36	4.5	0.2	D.L.	D.L.	0.346	0.238	D.L.
SW5A	D.L.	6	1.0	D.L.	D.L.	D.L.	0.170	D.L.	D.L.
SW5B	D.L.	5	0.8	D.L.	D.L.	D.L.	0.095	D.L.	D.L.
SW5C	D.L.	D.L.	0.6	D.L.	D.L.	0.099	0.118	D.L.	D.L.
SW5D	D.L.	6	0.7	D.L.	D.L.	0.108	0.081	D.L.	D.L.
SW5E	D.L.	5	0.8	D.L.	D.L.	0.110	0.160	D.L.	D.L.
W1	D.L.	49	6.5	0.3	15	0.359	0.589	0.288	D.L.
W2	D.L.	18	2.1	1.0	10	D.L.	0.212	0.118	D.L.
W3	D.L.	17	2.7	D.L.	D.L.	0.155	0.4	0.155	D.L.
NW3	D.L.	64	5.0	0.4	9	0.335	0.368	0.335	D.L.
NW4	D.L.	32	4.4	0.2	D.L.	0.217	0.244	0.136	D.L.
NW5	D.L.	23	3.3	0.2	D.L.	0.089	0.148	0.134	D.L.
NNW1	M	M	M	M	M	M	M	M	M
R1A	D.L.	100	14.9	0.8	D.L.	0.345	1.745	0.444	0.148
R1B	D.L.	100	13.8	0.7	16	M	2.126	M	M
R1C	D.L.	190	25.2	1.3	6	0.276	1.901	0.553	0.221
R1D	D.L.	110	16.1	1.0	15	0.330	1.783	0.660	0.248
R1E	4300	110	14.9	0.8	14	0.344	2.029	0.631	0.229
R2	12700	370	27.5	2.2	23	0.144	1.223	0.120	0.169
R3	5800	110	14.9	2.5	29	0.268	0.897	D.L.	D.L.
N4	D.L.	69	8.5	0.5	D.L.	D.L.	0.665	0.640	D.L.
N5	D.L.	40	5.9	0.2	D.L.	0.524	0.812	0.720	D.L.
BM	D.L.	9	0.3	D.L.	D.L.	0.097	D.L.	D.L.	D.L.
G1	8900	540	75.7	4.1	61	0.133	5.324	0.155	0.293
G5	15200	780	61.9	6.4	90	0.193	1.705	D.L.	D.L.
R1	D.L.	150	24.1	1.4	15	0.276	1.554	0.316	0.138
R2	11000	450	35.5	4.0	49	0.178	1.579	0.245	0.111
R3	7900	510	79.1	3.4	58	0.086	3.605	0.562	0.432
R4A	D.L.	160	18.3	8.9	11	0.185	3.049	D.L.	0.350
R4B	D.L.	110	14.9	0.7	D.L.	0.182	2.985	D.L.	0.377
R4C	D.L.	150	79.1	1.0	17	0.211	2.869	D.L.	0.369
R4D	5900	220	31.0	1.3	21	0.216	3.255	0.182	0.350
R4E	D.L.	180	26.4	1.3	32	0.275	3.379	0.138	0.350
ELS	D.L.	8	1.1	0.6	D.L.	0.143	0.136	D.L.	D.L.
RCH	D.L.	50	9.0	0.7	1	0.137	D.L.	D.L.	D.L.
NMR	D.L.	M	M	M	M	0.090	D.L.	D.L.	D.L.
SMT	D.L.	12	1.0	0.5	D.L.	0.447	0.214	0.223	D.L.
LC	D.L.	M	M	M	M	0.198	0.119	D.L.	D.L.
UT	D.L.	2	0.2	D.L.	D.L.	0.140	D.L.	D.L.	D.L.
LS	4900	140	18.4	1.0	20	0.241	2.798	0.135	0.241

Table 11. The intrasite variability of snowpack loadings of insoluble Al, V, Mn and of soluble Al, V, Fe, Ni (represented by the average percent standard deviation about the mean of five samples taken at each of the following sites: M, NW5, R4, N1).

LOADING OF	INTRASITE VARIABILITY (%)
Insoluble	
Al	24
V	35
Mn	44
Soluble	
Al	16
V	15
Fe	17
Ni	14

5. DISCUSSION

5.1 DEPOSITION PATTERNS AND MASS BALANCES

The deposition patterns of snowpack constituents originating mainly from the GCOS power house stack (Appendix 8.2 and 8.3) have several features in common that one might expect from the wind distribution in the area (Figure 5). Most deposition occurs in a strip running north and south from the source that corresponds to frequent valley winds (52% frequency). An easterly bulge in the deposition pattern reflects a small maximum in westerly and south-westerly winds. Maximum deposition generally occurs to the south of the source at a distance of 5 km. The deposition patterns of SO_4^- , NO_3^- (Figure 7) and of insoluble Al, V, Mn (Figure 8) clearly display the north-south axis and the easterly bulge.

Using the measured deposition patterns and known emission rates, the total amounts deposited in the snowpack within 25 km were calculated and compared to those emitted (Table 12). Since the soluble fraction of aluminum and vanadium deposition was generally less than 1 and 10%, respectively (see data in Table 10), their insoluble fraction essentially represents total deposition. It is assumed that the same is true for manganese. A large fraction of the aluminum, vanadium, and manganese released by the source as flyash was deposited within 25 km. However, over 98% of the more volatile oxides of sulphur and nitrogen were transported out of the area. Only 0.3% of the total sulphur released by the source was removed within 25 km. This is twice as high as the 0.14% found to be deposited in snow during the three-week period ending 2 March 1976 (Barrie and Whelpdale 1978). Both these results are consistent with those of a study around a sour gas plant in central Alberta where it was concluded that (during winter) less than 2% of the sulphur released was deposited within 40 km of the source (Summers and Hitchon 1973).

Particulate Al, V, and Mn are removed much more rapidly from the GCOS plume than are the oxides of sulphur and nitrogen.

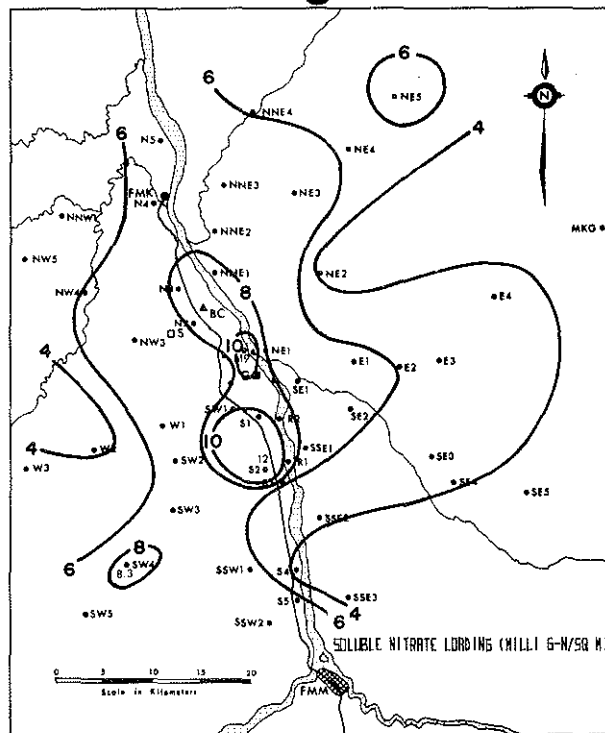
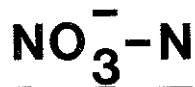
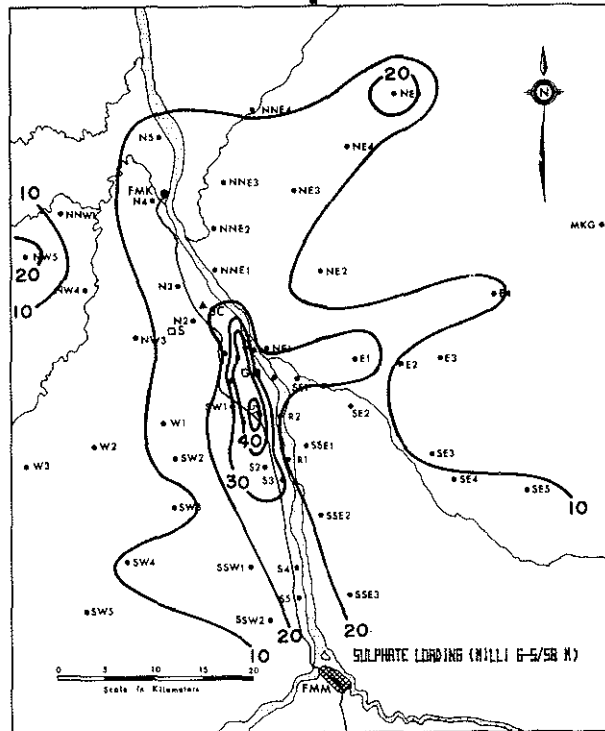
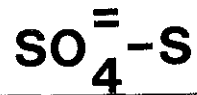


Figure 7. The spatial distribution of snowpack loading ($\text{mg}\cdot\text{m}^{-2}$) of sulphate and nitrate ions in the study area on 26 January 1978. G marks the location of the GCOS power plant.

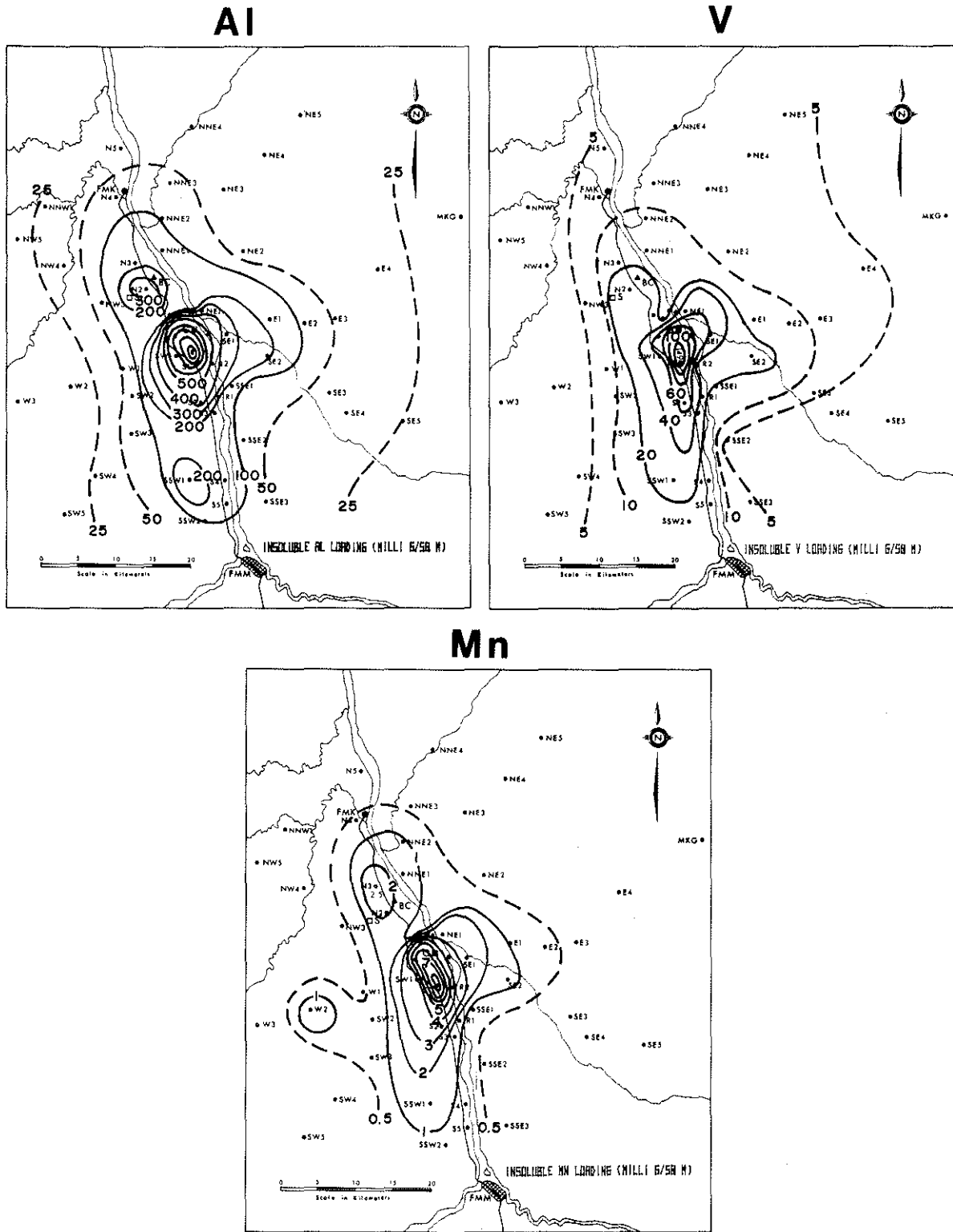


Figure 8. The spatial distribution of snowpack loading ($\text{mg}\cdot\text{m}^{-2}$) of insoluble aluminum, vanadium and manganese in the study area on 26 January 1978. G marks the location of the GCOS power plant.

Table 12. The mass budget of various substances released to the atmosphere by the GCOS power plant and deposited within 25 km from 17 November 1977 to 26 January 1978.

	AMOUNT (10^6 g)		FRACTION (%) DEPOSITED WITHIN 25 KM
	RELEASED	DEPOSITED WITHIN 25 KM	
<u>GASEOUS/PARTICULATE</u>			
$\text{SO}_2/\text{SO}_4^{2-}\text{-S}$	$7744 + 700^a$	23.3	0.30
$\text{NO}_x/\text{NO}_3^-\text{-N}$	$509 + 50^b$	10.2	2.0
<u>PARTICULATE</u>			
V	$49 + 7^c$	28.4	58
Al	$224 + 27^c$	208.0	93
Mn	$1.68 + 0.2^c$	1.66	99

^aCalculated using measured emission rates supplied by Alberta Environment.

^bCalculated by assuming the ratio of SO_x to NO_x emission rates reported by Shelfentook (1978) and measured SO_x emission rates.

^cDetermined using a particulate emission rate of 27 t/day and an average flyash content based on the data in Table 1.

The ratio of snowpack loading between Sites S1, 5 km from GCOS, and SSW2, 25 km from GCOS, is about 10:1 for insoluble Al, V, Mn and only 3:1 for SO_4^{--} and NO_3^- . The observed contrast in scavenging rates can be attributed largely to the preferential removal of large metal-bearing flyash particles (1 to 50 μm in diameter) over smaller sub-micron sulphate and nitrate particles or gaseous sulphur and nitrogen compounds (Clough 1973). During winter, pollutants are removed from the atmosphere by snow and by dry deposition processes. The latter involve sedimentation, interception, impaction, and brownian diffusion to the earth's surface. At temperatures below -25°C in a moist plume, a third pollutant scavenging mechanism is active, 'plume snow-out'. At such low temperatures, enough active ice nuclei are present to initiate the ice phase close to the source. Sufficient moisture is available in the plume that ice crystals develop, grow, and fall to the ground carrying pollutants with them. Presumably, ice crystals generated in the plume scavenge particulate flyash much more efficiently than gases. During the lifetime of the snowpack sampled, the air temperature was below -25°C about 25% of the time. Snow-out from the GCOS power-plant plume was observed frequently by AOSERP personnel at Mildred Lake. Melted snow samples collected below the plume by the authors contained soluble vanadium and sulphate concentrations up to 10 times higher than those in the snowpack. Scavenging by snow-out was probably a very effective scavenger of plume flyash for about 25% of the snowpack's lifetime. Another 2% of the time, scavenging by snow from weather systems likely occurred. Since 50 to 100% of flyash elements such as Al, V, and Mn were removed within 25 km (Table 12), dry deposition processes must have been active also in removing plume flyash from the atmosphere. Winds were calm (less than 1.5 m/s) 25% of the time during the snowpack's lifetime. In such situations, sedimentation of flyash particles 5 to 50 μm in diameter could be particularly important. A detailed discussion of the effectiveness of dry and wet pollutant removal processes in the AOSERP area based on this survey and several other studies cited in Section 1 has been reported elsewhere (Barrie 1979b).

5.2 MAJOR IONS AND SNOWPACK ACIDITY

The spatial distribution of snowmelt pH for the region is shown in Figure 9. In areas of high deposition near the source, pH has a maximum between 6 and 7. It drops off rapidly to the east and west, and less rapidly to the north and south along the river valley to values between 4.7 and 5.

An ion balance of major ions in snowmelt (Table 13) was used first to check the accuracy of analysis determining if positive and negative ion equivalents balanced and then to identify the dominant ions at each site. In general, the predominant ions in snow collected near the source are in order of decreasing equivalents: cations Ca^{++} , Mg^{++} , Na^+ , NH_4^+ , and H^+ ; and anions $\text{SO}_4^{=}$, NO_3^- , and Cl^- . In outlying areas having pH 4.7 to 5.1, H^+ , $\text{SO}_4^{=}$, and NO_3^- are the dominant ions. Alkaline snow near the source is probably due to calcium and magnesium oxides in flyash particles. As shown in Section 5.1, alkaline flyash particles are absent in outlying areas leaving the acidic oxides of sulphur and nitrogen to dominate the deposition. Between pH 5.1 and 7, calcium is the dominant positive ion while, below pH 5.1, hydrogen ions predominate (Figure 10). The observed relationship between these two ions further supports the hypothesis that calcium is provided by the dissolution of calcium oxides accompanied by the release of acid-neutralizing hydroxyl ions.

The spatial distribution of the hydrogen ion's contribution to the total positive ion equivalents in snowmelt is shown in Figure 11. It was the main positive-ion in sectors to the east-northeast and to the west of GCOS at distances beyond 5 km. The alkaline area marked by low H^+ contributions corresponds roughly to areas of high calcium deposition (Appendix 8.2).

5.3 PRINCIPAL COMPONENT AND CLUSTER ANALYSIS OF THE DATA

A statistical analysis of snowpack data from 43 sites was performed using two multivariate methods: a principal component analysis (PCA), and a cluster analysis. Snowpack loadings of H^+ , NH_4^+ , Na^+ , Mg^{++} , Ca^{++} , $\text{SO}_4^{=}$, NO_3^- , soluble silicate, insoluble Mn,

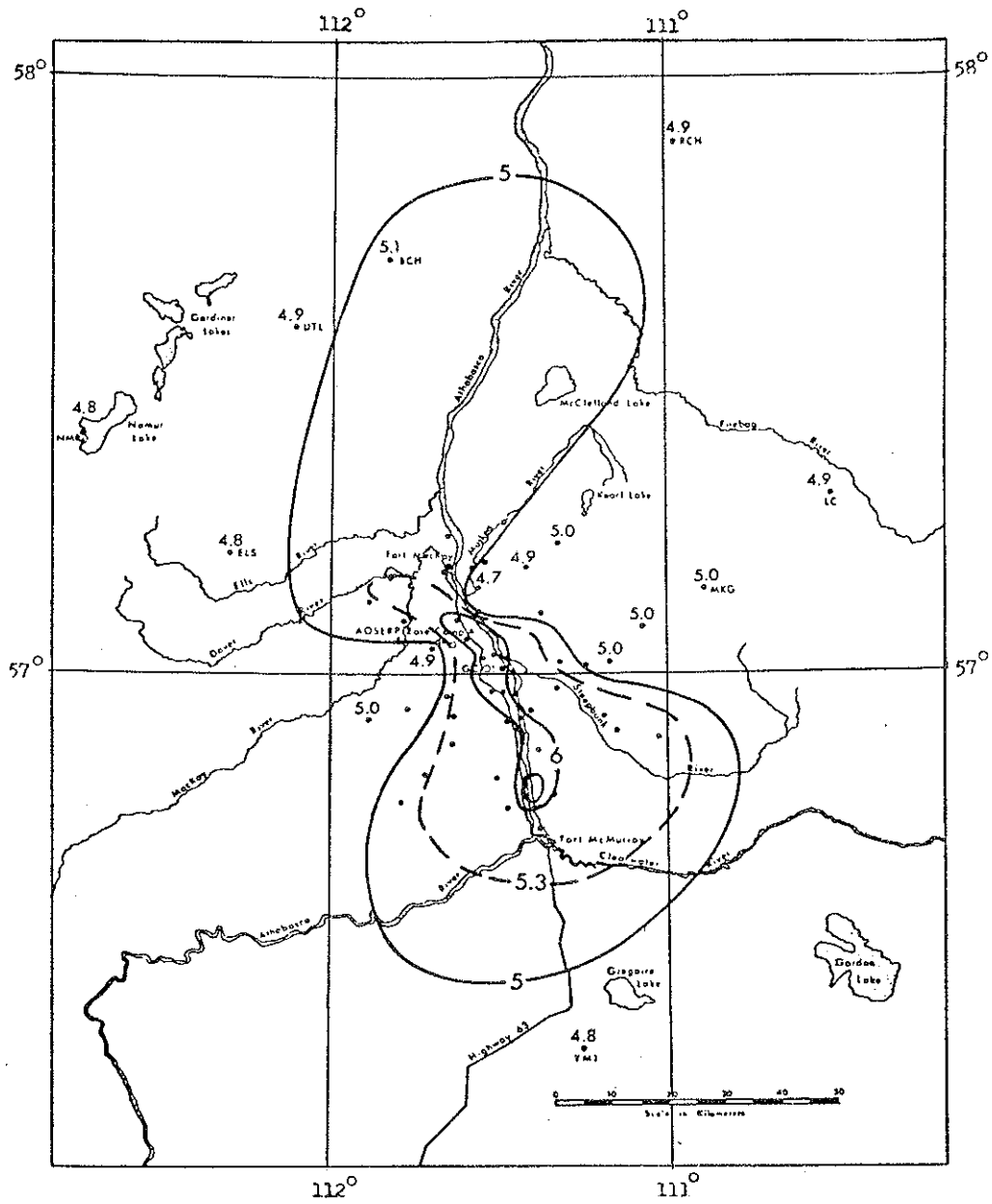


Figure 9. The spatial distribution of snowpack pH (Lab) in the study area on 26 January 1978.

Table 13. Results of an ion balance done with snowmelt major ion concentration for each site.

SITE	TOTAL +VE IONS	TOTAL -VE IONS	RATIO OF TOTAL	FRACTION OF TOTAL +VE ION EQUIVALENT DUE TO					FRACTION OF TOTAL -VE ION EQUIVALENT DUE TO				
	(10^{-6} eq.l $^{-1}$)	(10^{-6} eq.l $^{-1}$)	+VE/-VE	H ⁺	NH ₄ ⁺	Ca ⁺⁺	Mg ⁺⁺	Na ⁺	K ⁺	SO ₄ ⁼	NO ₃ ⁻	Cl ⁻	HCO ₃ ⁻
NN1	35.5 - 37.0	35.3 - 37.0	1.00	0.34	0.09	0.40	0.09	0.04	< 0.04	0.61	0.33	< 0.05	0.01
NN2	40.0 - 47.8	37.4 - 39.1	1.06	0.49	0.05	0.27	< 0.02	0.09	0.06	0.64	0.31	< 0.04	0.01
NN3	20.9 - 22.4	22.1 - 23.8	0.94	0.45	0.09	0.27	0.07	0.06	< 0.07	0.55	0.35	< 0.07	0.02
NN4	20.9 - 22.4	21.6 - 23.3	0.96	0.45	0.04	0.31	0.07	0.06	< 0.07	0.54	0.37	< 0.07	0.02
NE1	57.5	43.2 - 44.9	1.30	0.02	0.13	0.56	0.13	0.10	0.06	0.60	0.24	< 0.04	0.12
NE2	17.6 - 19.9	19.7 - 21.4	0.91	0.50	0.09	0.20	< 0.04	0.09	< 0.08	0.56	0.34	< 0.05	0.02
NE3	18.7 - 21.1	21.0 - 22.7	0.91	0.60	0.04	0.19	< 0.04	0.06	< 0.07	0.55	0.36	< 0.07	0.02
NE4	15.0 - 17.3	19.8 - 21.5	0.78	0.58	0.04	0.17	< 0.05	0.03	< 0.09	0.58	0.32	< 0.06	0.02
NE5	83.2 - 84.7	47.8 - 49.5	1.73	0.00	0.01	0.74	0.26	0.20	< 0.02	0.38	0.10	< 0.03	0.43
E1	45.1	40.6 - 42.3	1.11	0.17	0.02	0.15	0.04	0.30	0.25	0.68	0.20	< 0.04	0.02
E2	22.8 - 23.6	19.7 - 21.3	1.13	0.42	0.05	0.21	< 0.03	0.18	0.10	0.50	0.40	< 0.06	0.03
E3	14.0 - 17.2	18.0 - 19.7	0.83	0.58	0.06	0.17	< 0.05	< 0.05	< 0.09	0.51	0.30	< 0.09	0.03
E4	11.2 - 16.9	20.0 - 21.7	0.67	0.59	0.07	< 0.15	< 0.05	< 0.05	< 0.09	0.58	0.32	< 0.06	0.02
MA	8.5 - 13.4	16.9	0.65	0.47	0.04	< 0.19	0.12	< 0.06	< 0.11	0.44	0.37	0.13	0.05
EM	***	***	***	***	***	***	***	***	***	***	***	***	***
EC	10.5 - 16.3	19.4 - 21.1	0.66	0.61	0.03	< 0.15	< 0.05	< 0.05	< 0.09	0.41	0.48	< 0.05	0.03
MD	10.9 - 15.7	17.3 - 19.0	0.76	0.60	0.06	< 0.15	< 0.05	< 0.05	< 0.09	0.43	0.46	< 0.09	0.03
ME	10.8 - 15.6	22.7	0.60	0.60	0.05	< 0.15	< 0.05	< 0.05	< 0.09	0.44	0.44	0.10	0.02
SE1	31.4 - 31.3	32.6 - 34.2	0.96	0.12	0.11	0.51	0.12	0.03	< 0.05	0.66	0.25	< 0.05	0.04
SE2	16.3 - 19.2	19.6 - 21.3	0.88	0.41	0.03	0.31	< 0.04	0.07	< 0.08	0.59	0.30	< 0.06	0.03
SE3	31.3 - 32.8	33.1 - 34.6	1.34	0.02	0.04	0.46	0.30	0.07	< 0.05	0.35	0.24	< 0.07	0.34
SE4	15.6 - 18.8	22.0 - 23.7	0.75	0.21	0.40	0.21	< 0.04	< 0.05	< 0.08	0.61	0.27	< 0.07	0.02
SE5	47.6 - 49.2	43.9 - 42.6	1.16	0.01	0.02	0.71	0.18	0.04	< 0.03	0.38	0.08	< 0.04	0.50
SE11	17.5 - 21.7	24.5 - 26.2	0.75	0.48	0.12	0.24	< 0.04	< 0.04	< 0.07	0.62	0.29	< 0.06	0.02
SFE2	89.8 - 90.4	60.9 - 62.6	1.45	0.00	0.01	0.72	0.19	0.06	< 0.02	0.33	0.11	< 0.03	0.54
SFE3	***	***	***	***	***	***	***	***	***	***	***	***	***
S1	86.5	83.8	1.03	0.01	0.09	0.63	0.18	0.06	0.02	0.71	0.17	0.04	0.03
S2	48.7 - 53.3	51.4	0.95	0.08	0.06	0.50	0.16	0.17	< 0.03	0.61	0.24	0.12	0.03
S3	46.1	33.4	1.20	0.27	0.05	0.22	0.05	0.34	0.07	0.70	0.05	0.24	0.01
S4	61.5 - 63.1	30.9	1.22	0.00	0.02	0.63	0.23	0.08	< 0.02	0.44	0.03	0.33	0.42
S5	179.8	118.1	1.55	0.00	0.00	0.42	0.31	0.26	0.01	0.24	0.09	0.09	0.50
SSW1	27.3 - 28.8	27.6 - 29.3	0.93	0.14	0.18	0.35	0.14	0.14	< 0.05	0.58	0.32	< 0.06	0.05
SSW2	22.0 - 23.6	23.6 - 30.3	0.78	0.34	0.11	0.25	0.07	0.17	< 0.07	0.62	0.35	< 0.05	0.02
SW1	81.5	69.3	1.17	0.00	0.04	0.43	0.35	0.09	0.03	0.39	0.22	0.09	0.31
SW2	***	***	***	***	***	***	***	***	***	***	***	***	***
SW3	40.7 - 42.3	32.3	1.29	0.01	0.02	0.41	0.18	0.35	< 0.04	0.27	0.25	0.06	0.42
SW4	16.1 - 14.5	23.5 - 25.2	0.71	0.34	0.23	0.22	0.09	< 0.05	< 0.08	0.57	0.33	< 0.07	0.03
SW5A	19.9 - 21.4	19.9 - 21.6	0.99	0.19	0.06	0.35	0.23	0.10	< 0.07	0.46	0.40	< 0.08	0.06
SW5B	***	***	***	***	***	***	***	***	***	***	***	***	***
SW5C	16.4 - 17.9	19.5 - 21.2	0.84	0.44	0.05	0.22	0.09	0.07	< 0.09	0.47	0.42	< 0.08	0.03
SW5D	18.1 - 19.6	19.5 - 21.2	0.93	0.40	0.07	0.25	0.13	0.07	< 0.08	0.47	0.42	< 0.08	0.03
SW5E	27.5 - 29.0	20.1 - 21.8	1.35	0.05	0.05	0.52	0.26	0.07	< 0.05	0.40	0.37	< 0.05	0.15
w1	16.4 - 15.3	21.9	0.80	0.53	0.07	0.16	< 0.04	0.12	< 0.05	0.48	0.37	0.12	0.01
w2	271.0	129.3	2.10	0.00	0.01	0.20	0.29	0.47	0.03	0.09	0.06	0.02	0.62
w3	***	***	***	***	***	***	***	***	***	***	***	***	***
N13	19.8 - 22.1	19.0 - 20.7	1.06	0.57	0.05	0.18	< 0.04	0.10	< 0.07	0.48	0.41	< 0.05	0.02
N14	15.4 - 17.8	17.9 - 19.6	0.88	0.45	0.04	0.26	< 0.05	0.10	< 0.09	0.45	0.43	< 0.09	0.03
N15	673.2	302.5 - 304.2	2.22	0.00	0.01	0.11	0.42	0.45	0.02	0.09	0.03	< 0.01	0.68
NNW1	16.3 - 17.8	17.3 - 19.0	0.94	0.28	0.05	0.28	0.13	0.12	< 0.09	0.46	0.39	< 0.09	0.06
N1A	45.3 - 47.4	41.2	1.13	0.02	0.05	0.58	0.23	0.09	< 0.03	0.55	0.28	0.05	0.13
N1B	40.4 - 42.0	38.2	1.08	0.04	0.09	0.48	0.24	0.12	< 0.04	0.56	0.30	0.05	0.09
N1C	38.9 - 40.4	38.6	1.03	0.05	0.06	0.34	0.20	0.11	< 0.04	0.58	0.30	0.05	0.07
N1E	62.6	41.6	1.51	0.01	0.04	0.56	0.20	0.14	0.06	0.40	0.27	0.05	0.20
w1E	51.8 - 53.3	41.1	1.28	0.01	0.03	0.61	0.23	0.05	< 0.03	0.53	0.26	0.04	0.10
N2	135.6 - 137.1	77.7	1.75	0.00	0.01	0.76	0.20	0.02	< 0.01	0.27	0.16	0.03	0.50
N3	73.0 - 74.6	53.4 - 55.1	1.36	0.00	0.01	0.67	0.28	0.02	< 0.02	0.30	0.19	< 0.03	0.43
N4	24.5 - 26.0	22.9 - 24.6	1.06	0.31	0.02	0.38	0.09	0.13	< 0.06	0.51	0.40	< 0.07	0.03
N5	22.8 - 23.6	22.3 - 24.0	1.00	0.34	0.05	0.34	< 0.03	0.17	0.06	0.52	0.30	< 0.07	0.03
B1	14.2 - 16.6	18.7 - 18.4	0.88	0.48	0.07	0.15	< 0.05	0.13	< 0.09	0.68	0.19	< 0.09	0.04
G1	50.6 - 50.1	48.9	1.21	0.01	0.06	0.62	0.23	0.05	< 0.03	0.52	0.28	0.06	0.14
G5	151.0 - 152.5	107.6	1.41	0.00	0.02	0.69	0.24	0.04	< 0.01	0.45	0.13	0.03	0.39
F1	143.5	78.6	1.83	0.00	0.02	0.42	0.20	0.32	0.04	0.41	0.20	0.05	0.34
R2	57.2 - 53.7	56.5	1.03	0.01	0.13	0.59	0.17	0.07	< 0.03	0.40	0.30	0.07	0.15
R3	44.7 - 46.2	51.3	0.89	0.05	0.14	0.54	0.16	0.08	< 0.03	0.65	0.24	0.09	0.04
R4A	126.4	80.4	1.57	0.00	0.13	0.55	0.19	0.10	0.03	0.44	0.16	0.04	0.33
R4B	77.8 - 79.3	54.2 - 55.9	1.43	0.01	0.11	0.63	0.19	0.05	< 0.02	0.55	0.10	< 0.03	0.24
R4C	74.7	63.5	1.18	0.00	0.11	0.60	0.19	0.07	0.03	0.52	0.10	0.03	0.27
R4D	80.5	65.5	1.23	0.00	0.11	0.59	0.19	0.08	0.03	0.53	0.18	0.03	0.26
R4E	80.5	68.6	1.17	0.00	0.09	0.59	0.20	0.09	0.02	0.50	0.17	0.03	0.25
ELS	***	***	***	***	***	***	***	***	***	***	***	***	***
FCH	***	***	***	***	***	***	***	***	***	***	***	***	***
NNF	16.8 - 22.6	14.7 - 16.3	1.27	0.70	0.04	< 0.11	< 0.04	< 0.04	< 0.07	0.54	0.34	< 0.10	0.02
SNT	20.0 - 14.8	22.9 - 24.6	0.94	0.64	0.11	< 0.10	< 0.03	0.05	< 0.06	0.66	0.26	< 0.07	0.01
LC	***	***	***	***	***	***	***	***	***	***	***	***	***
UT	***	***	***	***	***	***	***	***	***	***	***	***	***
LS	108.4	108.9	1.00	0.00	0.14	0.63	0.14	0.04	0.05	0.44	0.23	0.23	0.10

BICARBONATE CALCULATED FROM MEASURED-PH ASSUMING EQUILIBRIUM WITH 330 ppm(v) CO₂.

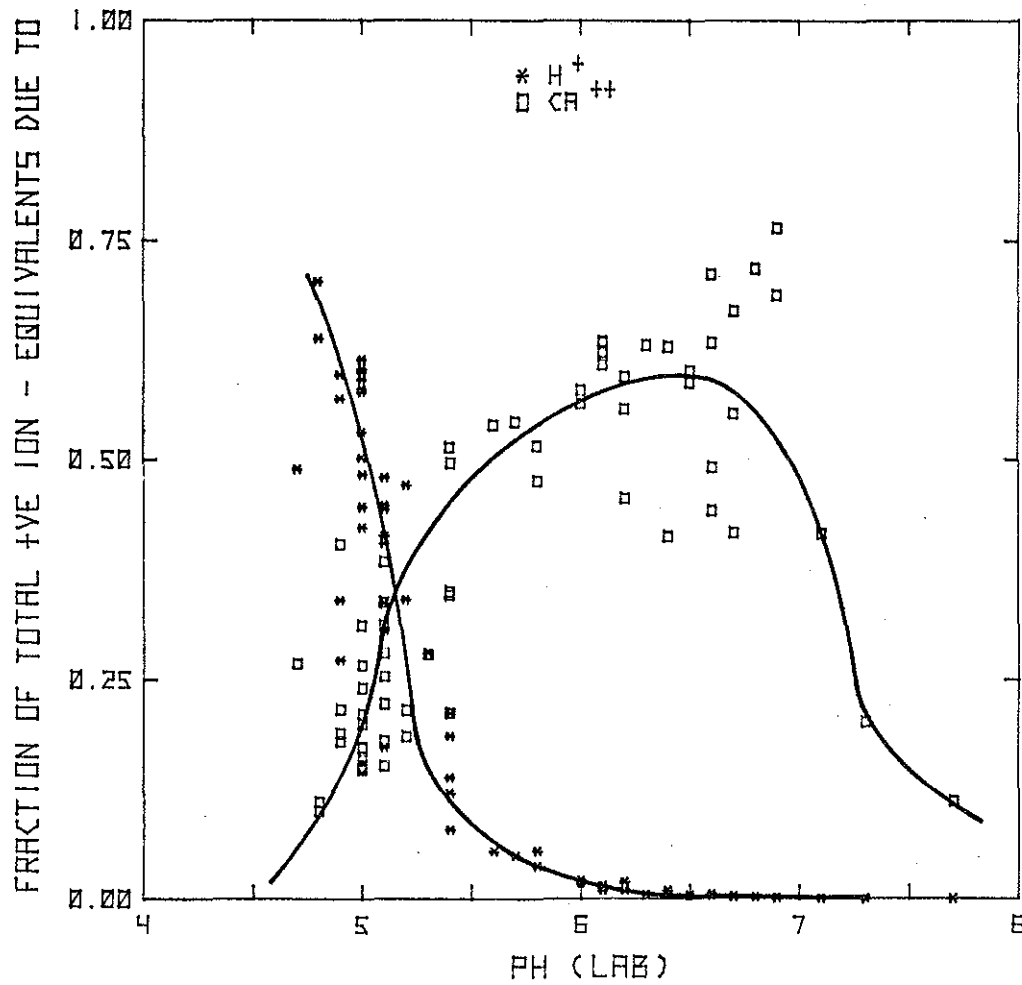


Figure 10. The contribution of hydrogen and calcium ions to the total positive ion equivalents in snowmelt collected from the oil sands area 26 January 1978 as a function of pH (Lab).

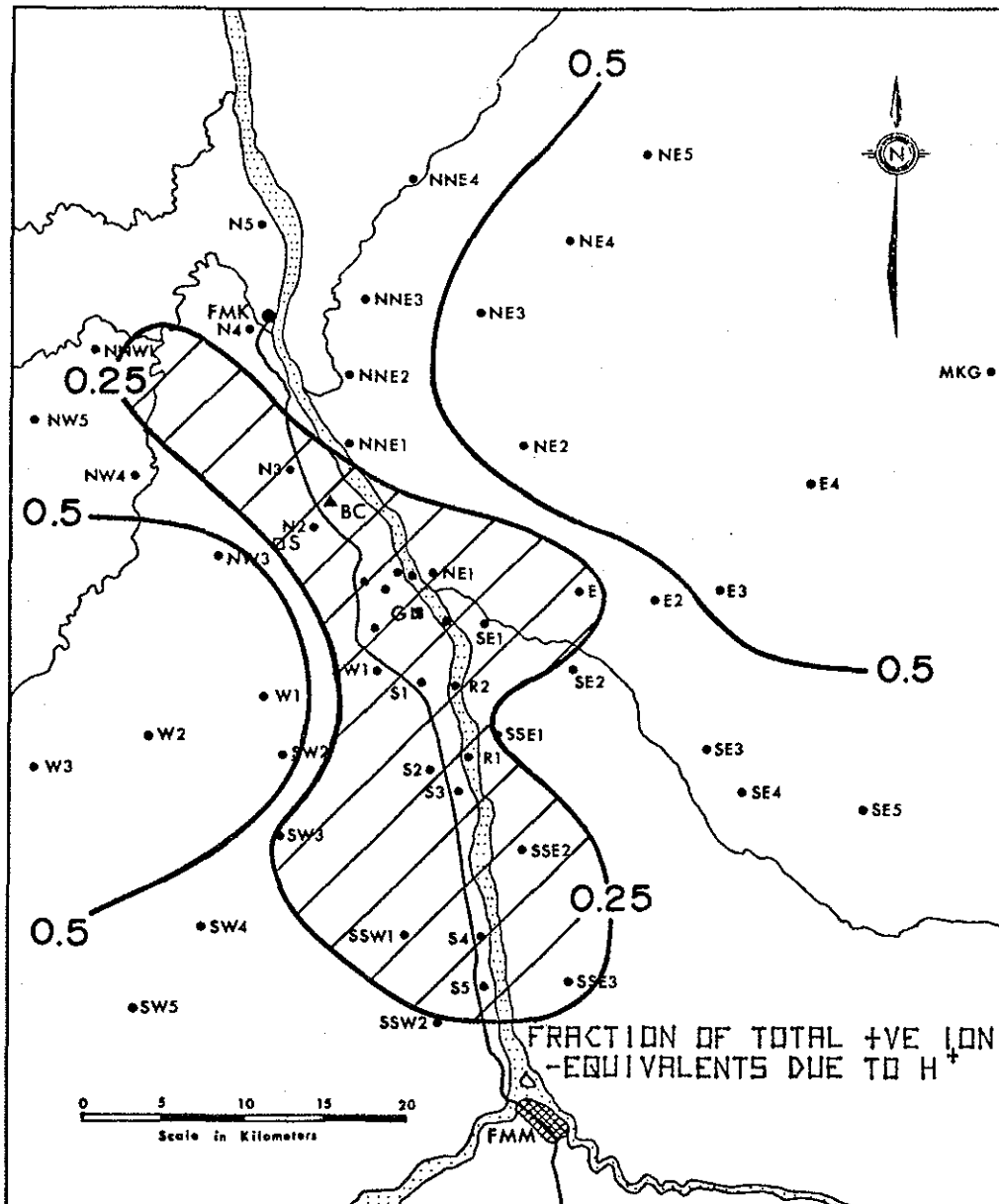


Figure 11. The spatial distribution of the contribution of hydrogen ions to the total positive ion equivalents in snowmelt collected from the oil sands area 26 January 1978. The hatched area is where hydrogen ion contributes less than 25% to the total positive ion equivalents.

insoluble Al, and insoluble V were used in the analysis. A PCA with subsequent orthogonal (varimax) rotation to simple structure was conducted with specific programs from the NT-SYS Package of Multivariate Statistical Programs (Rohlf et al. 1974). Two clustering techniques, a complete and an unweighted pair-group method using centroid averaging, were used from the NT-SYS package.

A PCA reduces the dimensionality of a data set by explaining its variance in terms of a reduced number of new variables or principal components. The principal components, each of which is a linear combination of the original variables, can then be rotated to simple structure. This rotation may allow for a more meaningful interpretation of the principal components. The sites may then be plotted against the first three principal components to provide some visual presentation of the analytical solution. In addition to the PCA, a cluster analysis was carried out to select sites having similar snowmelt chemistry. The groups selected in this manner closely resembled those obtained from the PCA. Most locations in each set of sites could be associated with one another intuitively after having seen the deposition patterns. However, one group of seven sites (NW5, NE5, W2, S5, S4, SSE2, and N3) stood out as geographically unrelated to one another. Snowmelt from these locations had high sodium and magnesium values. It is believed that somehow the sample had become contaminated by surface water presumably from the frozen stream or lake surfaces above which they were collected. After deleting data for the seven surface-water contaminated sites, PCA and cluster analyses were repeated on the reduced data set. The first four principal components extracted explained 86% of the variance. The chemical constituents associated with each component were as follows:

1. $\text{SO}_4^{=}$, NO_3^{-} , NH_4^{+}
2. Soluble silicate, Ca^{++} , Mg^{++}
3. H^{+} , Mg^{++} , Ca^{++}
4. $\text{SO}_4^{=}$, Insoluble -Al, V, Mn

In the third component, H^+ showed a strong negative correlation with the other major members Ca^{++} and Mg^{++} . In view of the observed relationships between H^+ and Ca^{++} (Figure 10), this result was not unexpected.

Components 1, 3, and 4 were selected to form the axes of a three-dimensional diagram in which the position of a site is determined by the magnitude of each of its components. When all sites are plotted in this manner, a pattern is evident (Figure 12). Most sites fall along a line running from the rear lower left (corresponding to low Ca^{++}/Mg^{++} - high H^+ ; low $Al/V/Mn/SO_4^{=}$ and low $NH_4^+/SO_4^{=} / NO_3^-$) to a point in the front upper right which is high in all constituents except H^+ (the implied negative correlation between H^+ and Mg^{++}/Ca^{++} should be noted. This was considered above).

The exceptions to the general pattern of three-dimensional site distribution discussed above are the background Sites BM, M, SMT and Site LS near the source. They clearly do not fall amongst the other sites. BM, M and SMT are remote 'background' locations. LS is about 4 km north of the source.

A cluster analysis was also used to identify groups of sites with similar chemistry. It was found that the complete set of sites was comprised of seven distinct sub-sets. They are identified with letters in the principal component graph in Figure 12. In addition, the geographical location of each subset is depicted on a map of the study area in Figure 13. Not only are sites in each cluster analysis group clumped together in the principal component graph but also they are geographically related to one another.

Closer to the source, snowmelt exhibits considerably more variation in its principal components (i.e., in its chemical composition) than it does in outlying areas. For instance, sites in Group F 15 to 25 km away are very close together while sites in Group A 5 km away are more scattered. Nevertheless it is felt that Group F is a distinct sub-set.

Two of the principal components plotted in Figure 12 may be related to different types of emissions from GCOS; the $Al/V/Mn/SO_4^{=}$

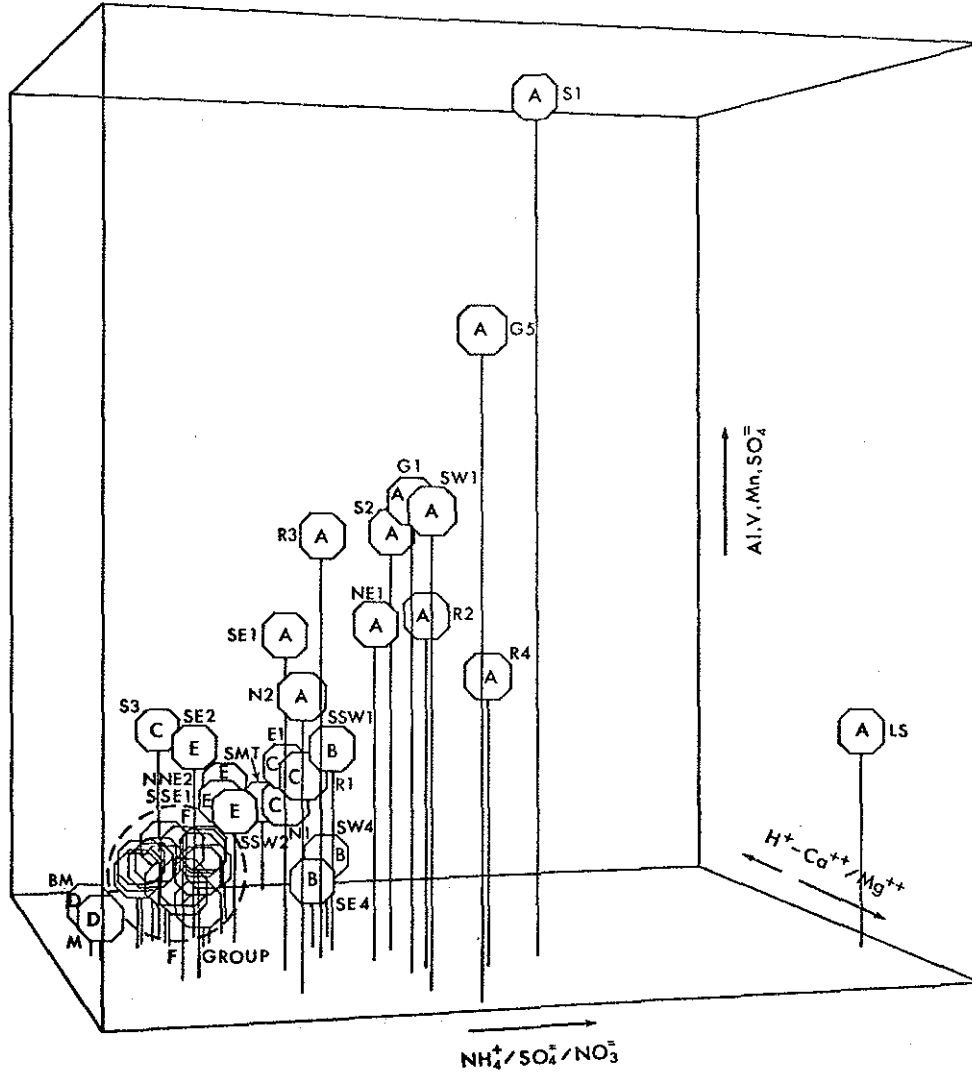


Figure 12. A three-dimensional representation of a principal component analysis of the snowpack loading data analysis. Groups of sites identified by a cluster analysis are identified by letters. The geographical location of each group is shown in Figure 13.

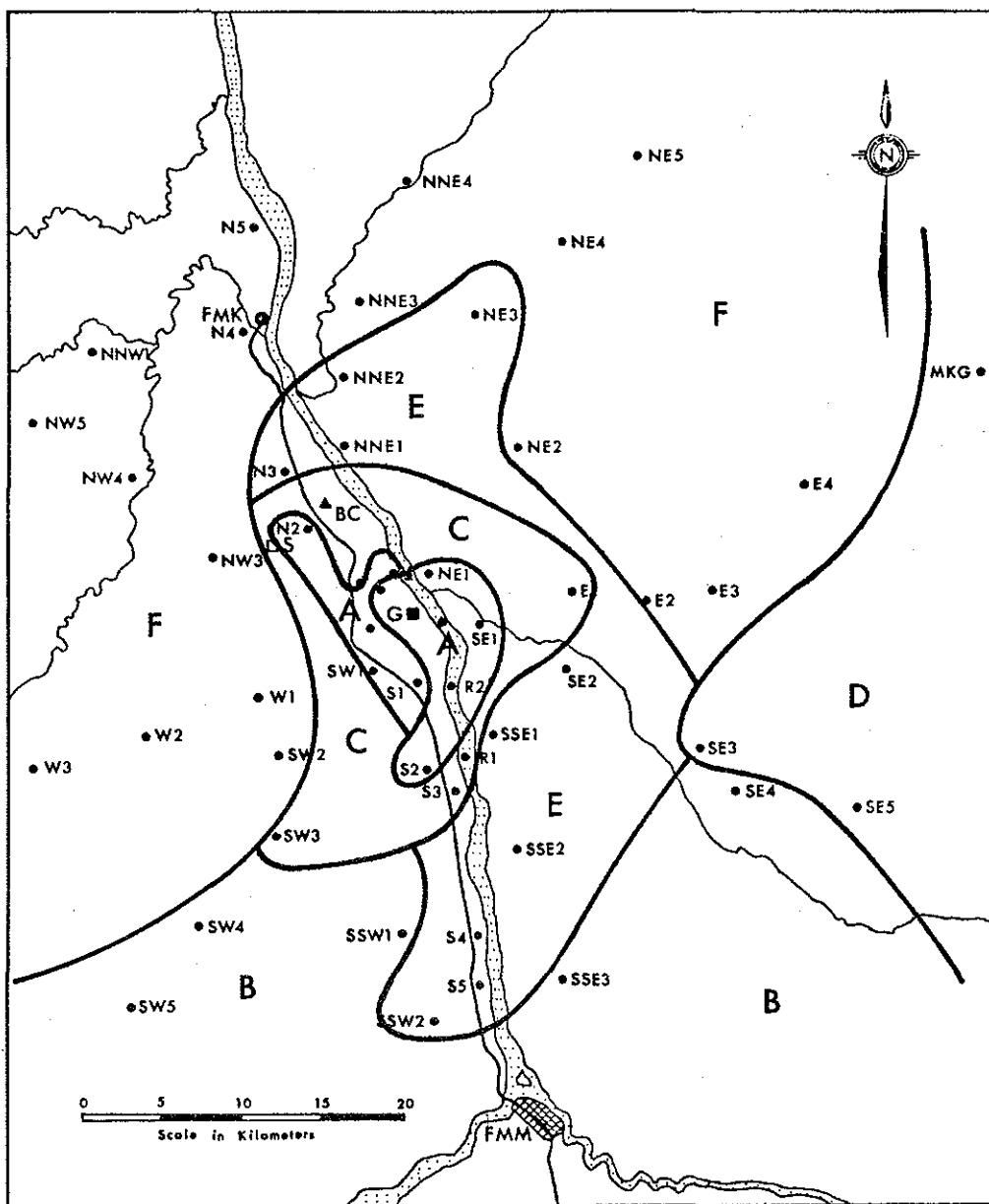


Figure 13. The geographical location of groups of sites identified as having similar snow chemistry by cluster analysis. The groups are also shown in Figure 12.

component is associated with gaseous and particulate emissions of the oxides of sulphur and nitrogen and of ammonia. In general, each component decreases with increasing distance from the source. The rate of decrease can be assessed quantitatively by comparing the average of each component for a set of sites near the source with those of a group of sites in an outlying area. This was done with sites in areas A and F in Figure 13. The results were as follows:

	Ratio close-in (F)/outlying sites (A)
Flyash component (Component 4)	8:1
Oxides of Sulphur and Nitrogen Component (component 1)	5:1

The influence of flyash constituents drops off more rapidly with distance from the source than that of gaseous constituents. The same conclusion was drawn in Section 5.1 using snowpack loading data.

6. CONCLUSIONS

A snow chemistry survey is an economical and effective way of establishing the extent and magnitude of wintertime deposition of air pollutants in the Athabasca Oil Sands region. In the winter of 1977-78, particulate and gaseous substances released to the atmosphere from the GCOS power plant stack were deposited mainly along the Athabasca River valley. Significant departures from background snowpack loadings were noted for flyash particulate matter as far north and south of the pollutant source as 25 km. To the east and west, effects of such emissions on deposition decreased much more rapidly reaching background within about 10 km. This pattern of deposition is consistent with the air motions observed during the winter.

Evidence from snowpack pH measurements suggests that acidic oxides of nitrogen and sulphur affect deposition in a much larger region than flyash constituents do. Consequently, snow near the source is alkaline because of a predominance of flyash in deposited matter and acidic in outlying areas where oxides of sulphur and nitrogen are the major pollutants.

The results of this study are summarized in the following conclusions:

1. Of the total sulphur and nitrogen oxides released by the source during the 70 d lifetime of the snowpack sampled, only 0.3 and 2% were deposited within 25 km of the source, respectively. On the other hand, at least 50% of such flyash constituents as Al, Mn, and V came down within 25 km.
2. The soluble fraction of total vanadium in the snowpack ranged from 1 to 10%. Aluminum was less than 1% soluble.
3. Plume snow-out which occurs at temperatures below about -25°C in the GCOS power plant plume is a viable pollutant scavenging mechanism in cold winter months.

4. The snowpack is alkaline (pH 6 to 7) near the source with Ca^{++} , $\text{SO}_4^{=}$, NO_3^- the predominant ions. In outlying areas, it is slightly acidic (pH 4.7 to 5) and H^+ , $\text{SO}_4^{=}$, and NO_3^- dominate snowmelt ion chemistry.

In the next decade as more oil extraction operations appear in the Fort McMurray region, both gaseous and particulate atmospheric emissions will increase. By regularly monitoring the chemical composition of the atmosphere as well as that of the snowpack in winter and of rain in summer in northern Alberta and Saskatchewan, the impact of emissions, especially the acidic ones, can be assessed. Although all of these activities are being undertaken by AOSERP, the area covered is limited to northeastern Alberta. There is a need to monitor over much larger areas downwind of the AOSERP source region, especially in northern Saskatchewan and in the Northwest Territories.

7. REFERENCES CITED

- Barrie, L.A. 1979a. The concentration and deposition of sulphur compounds and metals around the GCOS oil extraction plant. Pages 186 to 212 in Fanaki et al. Air System Summer Field Study in the AOSERP Study Area, June 1977. Prep. for the Alberta Oil Sands Environmental Research Program by Environment Canada, Atmospheric Environment Service. AOSERP Report 68. 248 pp.
- Barrie, L.A. 1979b. The fate of particulate emissions from an isolated power plant in the oil sands area of western Canada. Annals of New York Academy of Sciences, Vol. 14, Aerosols: Anthropogenic and Natural Sources and Transport (Conference Proceedings).
- Barrie, L.A., V. Nespiak and J. Arnold. 1978. Chemistry of rain in the Athabasca Oil Sands Region: summer 1977. Atmospheric Environment Service Report, ARQT 3-78.
- Barrie, L.A. and J.L. Walmsley. 1978. A study of sulphur dioxide deposition velocities to snow in northern Canada. Atmos. Envir. 12:2321-2332.
- Barrie, L.A. and D.M. Whelpdale. 1978. Background air and precipitation chemistry. Pages 124 to 159 in Fanaki, F. Meteorology and Air Quality Winter Field Study in the AOSERP Study Area, March 1976. Prep. for the Alberta Oil Sands Environmental Research Program by Atmospheric Environment Service. AOSERP Report 27. 249 pp.
- Clough, W.S. 1973. Transport of particles to surfaces. Aerosol Science. 4:227-234.
- Johannessen, M. and A. Henriksen. 1978. Chemistry of snow meltwater: changes in concentration during melting. Water Resources Res. 14(4):615-619.
- Rohlf, F.J., J. Kishpaught and D. Kirk. 1974. NT-SYS numerical taxonomy system of multivariate statistical program. State Univ. of New York at Stony Brook, Stony Brook, New York.
- Shelfentook, W. 1978. An inventory system for atmospheric emissions in the AOSERP study area. Prep. for the Alberta Oil Sands Environmental Research Program by SNC Tottrup Ltd. AOSERP Report 29. 58 pp.
- Summers, P.W. and B. Hitchon. 1973. Source and budget of sulphate in precipitation from central Alberta, Canada. J. Air Poll. Cont. Assoc. 23:194-199.

8. APPENDIX

8.1 THE SPATIAL DISTRIBUTION OF THE MEASURED CONCENTRATION OF SOLUBLE SNOWMELT CONSTITUENTS

Two maps are shown for each constituent: one with isopleths of concentration, one with the measured snowmelt concentration plotted beside each site marker. Maps are given for the following constituents: pH (lab), SO_4^- , Cl^- , NO_3^- , Silicate SiO_2 , NH_4^+ , K^+ , Na^+ , Mg^{++} , Ca^{++} , alkalinity, and soluble Al, V, Fe, and Ni.

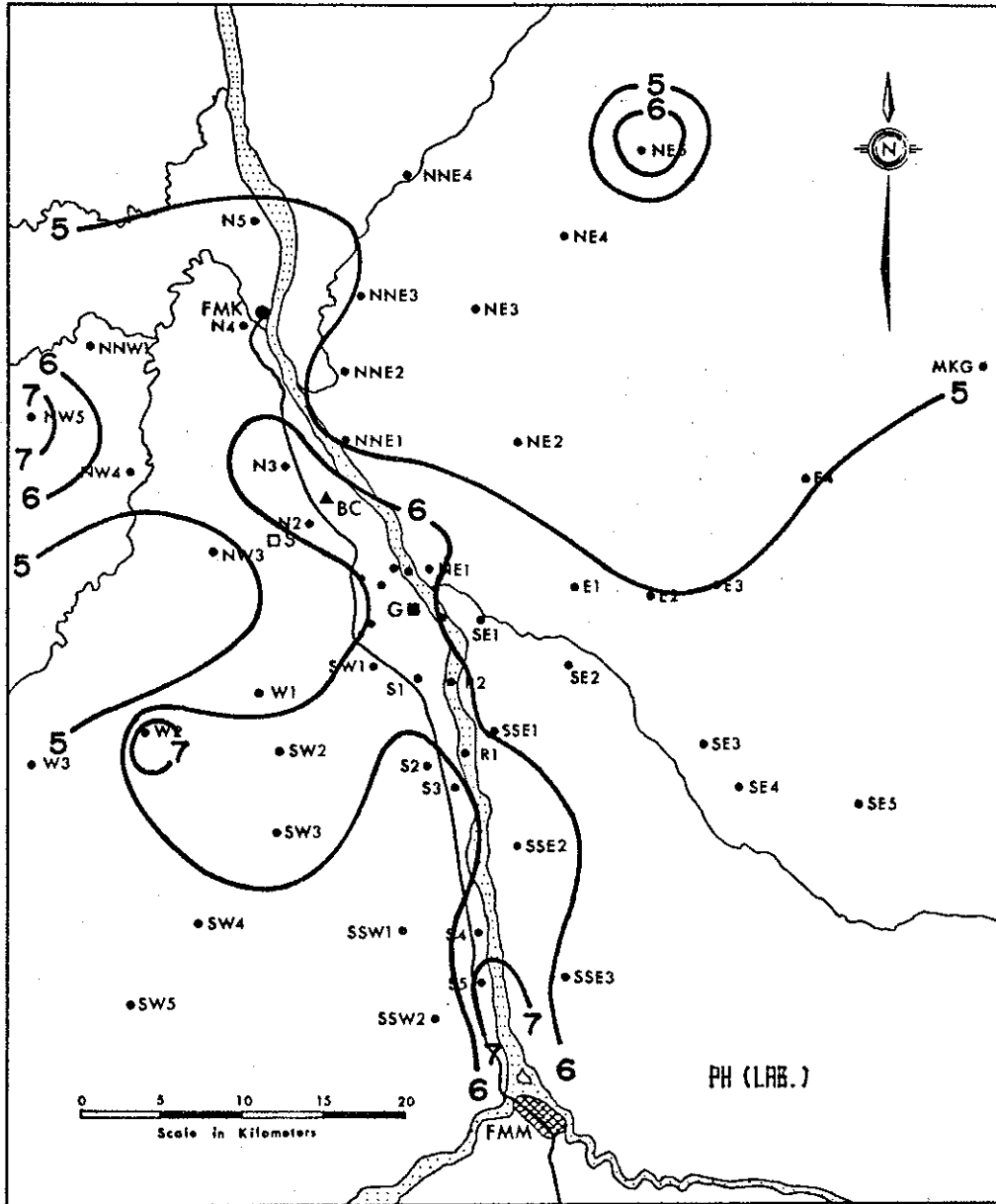


Figure 14. Spatial distribution of laboratory pH measurements.

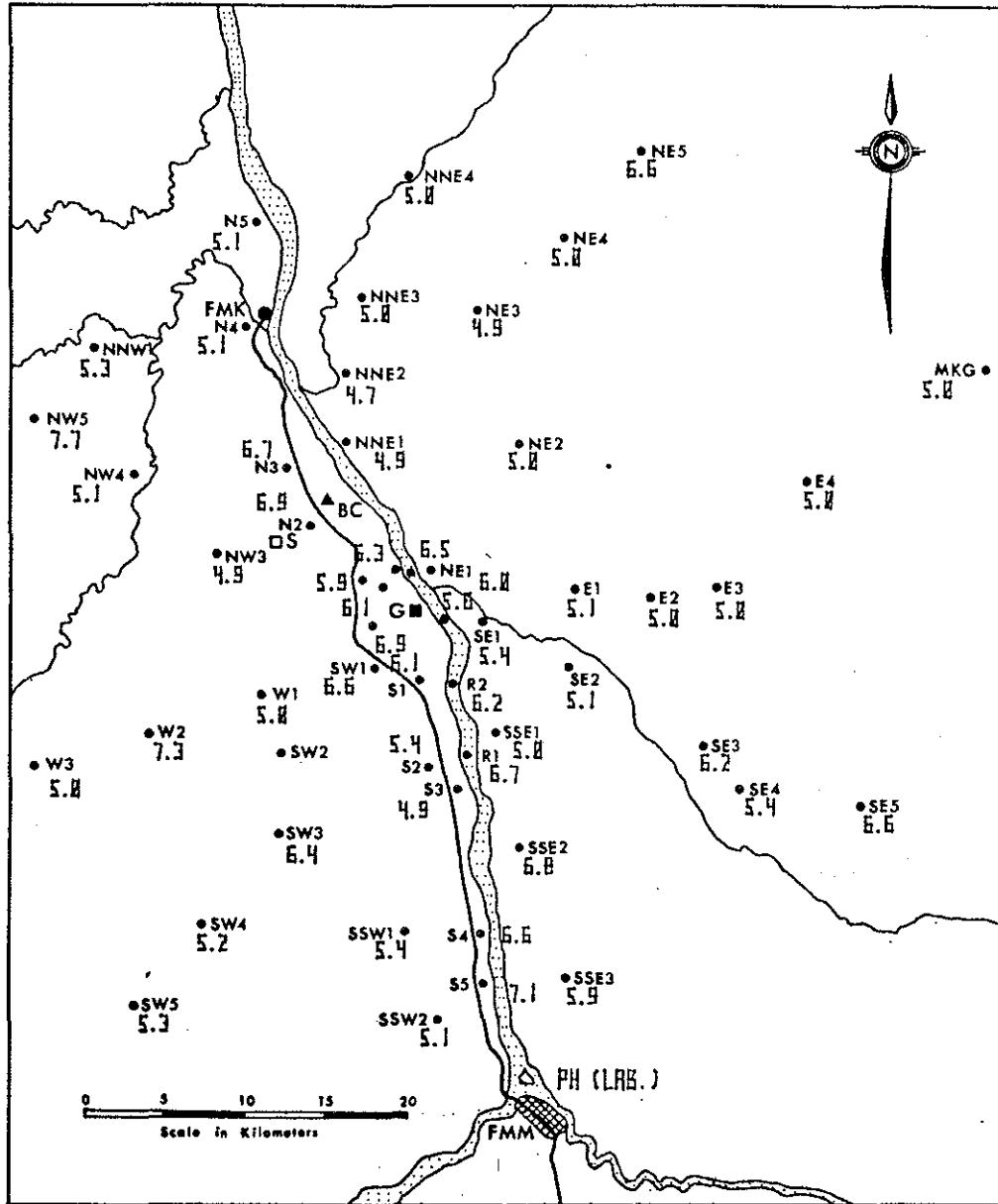


Figure 15. Plotted laboratory pH snowmelt at sampling sites.

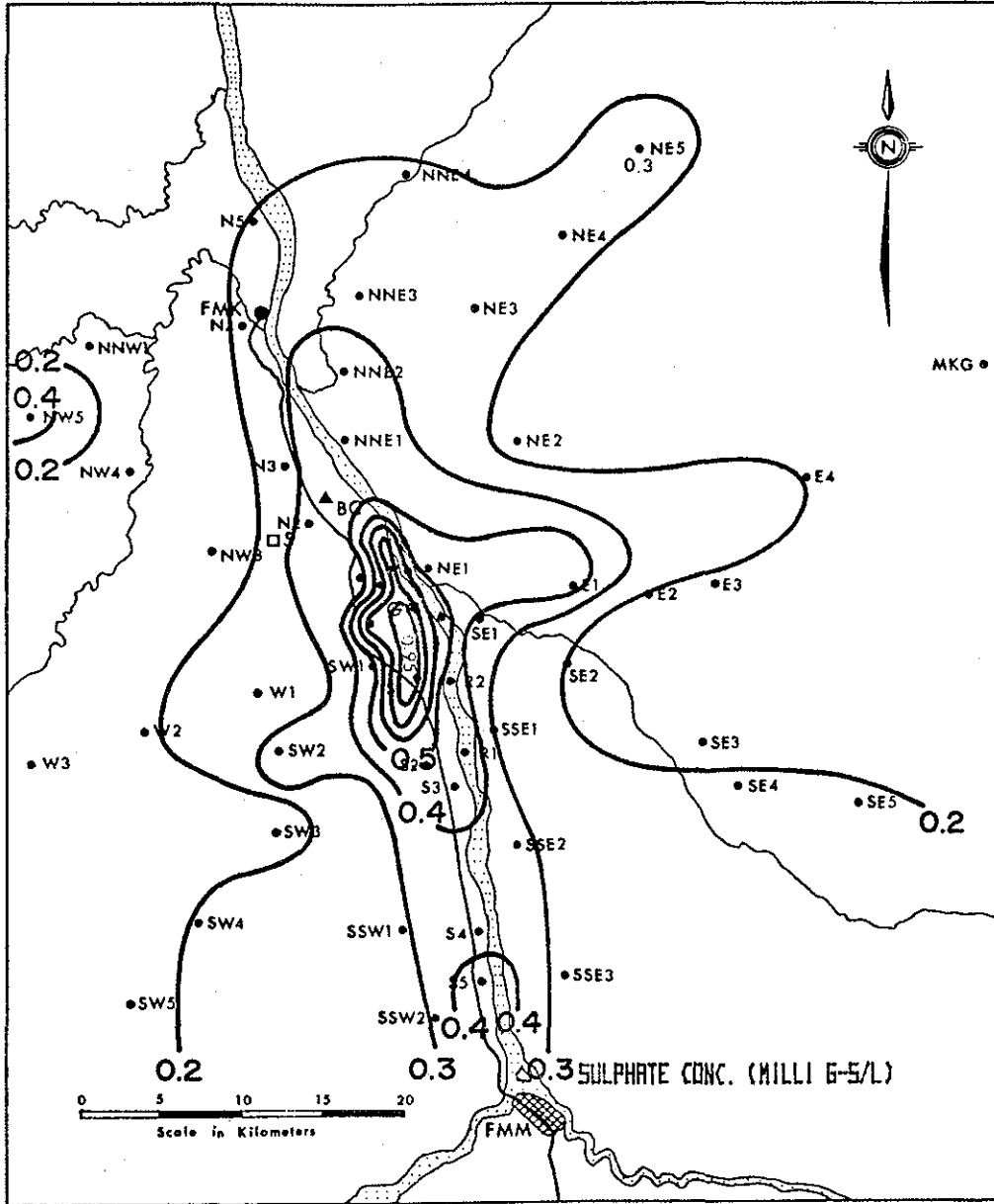


Figure 16. Spatial distribution of SO_4 measurements.

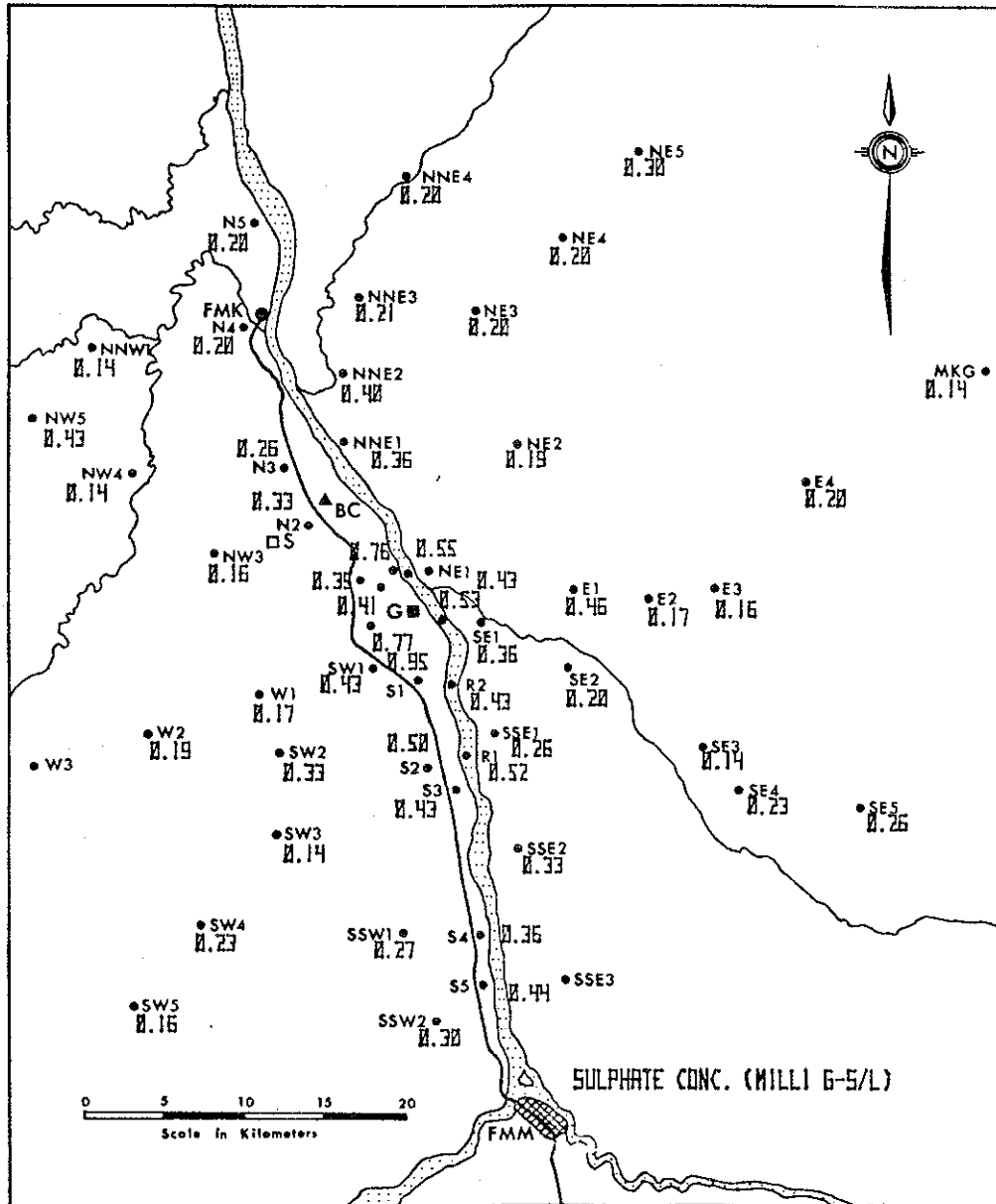


Figure 17. Plotted values of SO_4 from snowmelt at sampling sites.

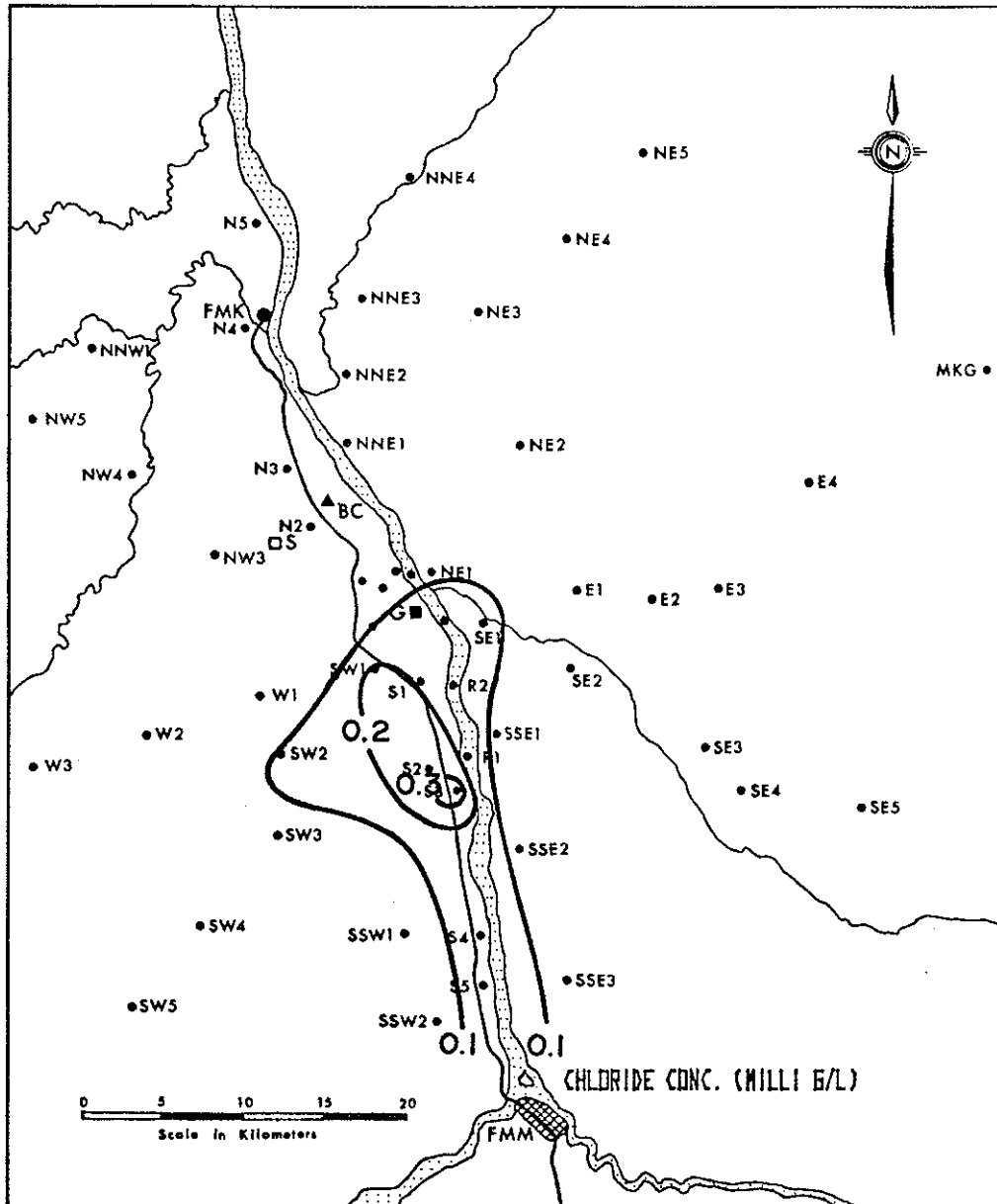


Figure 18. Spatial distribution of Cl^- measurements.

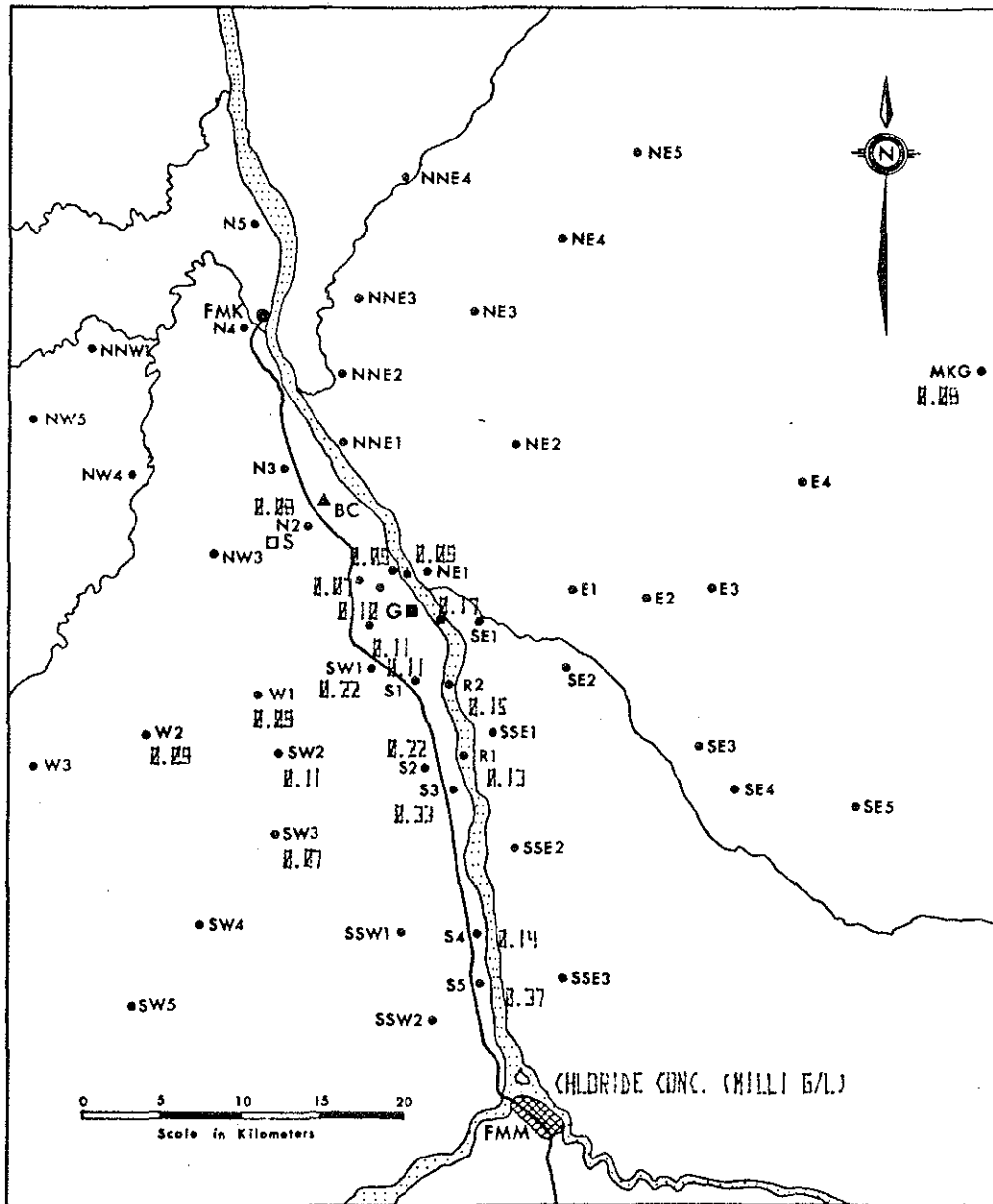


Figure 19. Plotted values of Cl^- from snowmelt at sampling sites.

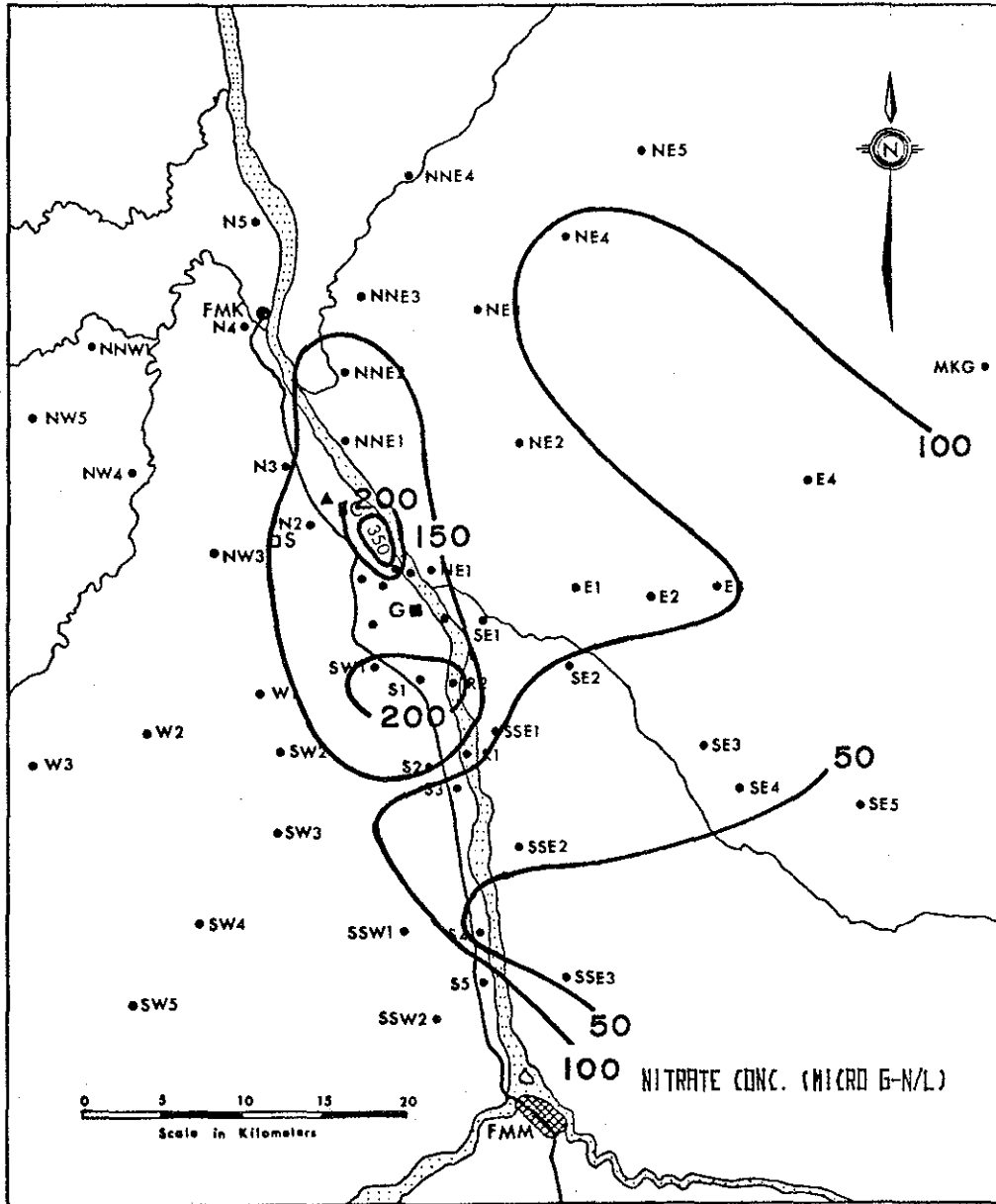


Figure 20. Spatial distribution of NO_3^- measurements.

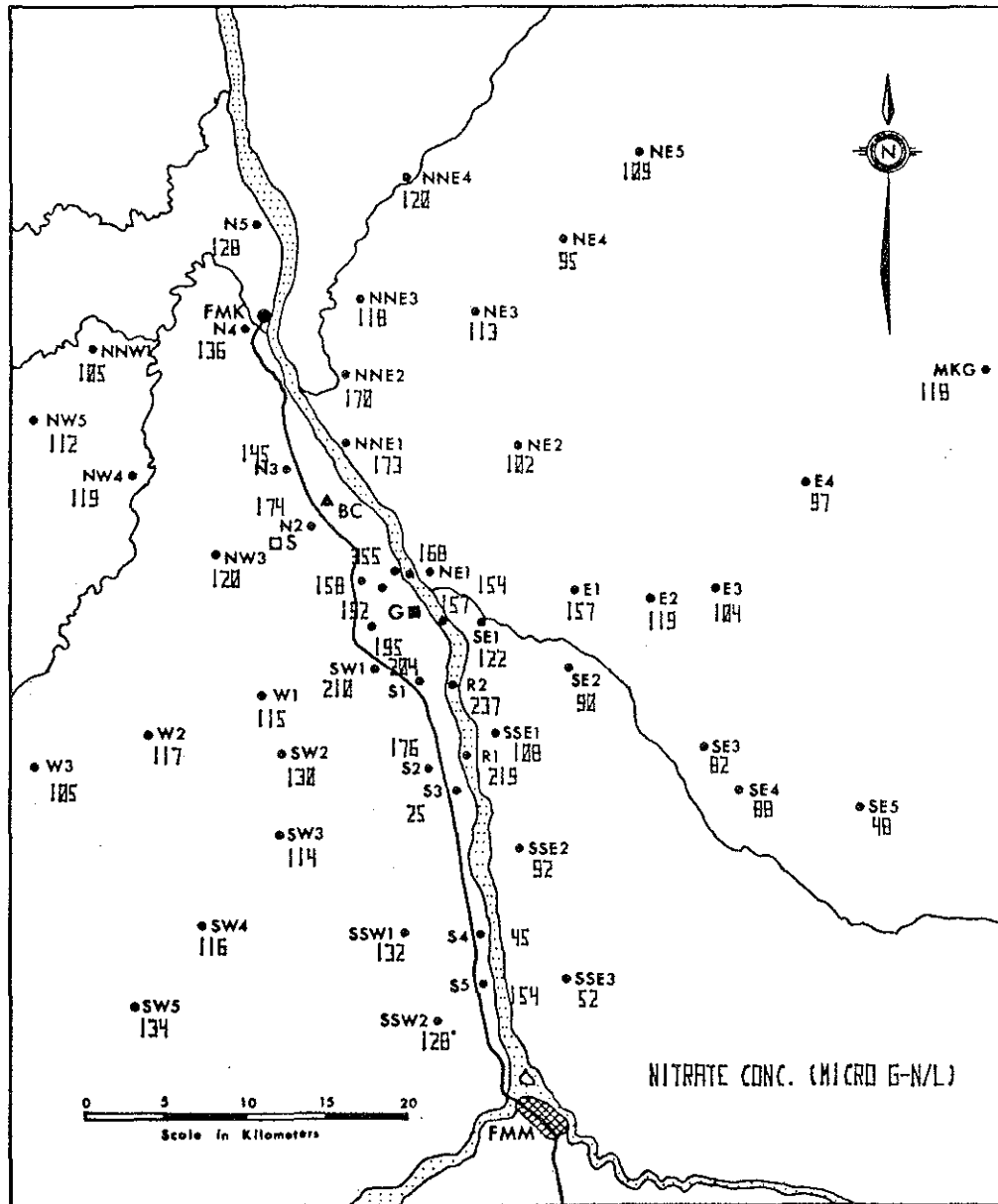


Figure 21. Plotted values of NO_3^- from snowmelt at sampling sites.

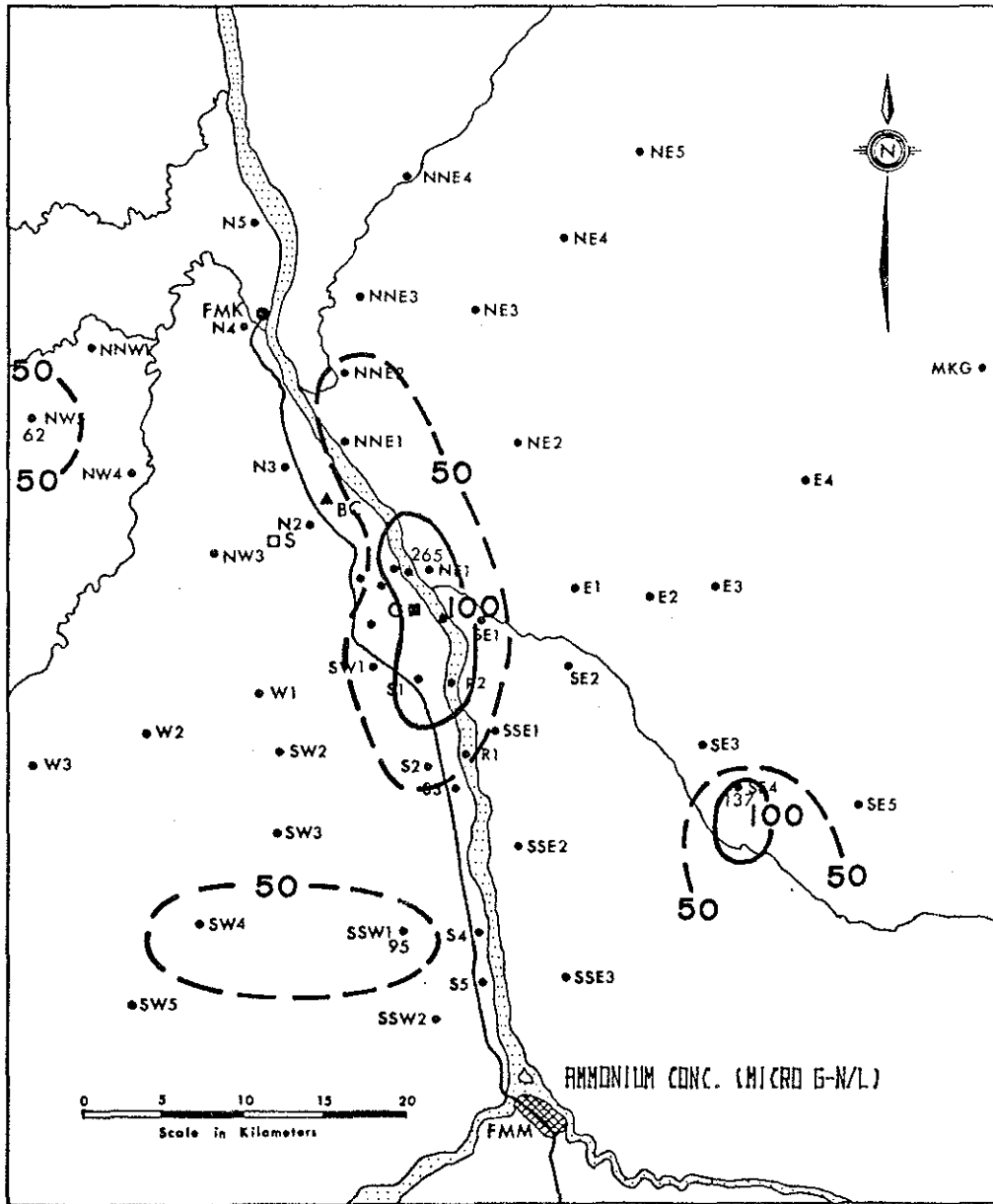


Figure 24. Spatial distribution of NH_4^+ measurements.

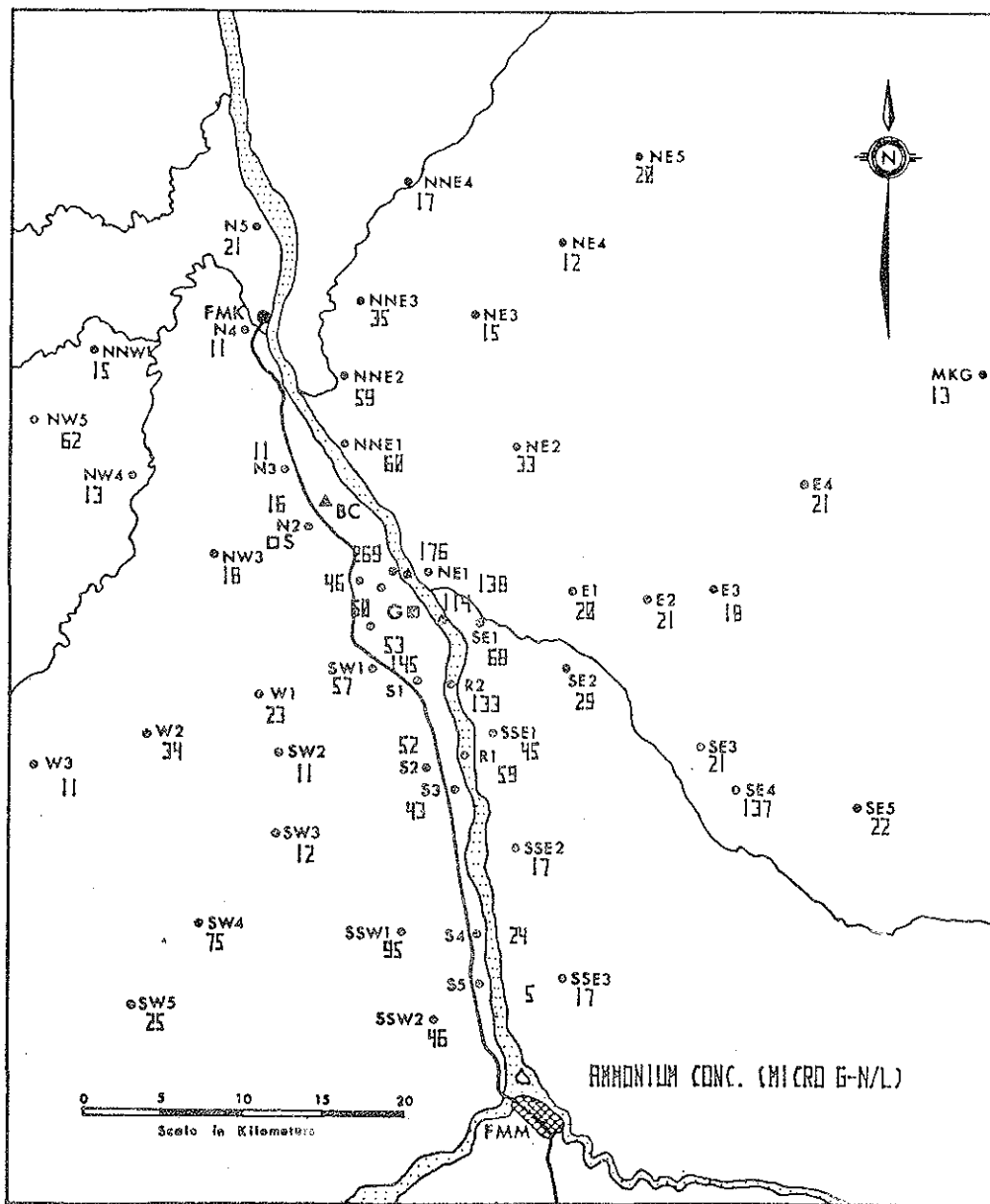


Figure 25. Plotted values of NH_4^+ from snowmelt at sampling sites.

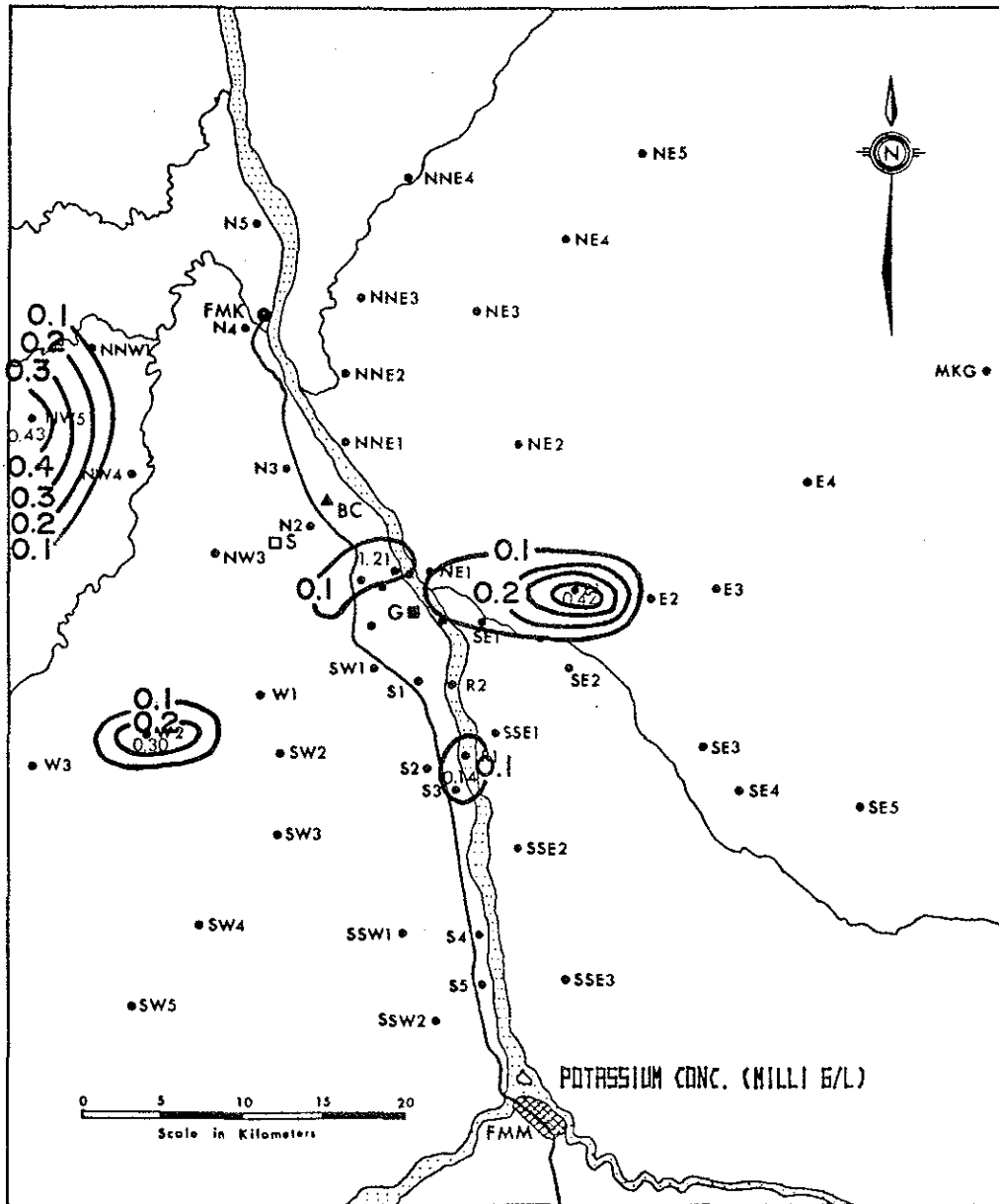


Figure 26. Spatial distribution of K^+ measurements.

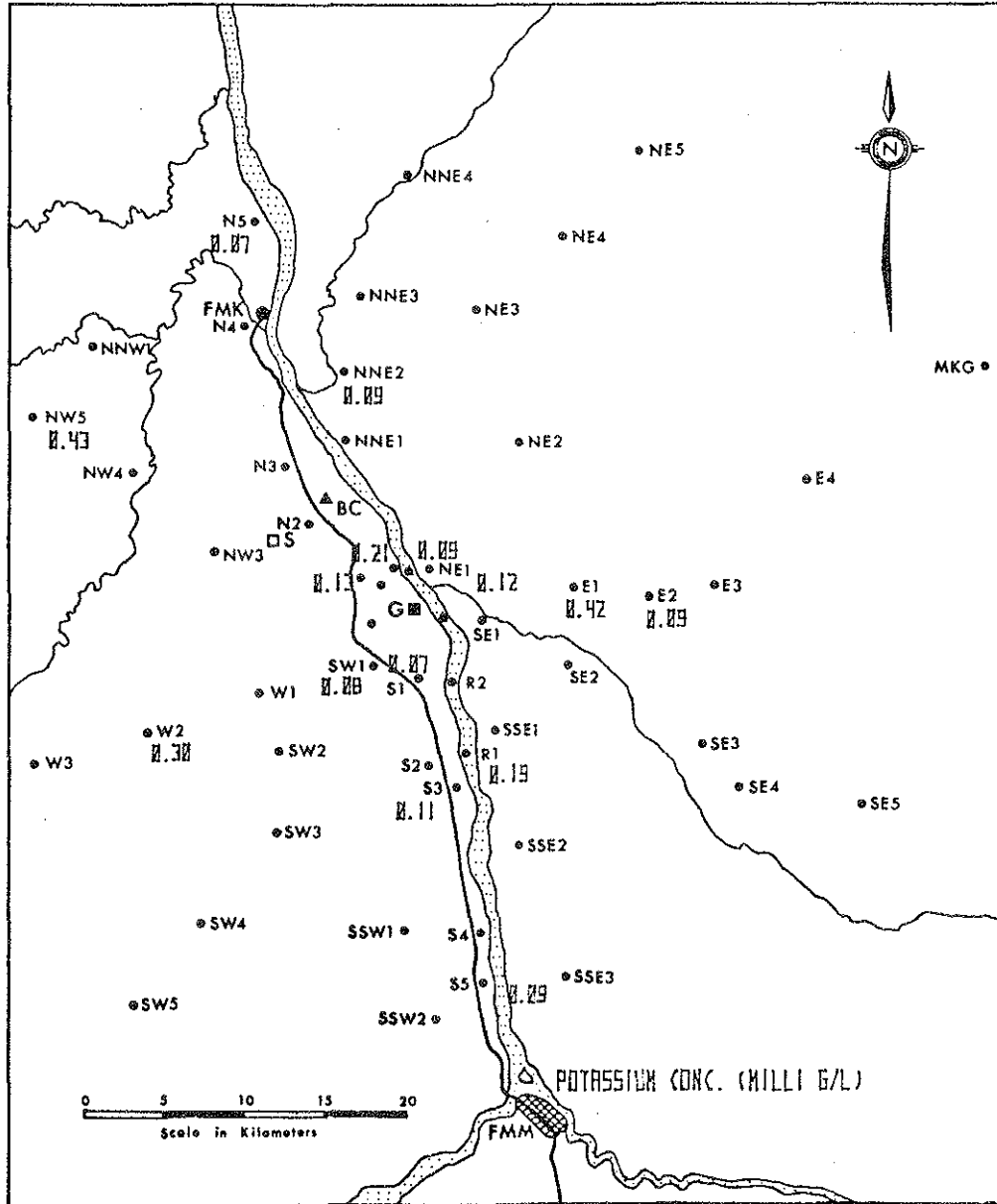


Figure 27. Plotted values of K^+ from snowmelt at sampling sites.

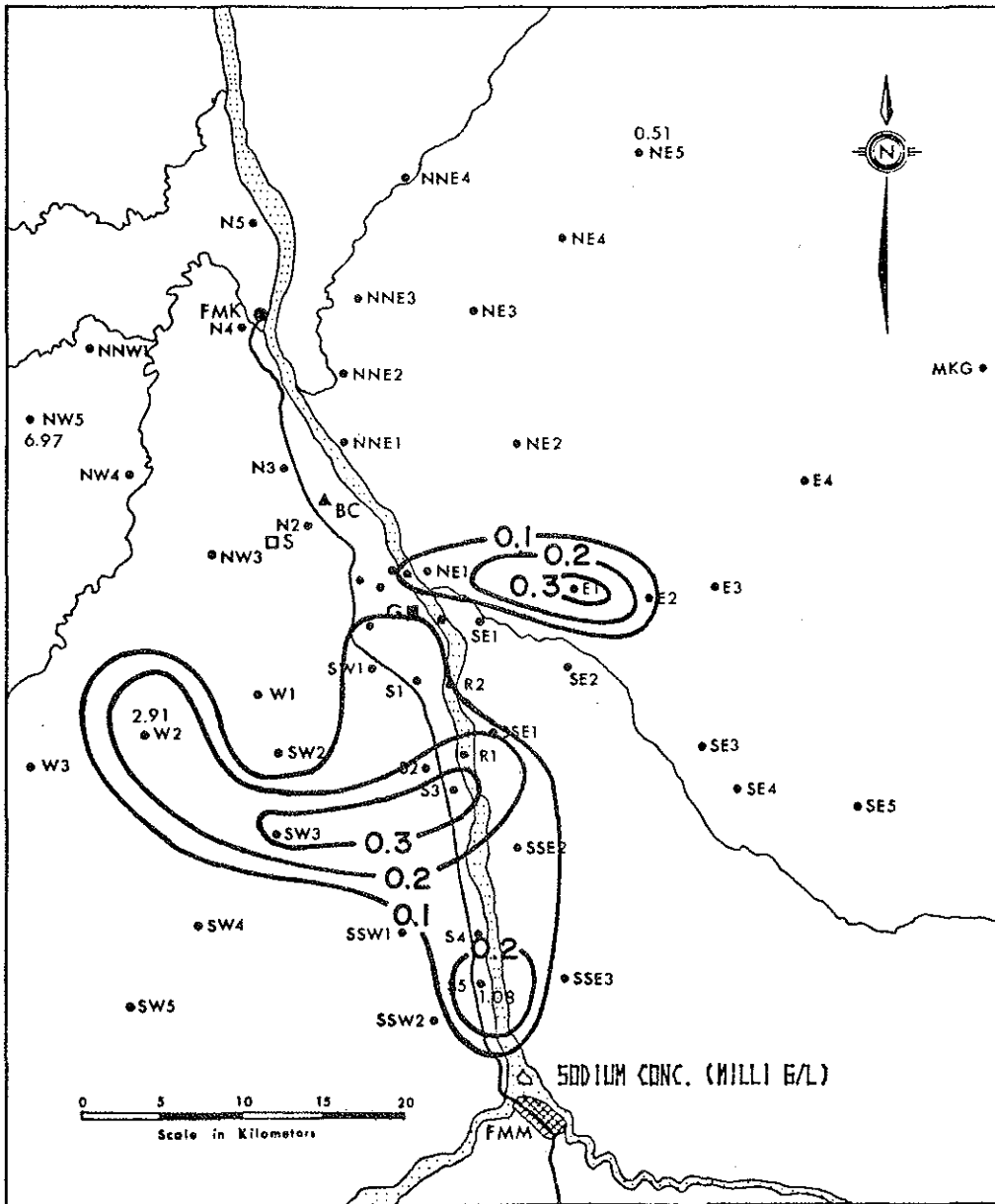


Figure 28. Spatial distribution of Na⁺ measurement.

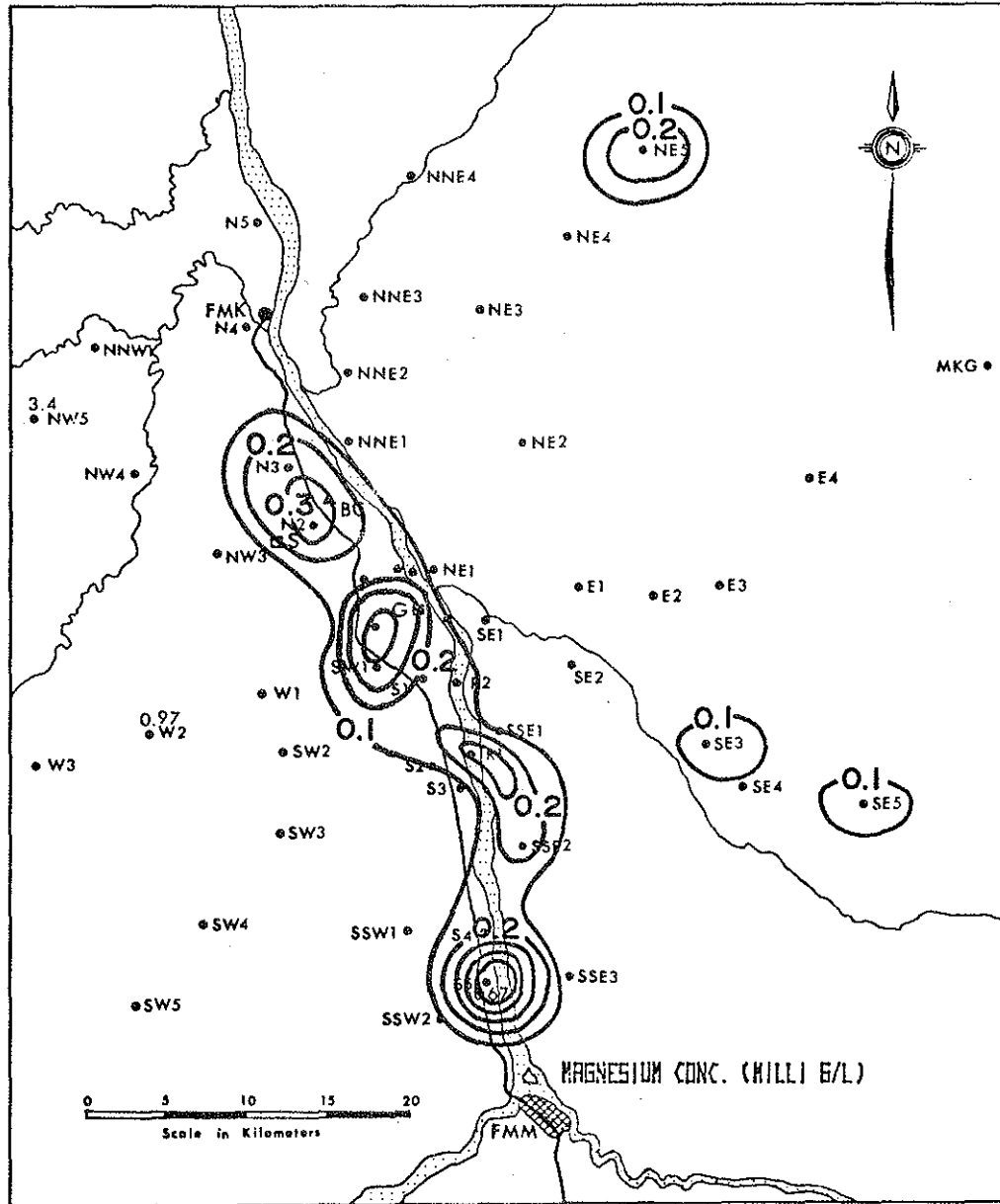
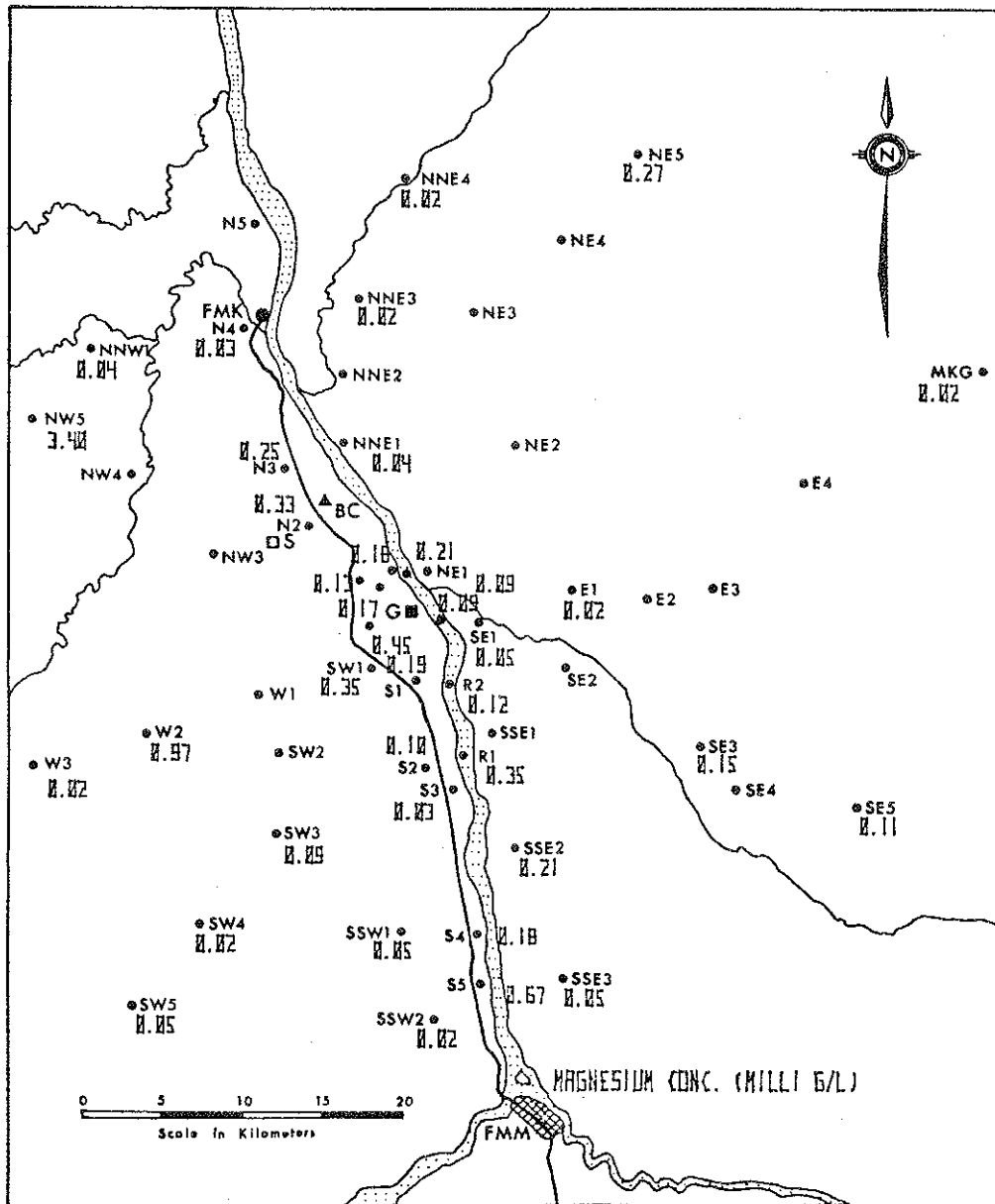


Figure 30. Spatial distribution of Mg^{++} measurements.



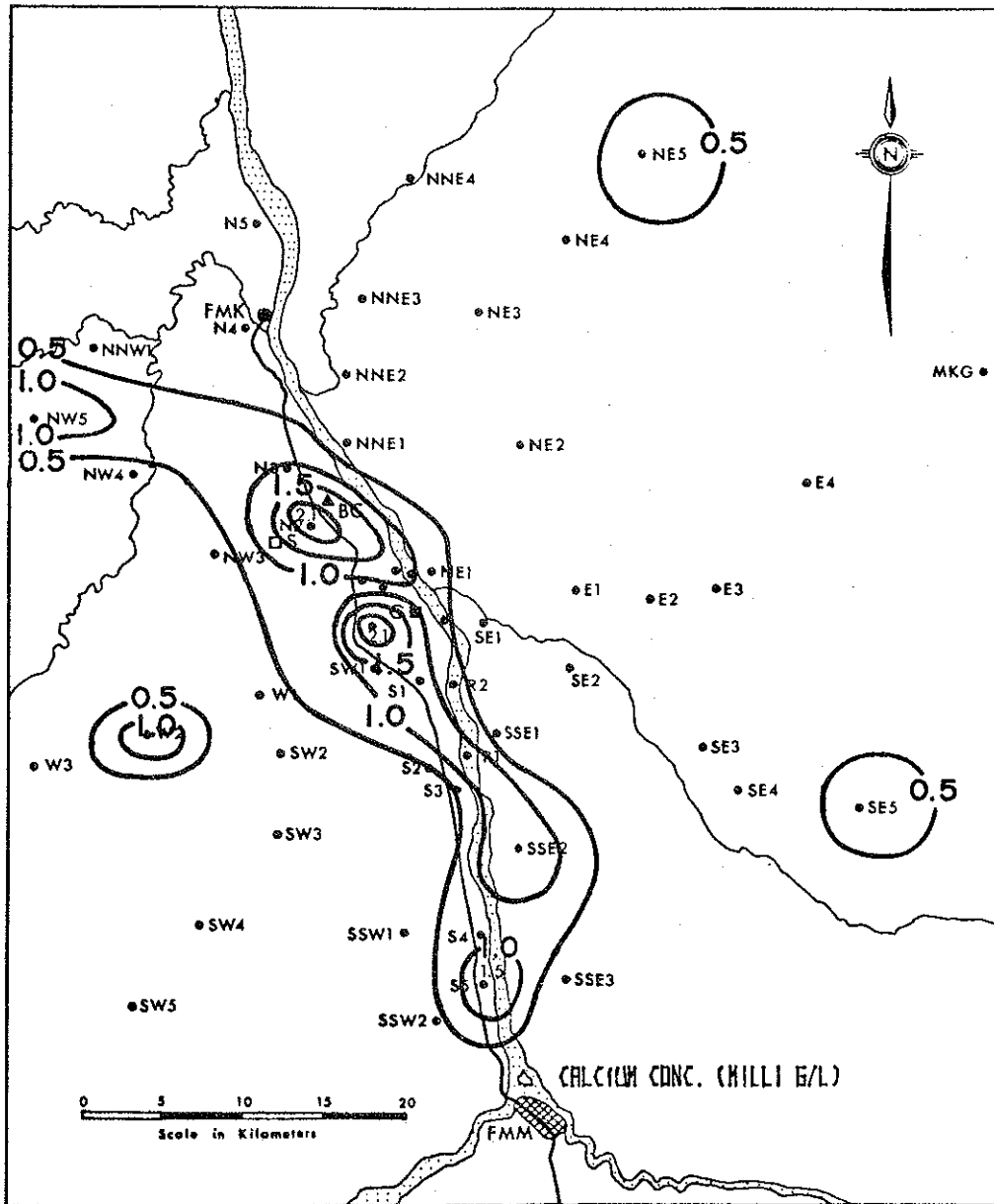


Figure 32. Spatial distribution of Ca⁺⁺ measurements.

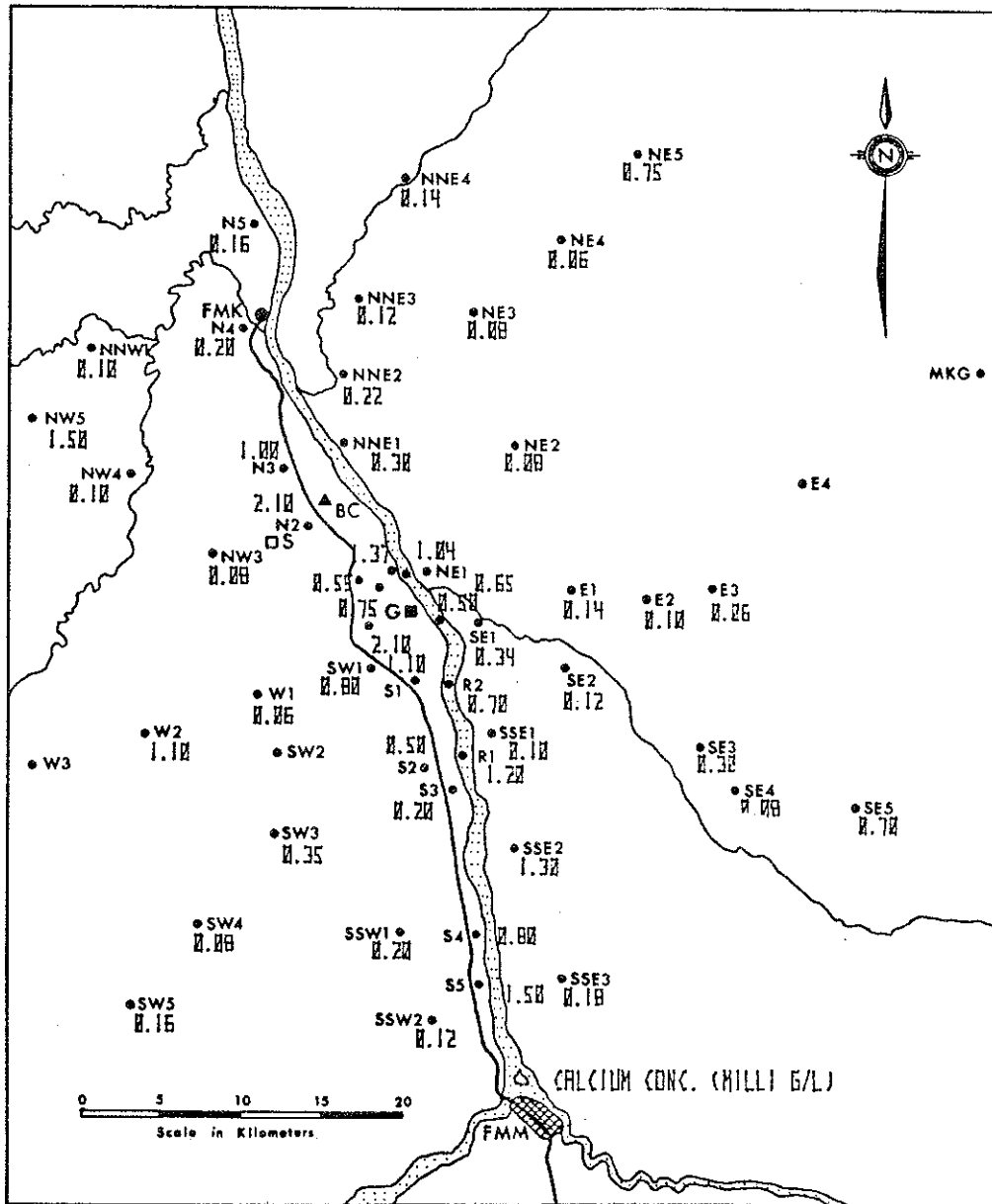


Figure 33. Plotted values of Ca^{++} from snowmelt at sampling sites.

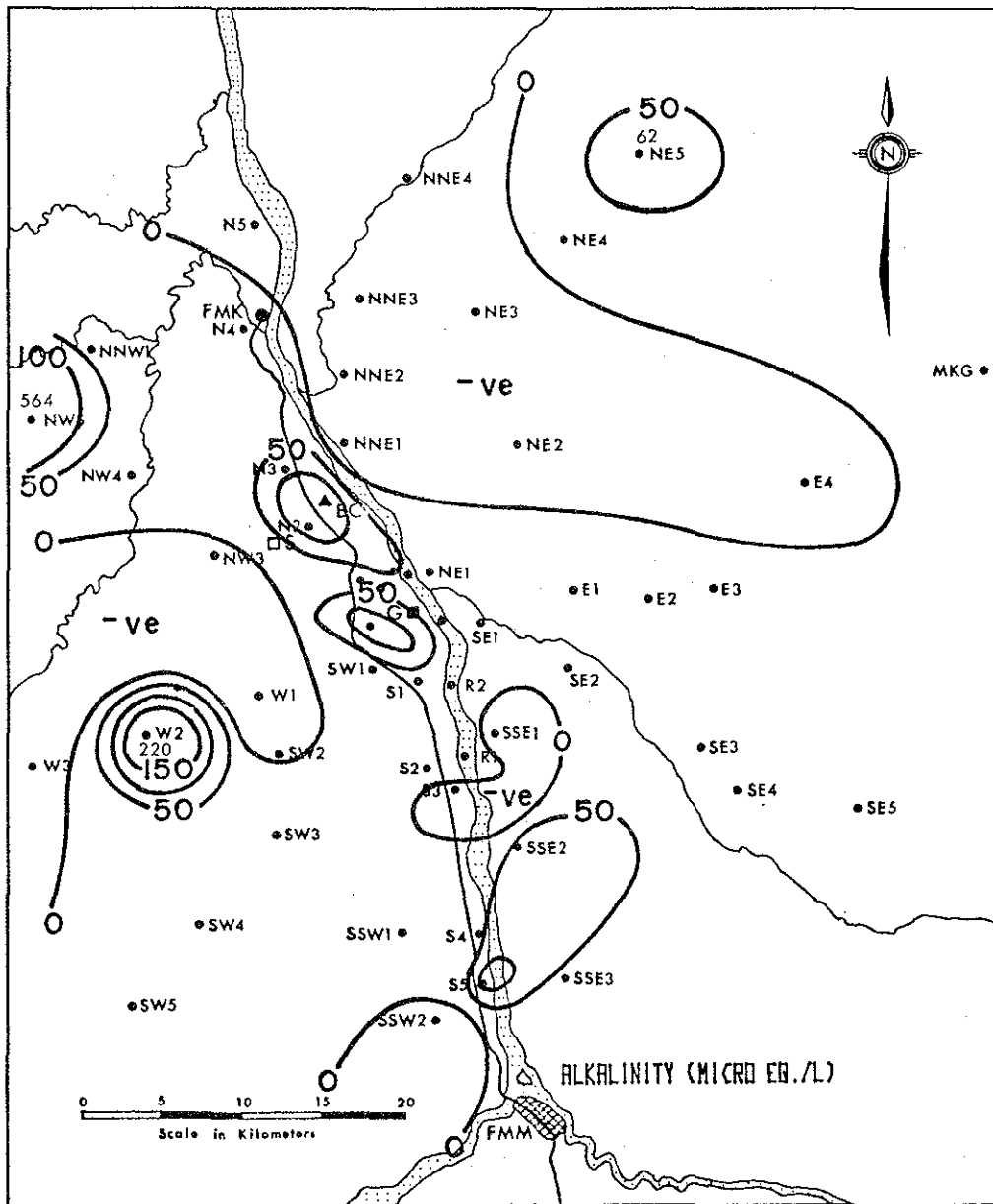


Figure 34. Spatial distribution of alkalinity measurements.

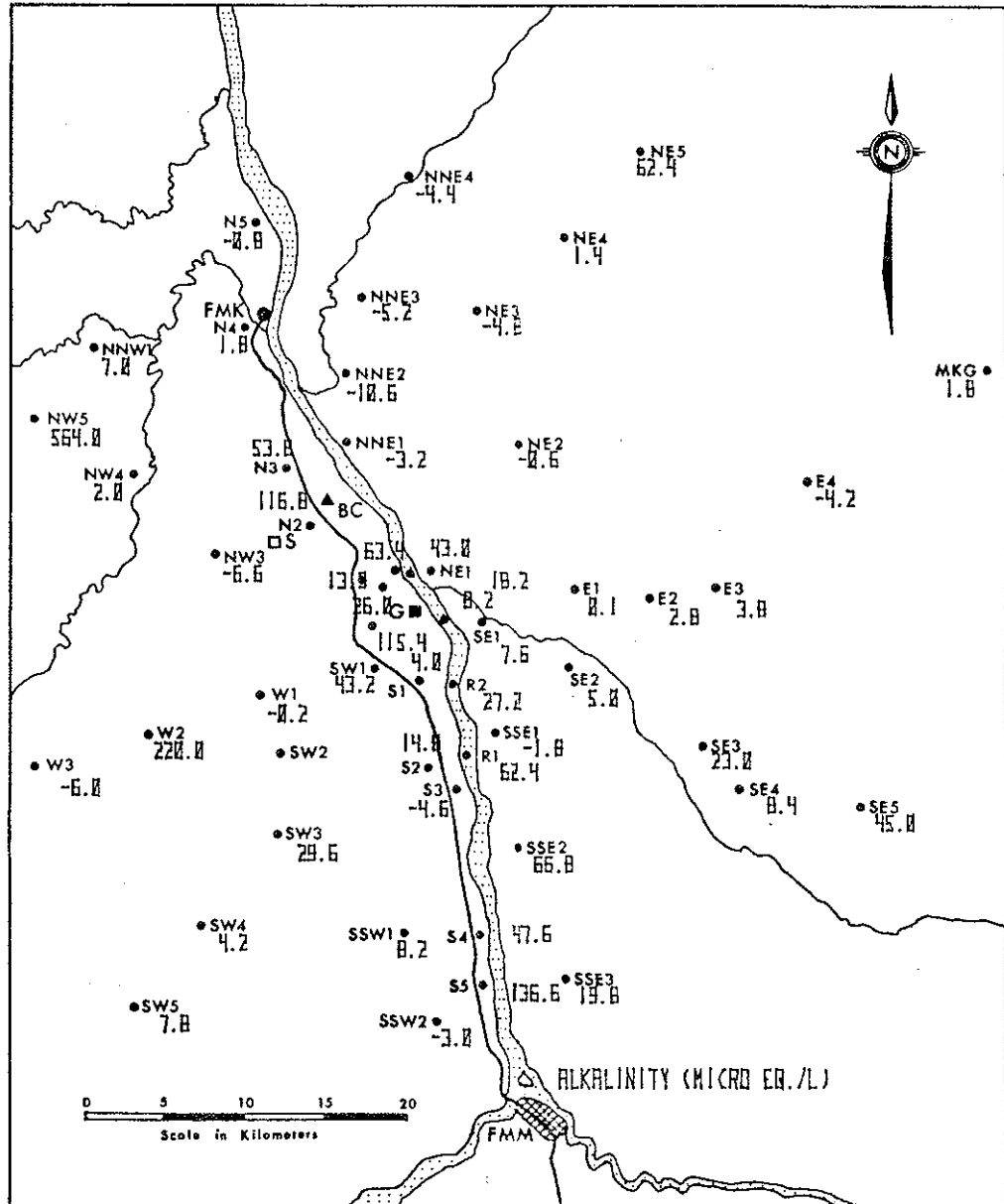


Figure 35. Plotted values of alkalinity at sampling sites.

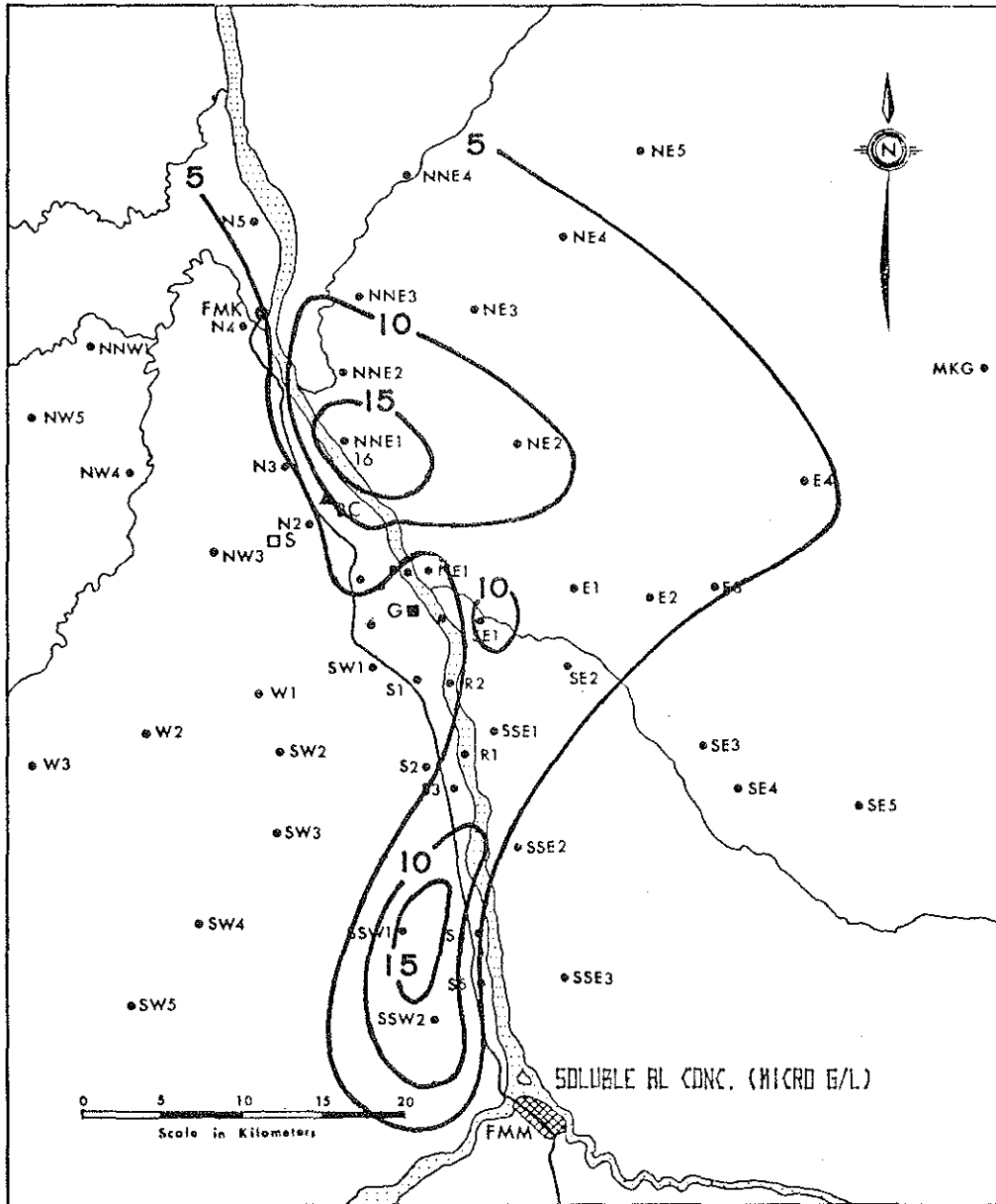


Figure 36. Spatial distribution of soluble aluminum concentration.

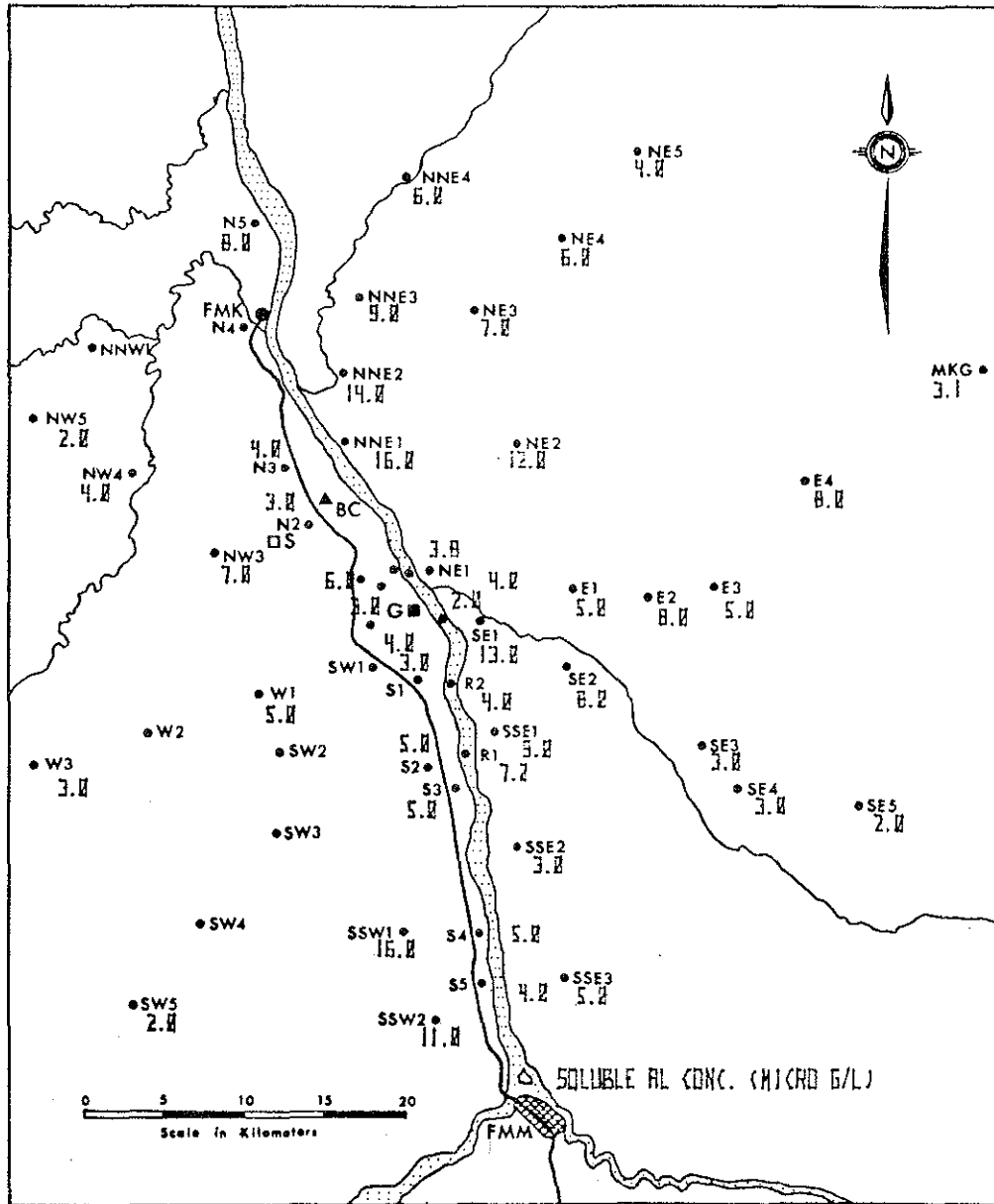


Figure 37. Plotted values of soluble aluminum concentrations at sampling sites.

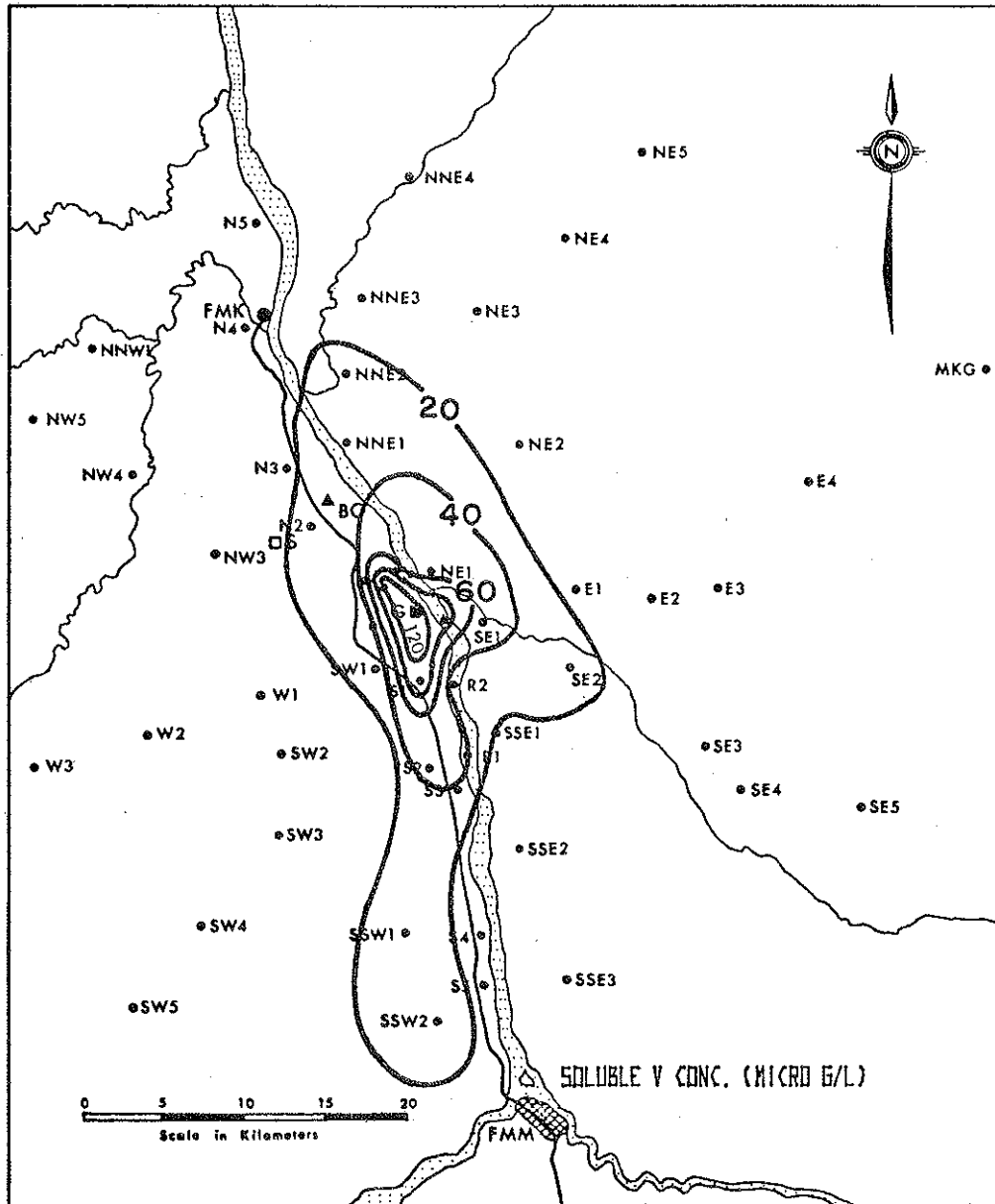


Figure 38. Spatial distribution of soluble vanadium concentration.

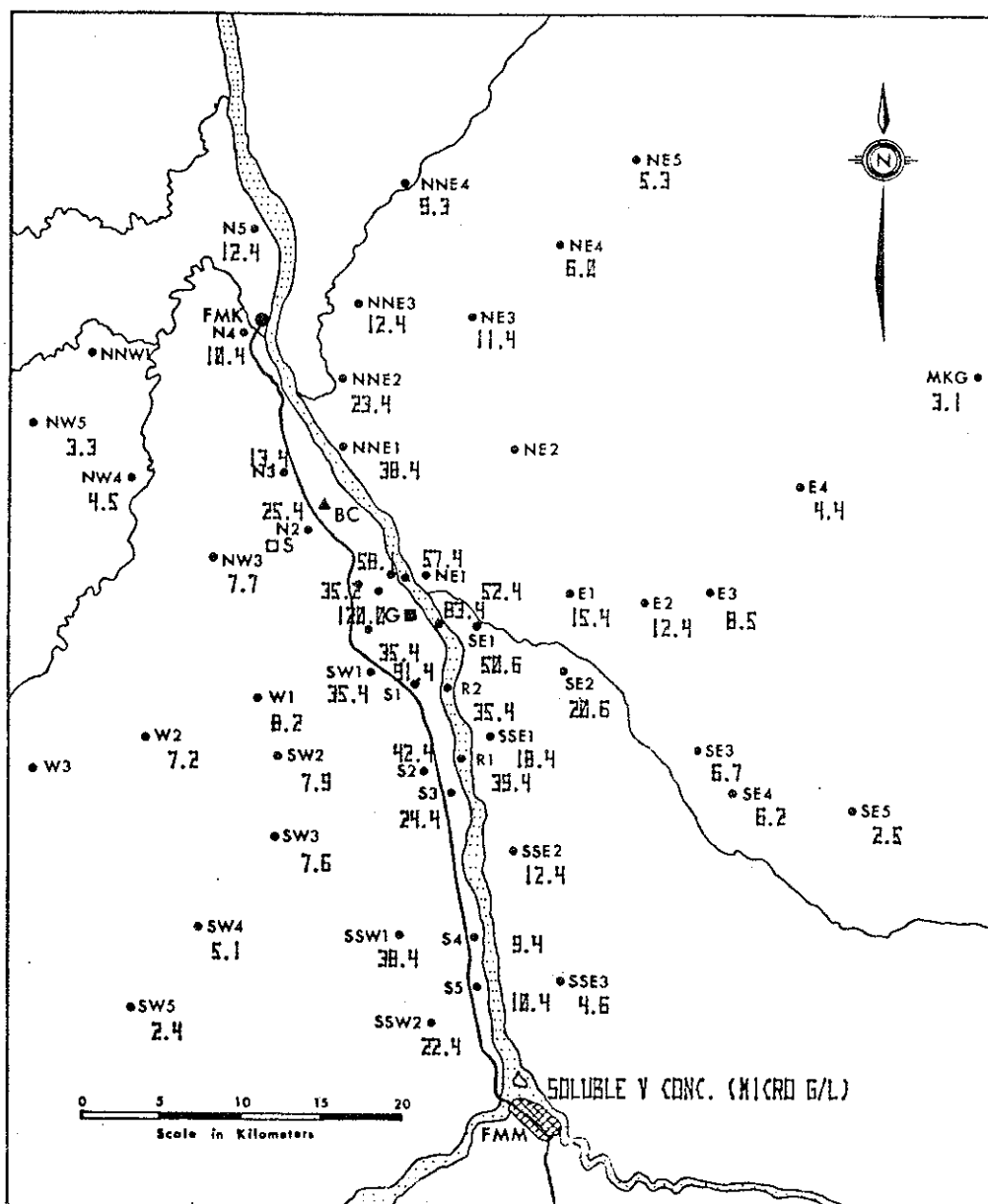


Figure 39. Plotted values of soluble vanadium concentration at sampling sites.

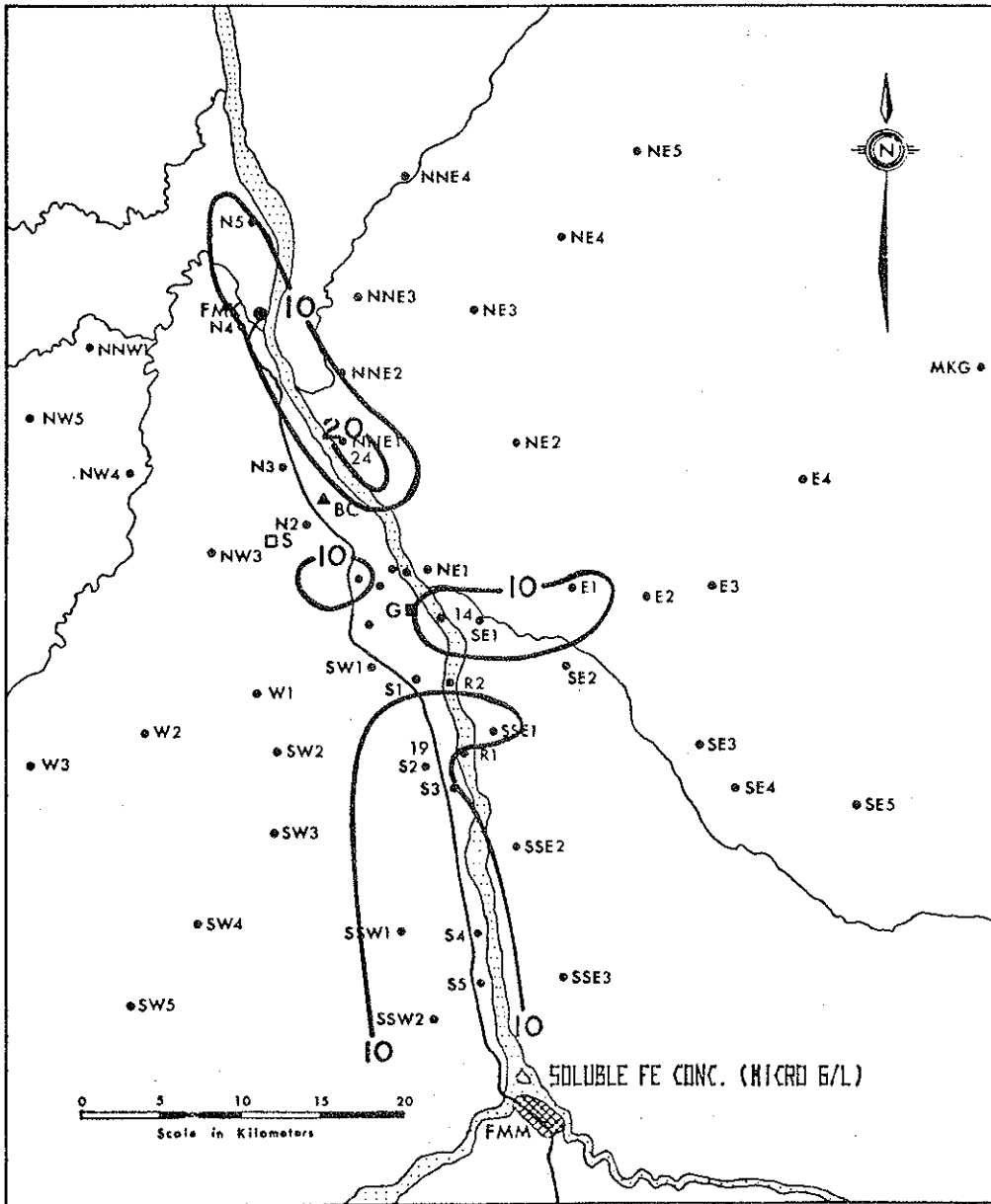


Figure 40. Spatial distribution of soluble iron concentration.

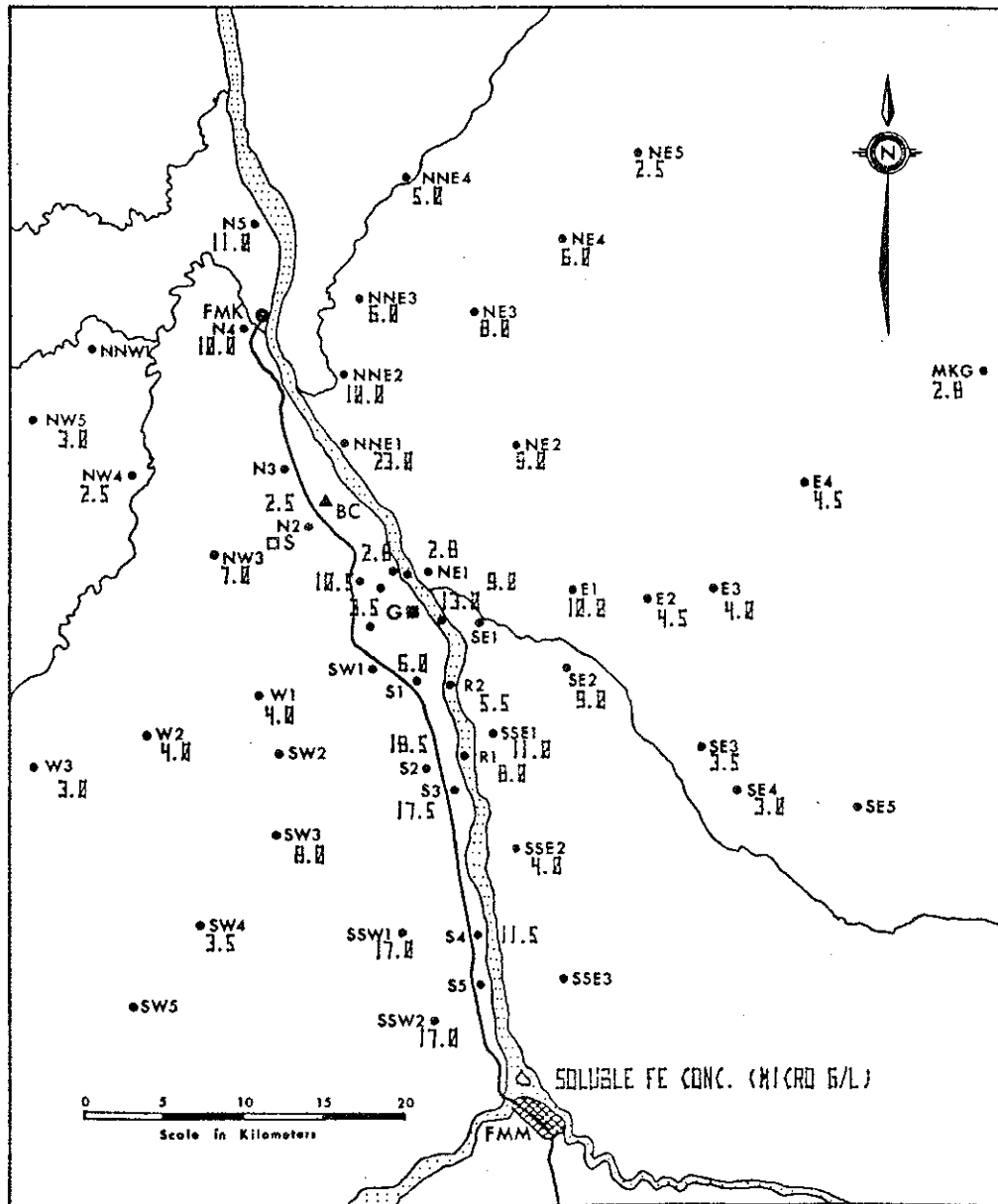


Figure 41. Plotted values of soluble iron concentrations at sampling sites.

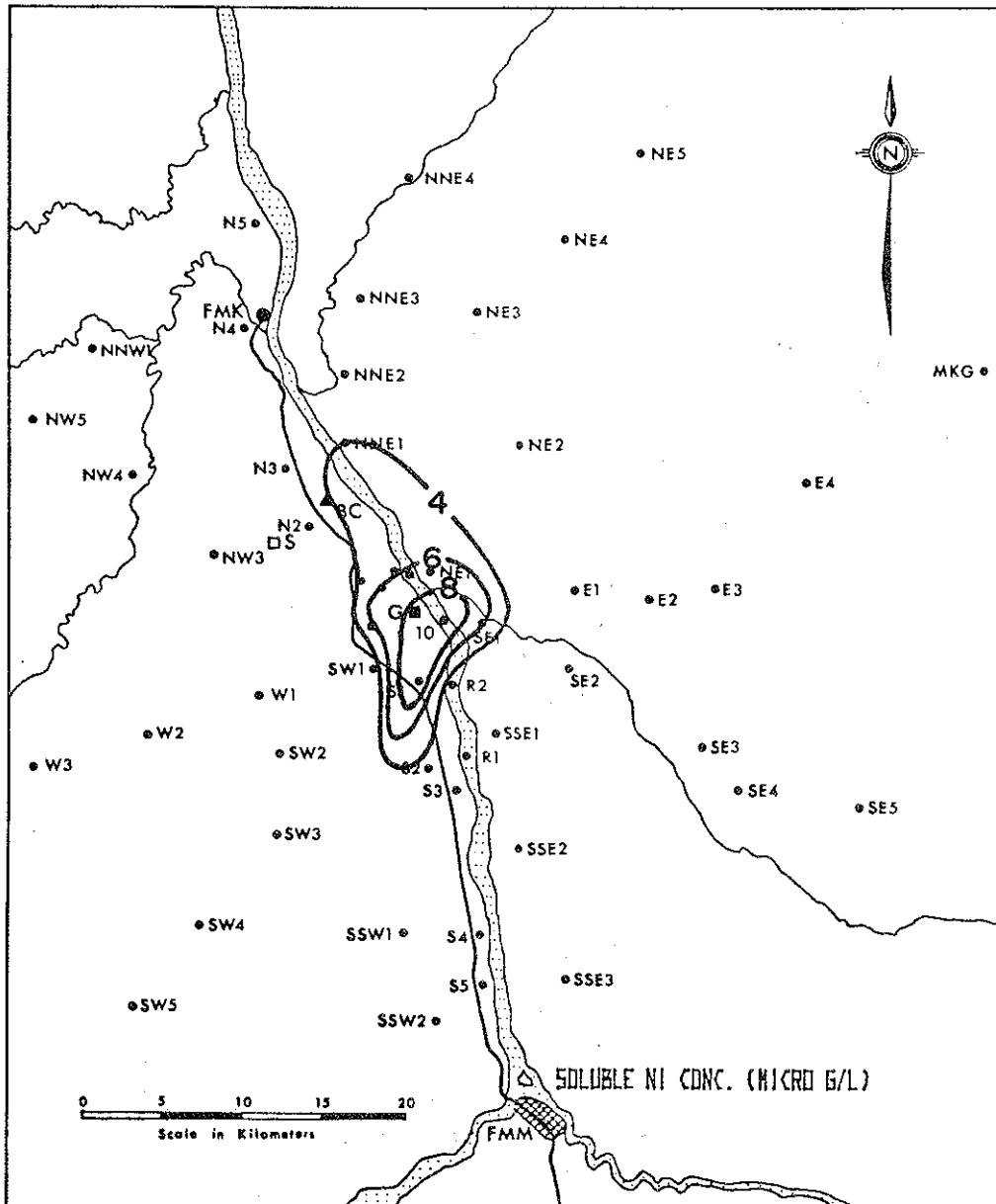


Figure 42. Spatial distribution of soluble nickel concentration.

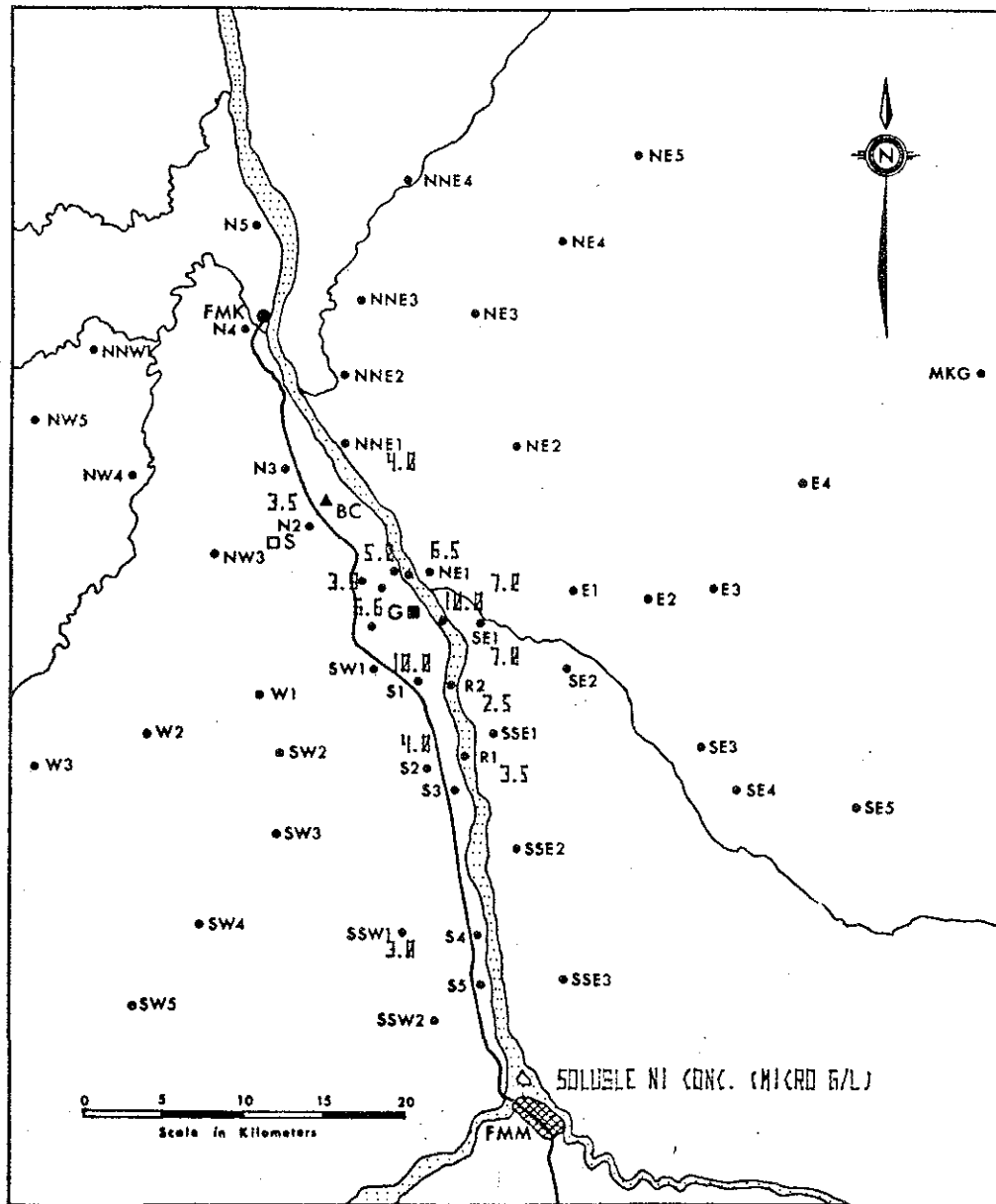


Figure 43. Plotted values of soluble nickel concentrations at sampling sites.

8.2 THE SPATIAL DISTRIBUTION OF MEASURED SNOWPACK LOADINGS
OF MAJOR IONS

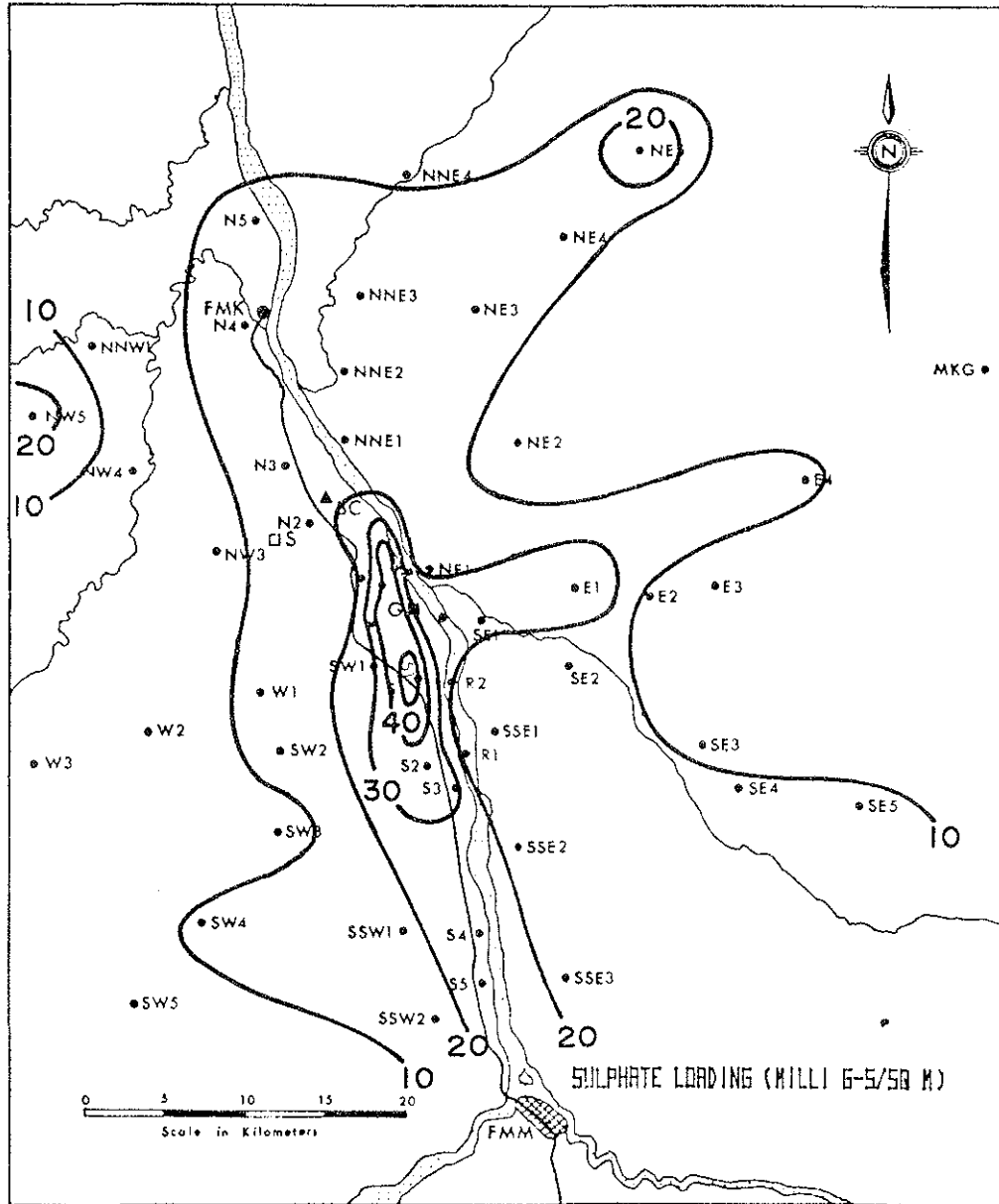


Figure 44. Spatial distribution of SO_4 snowpack loading.

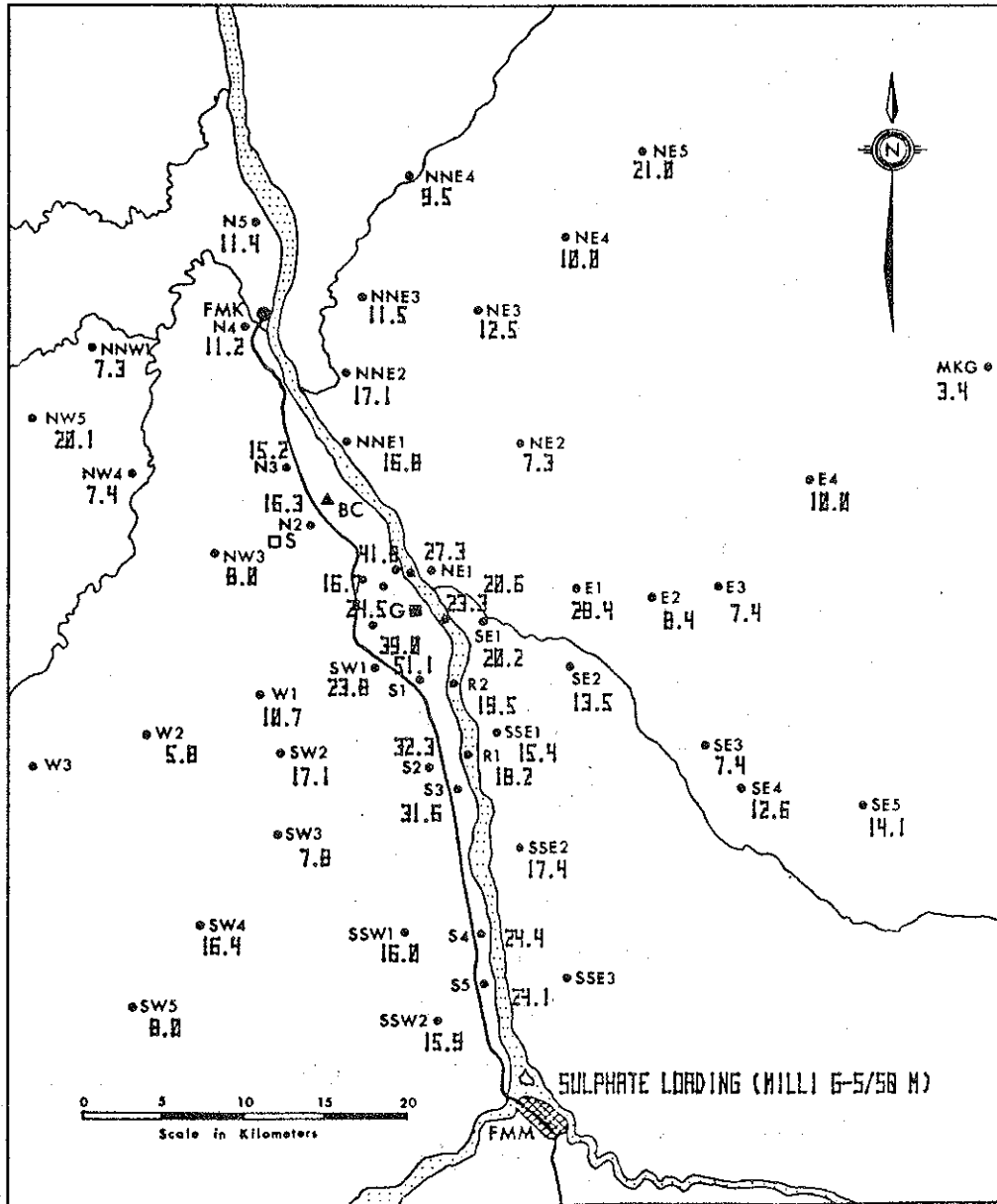


Figure 45. Plotted values of $\text{SO}_4^{=}$ snowpack loading at sampling sites.

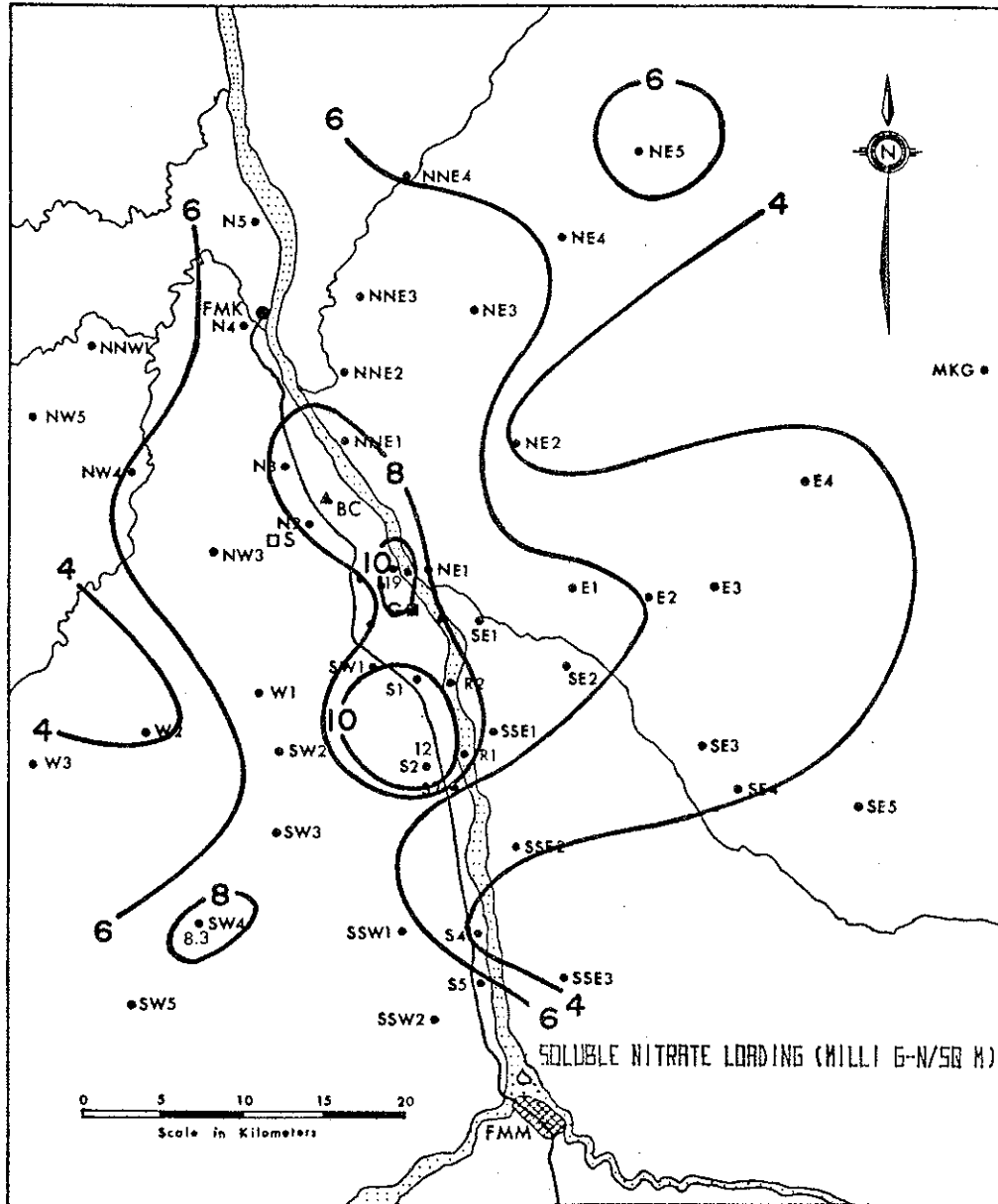


Figure 46. Spatial distribution of NO_3^- snowpack loading.

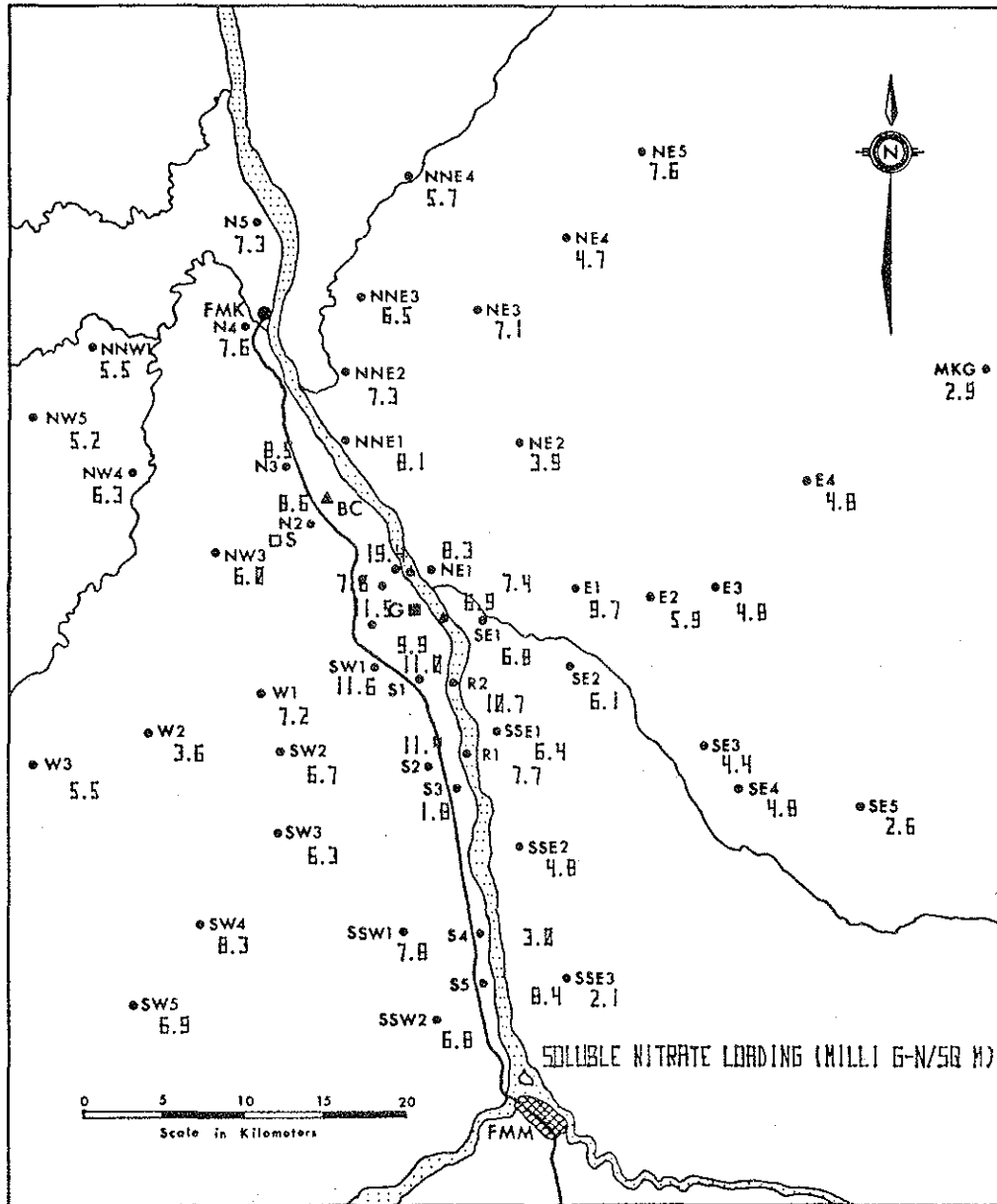


Figure 47. Plotted values of NO_3^- snowpack loading at sampling sites.

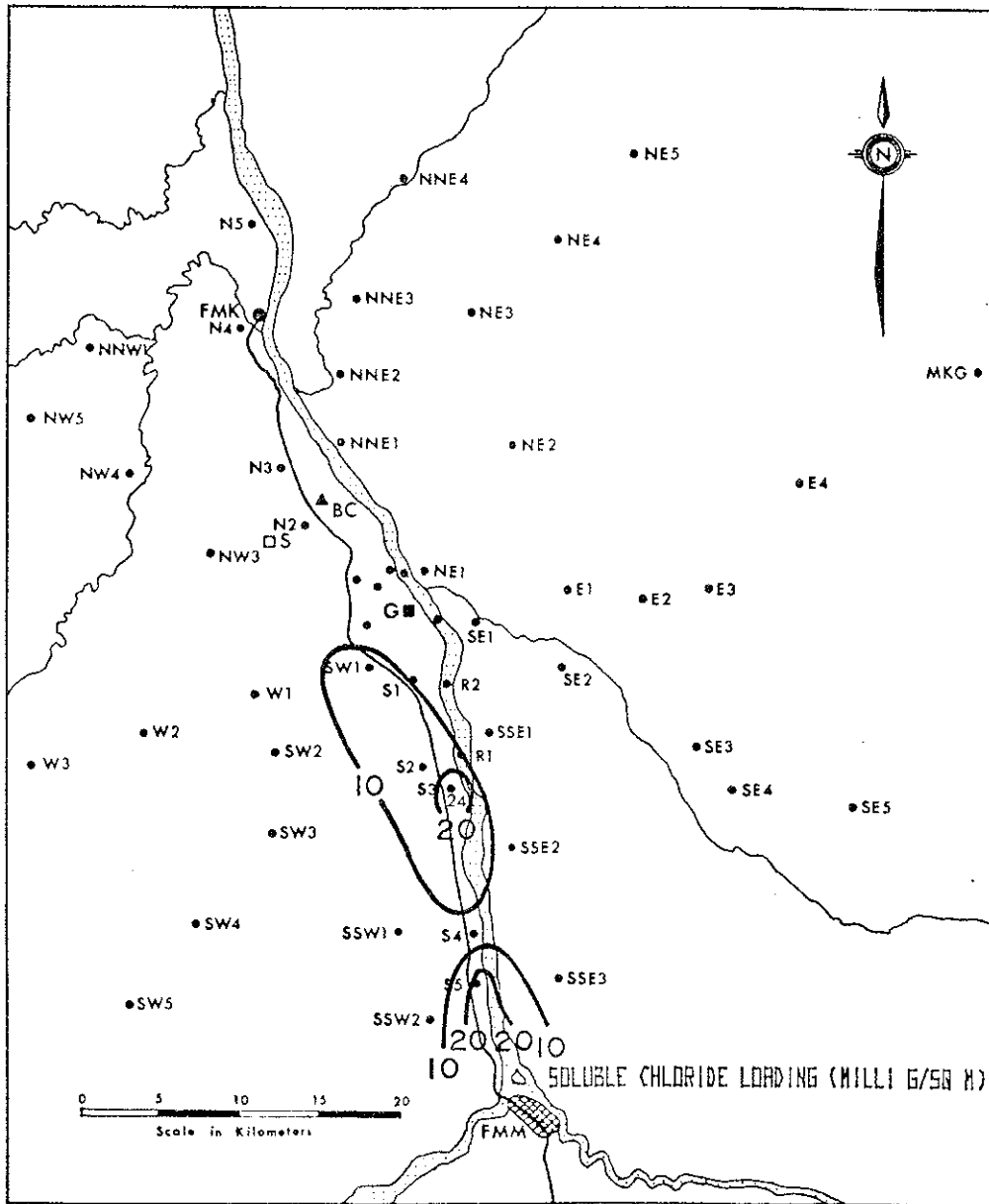


Figure 48. Spatial distribution of Cl^- snowpack loading.

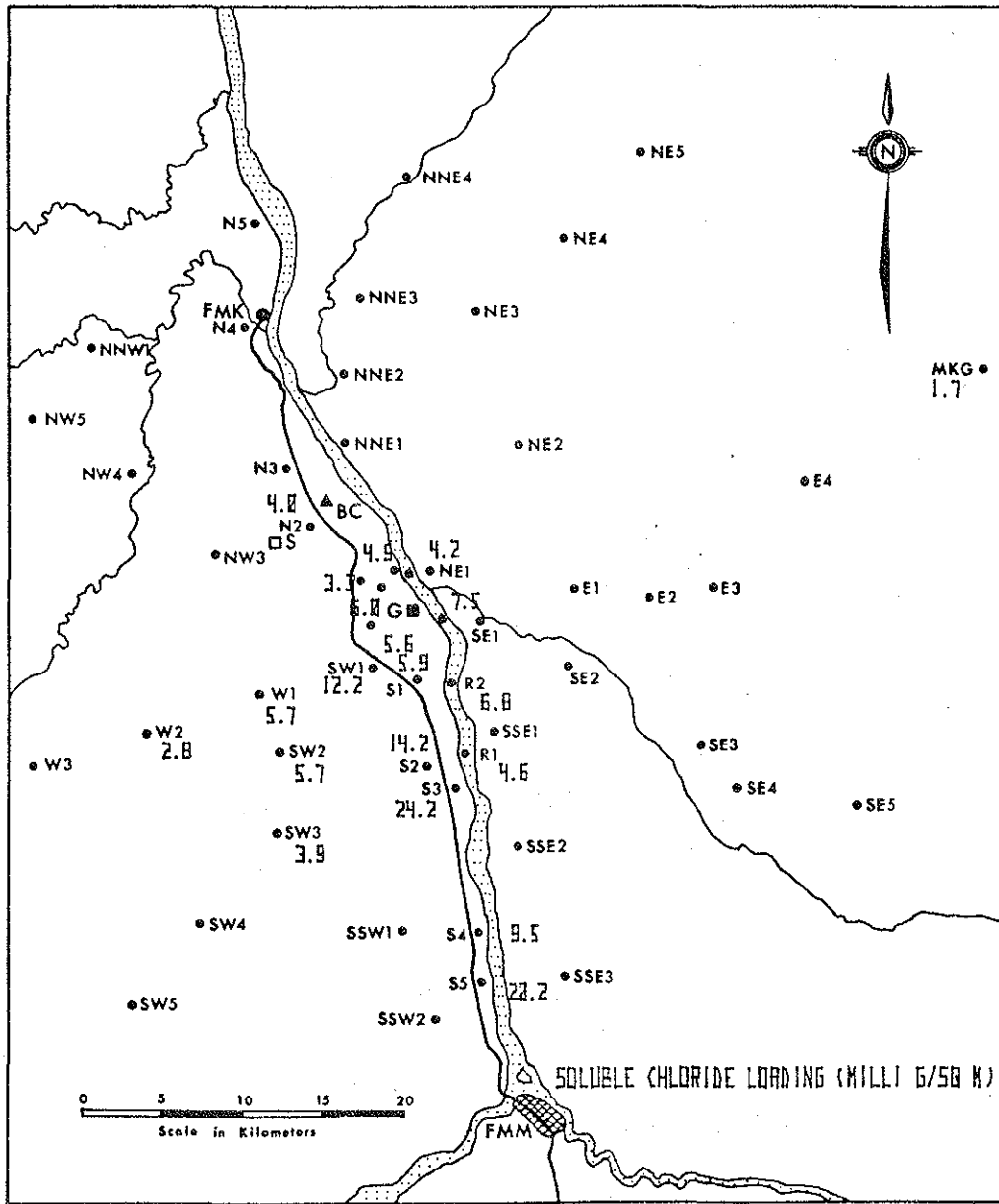


Figure 49. Plotted values of Cl^- snowpack loading at sampling sites.

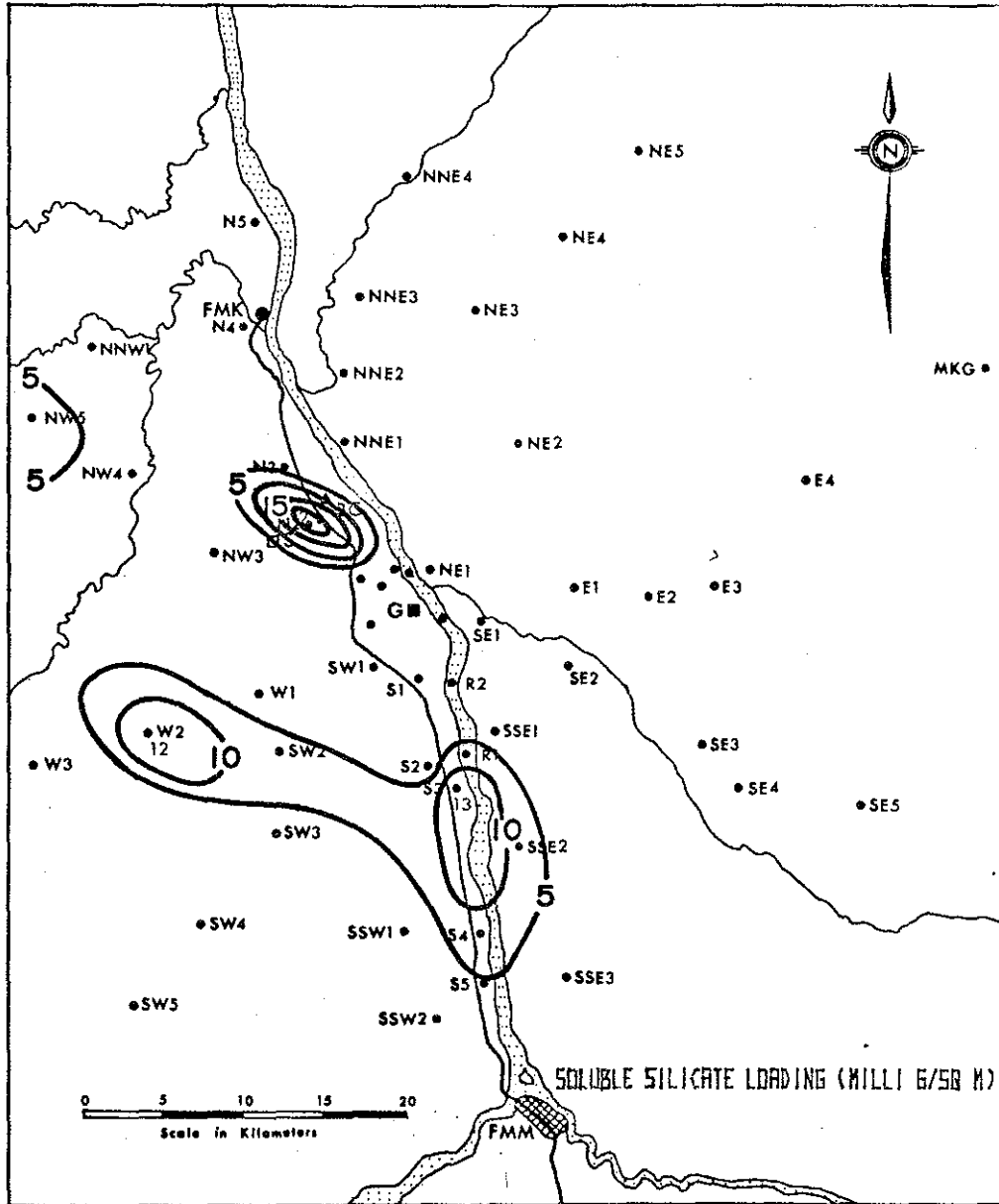


Figure 50. Spatial distribution of silicate snowpack loading.

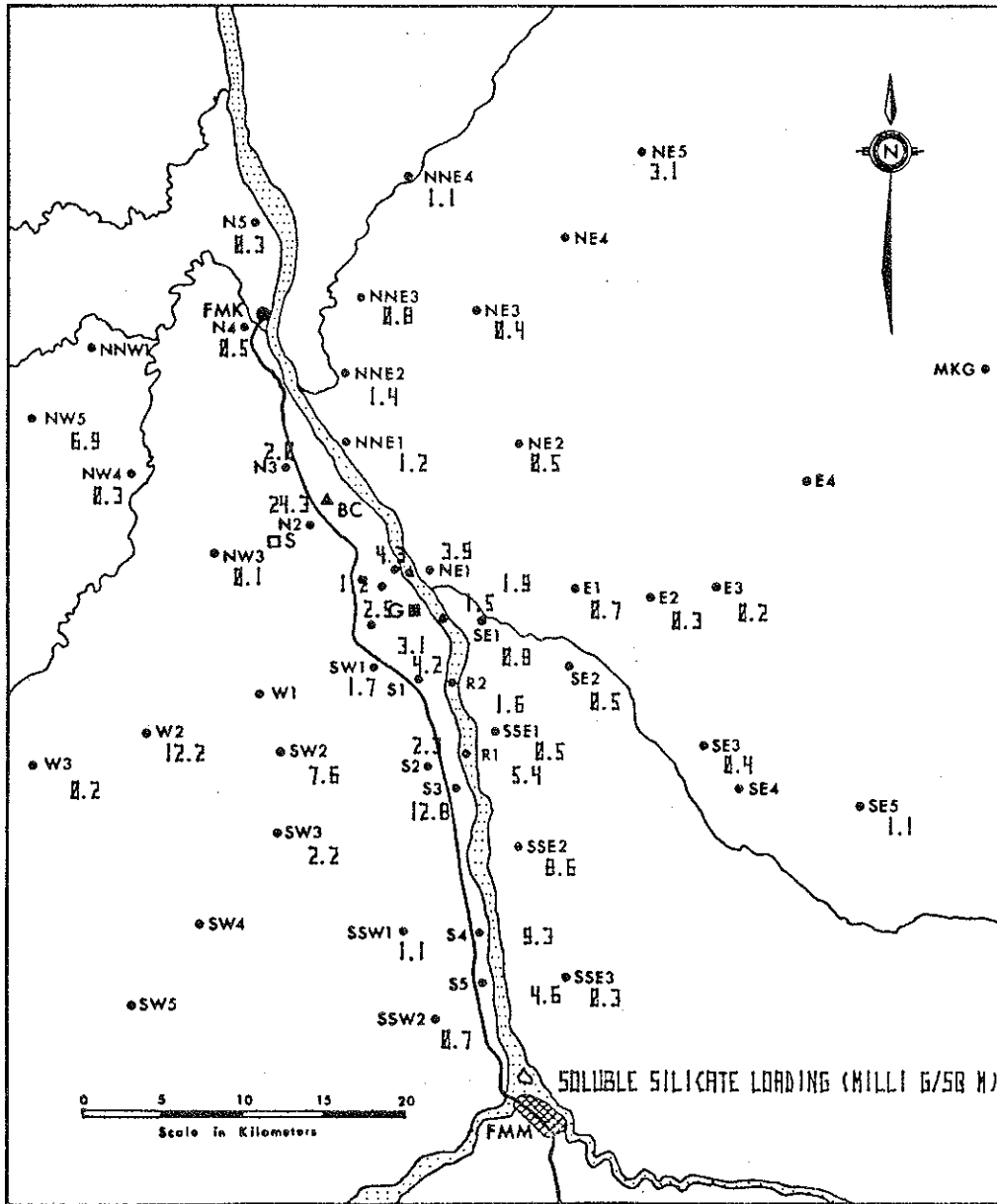


Figure 51. Plotted values of silicate snowpack loading at sampling sites.

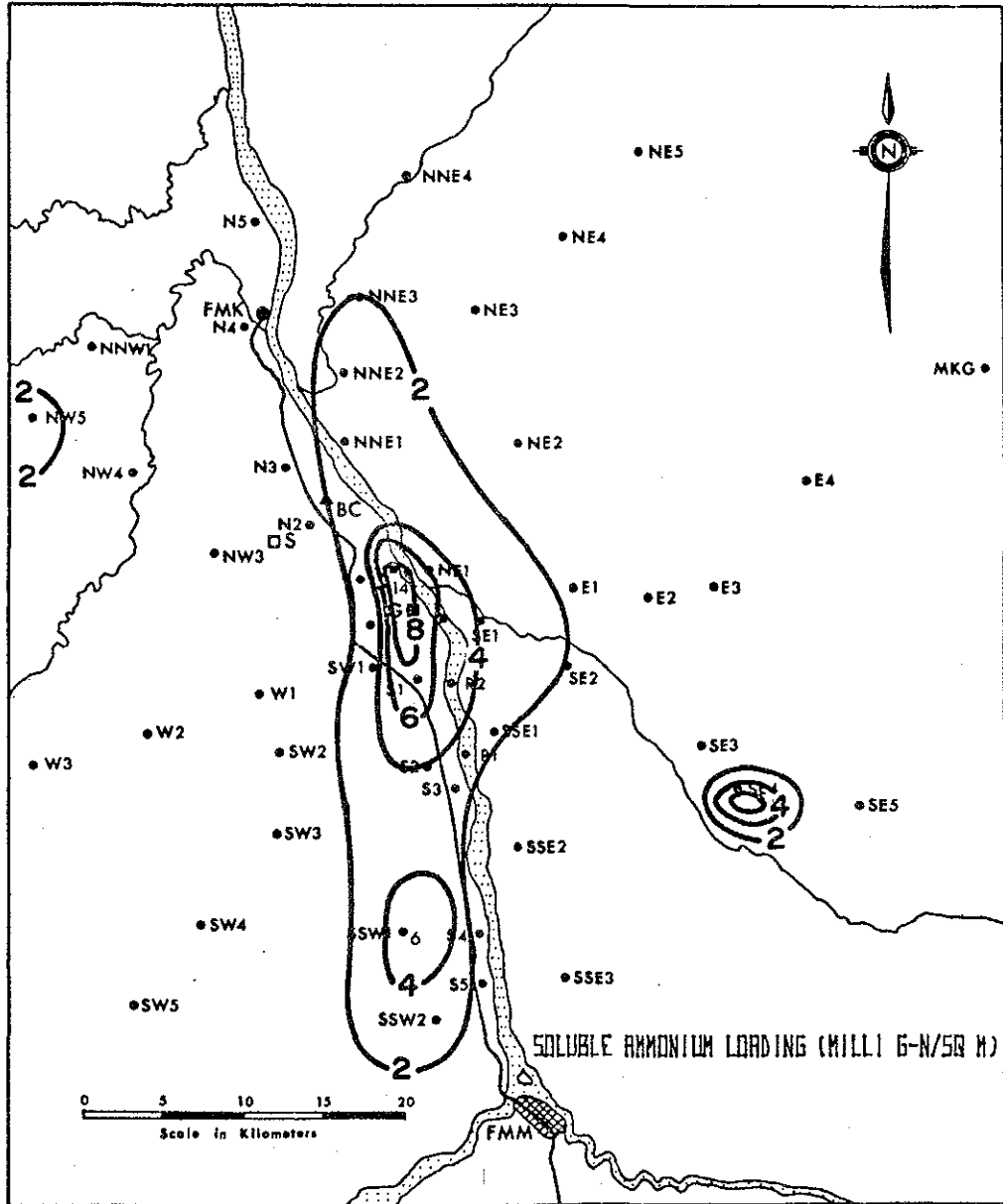


Figure 52. Spatial distribution of NH_4^+ snowpack loading.

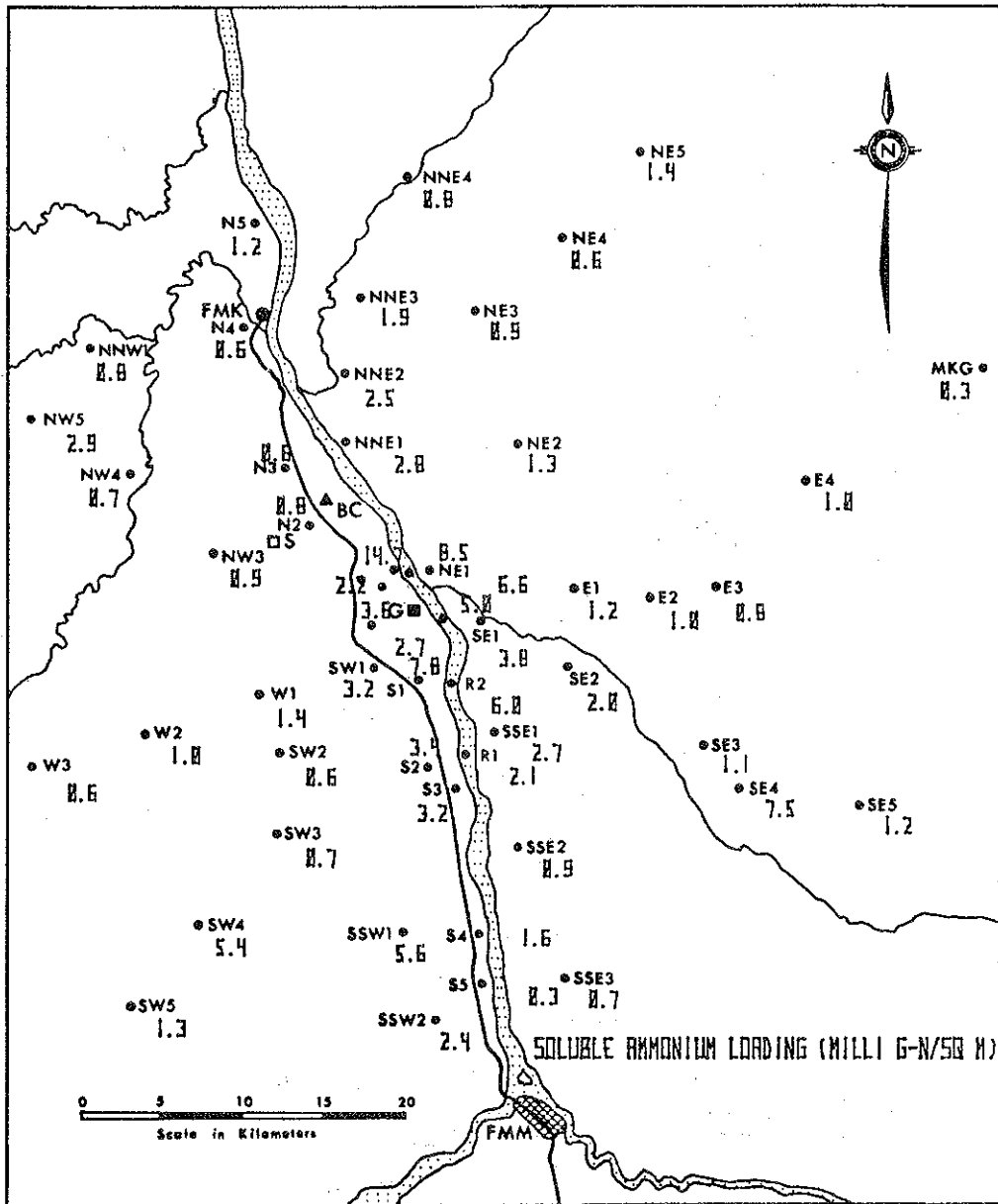


Figure 53. Plotted values of NH_4^+ snowpack loading at sampling sites.

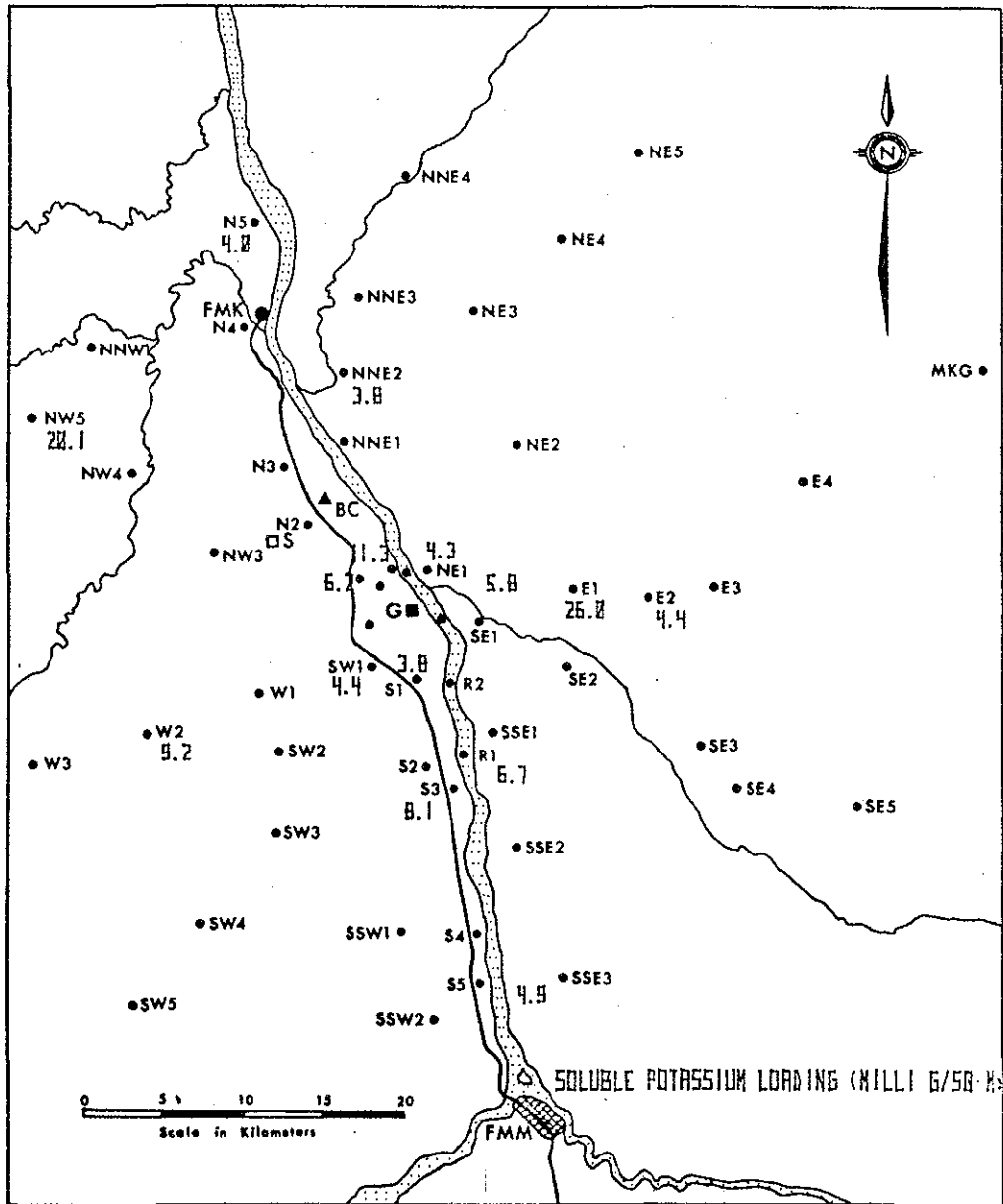


Figure 54. Plotted values of K^+ snowpack loading at sampling sites.

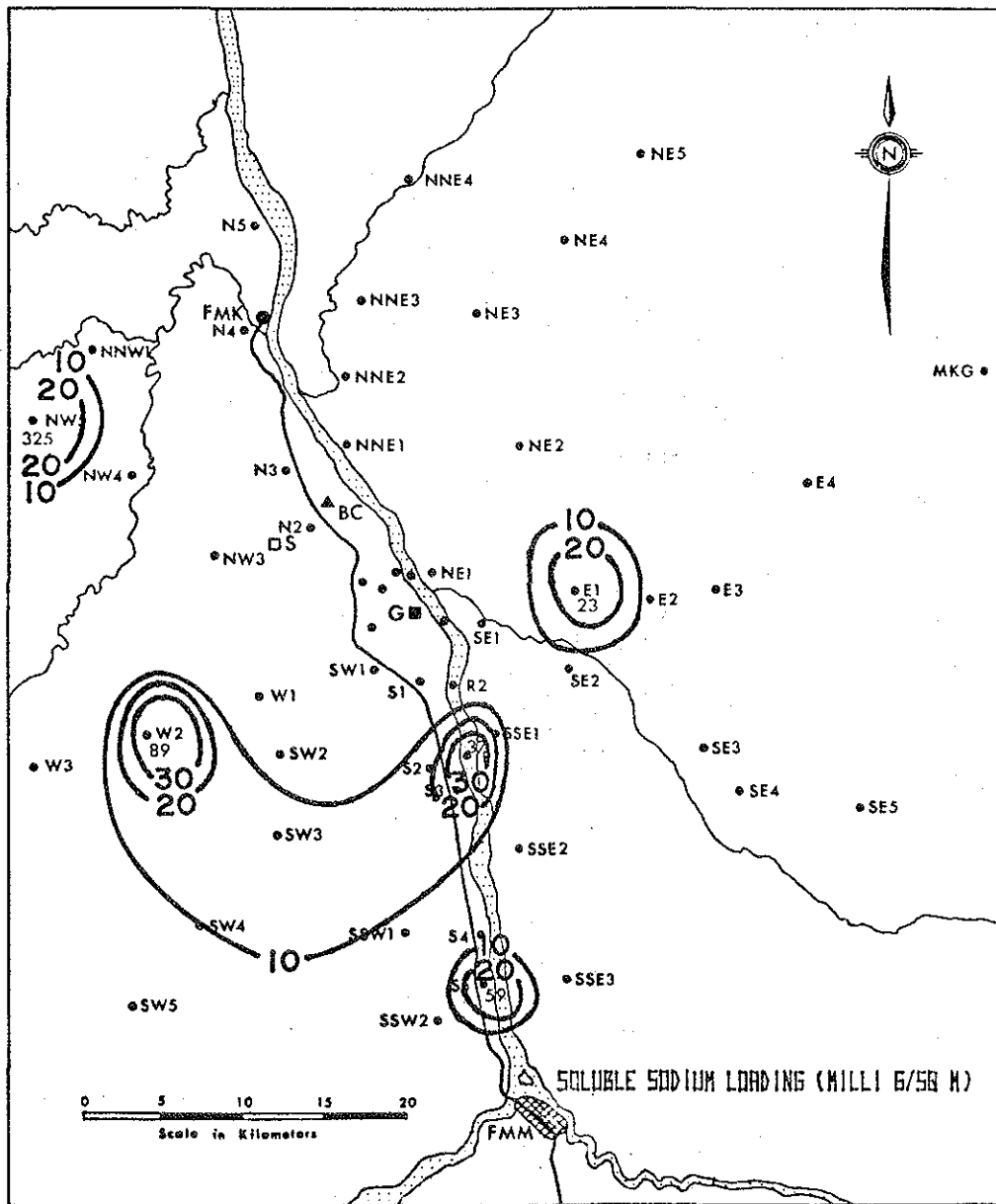


Figure 55. Spatial distribution of Na^+ snowpack loading.

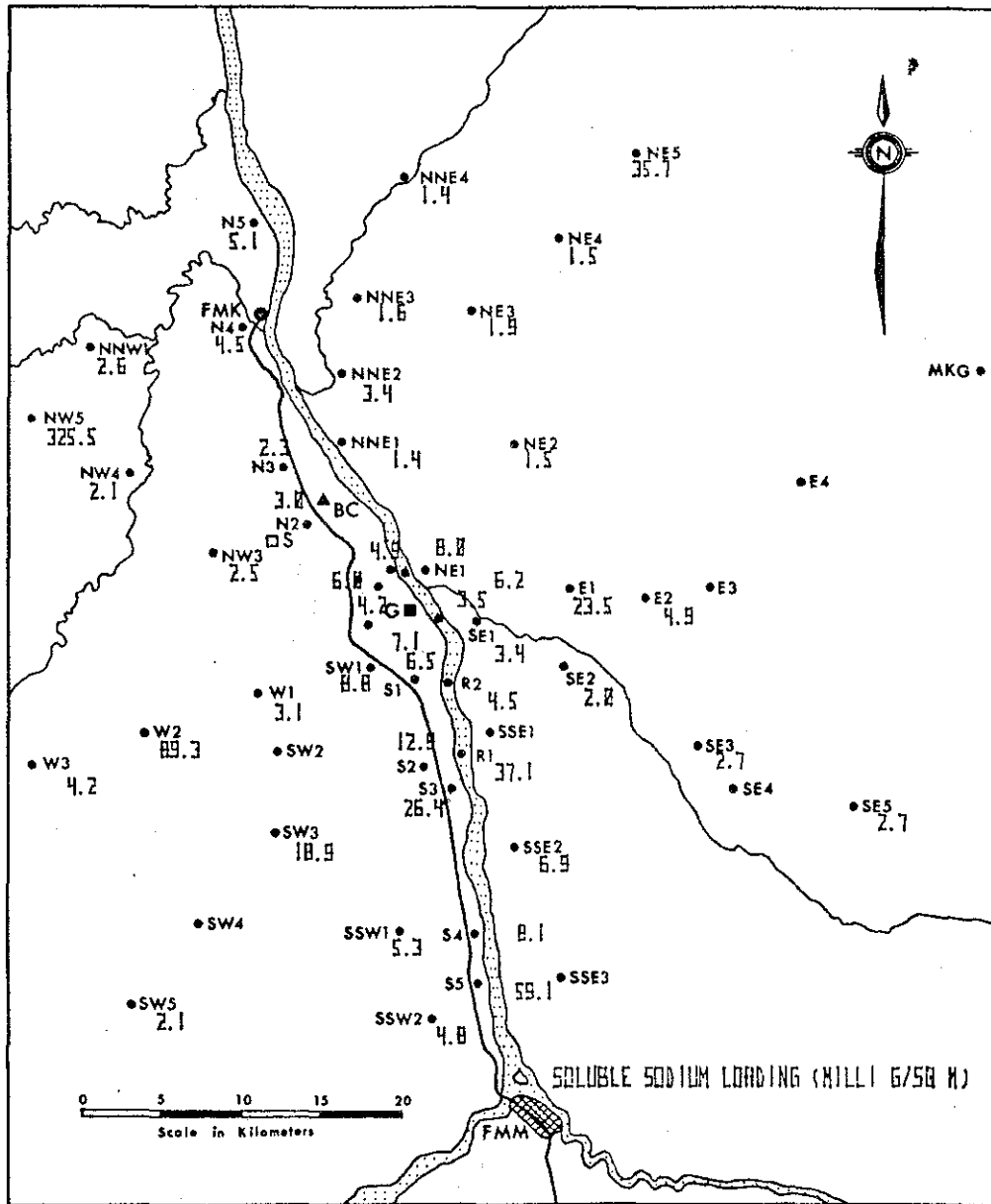


Figure 56. Plotted values of Na^+ snowpack loading at sampling sites.

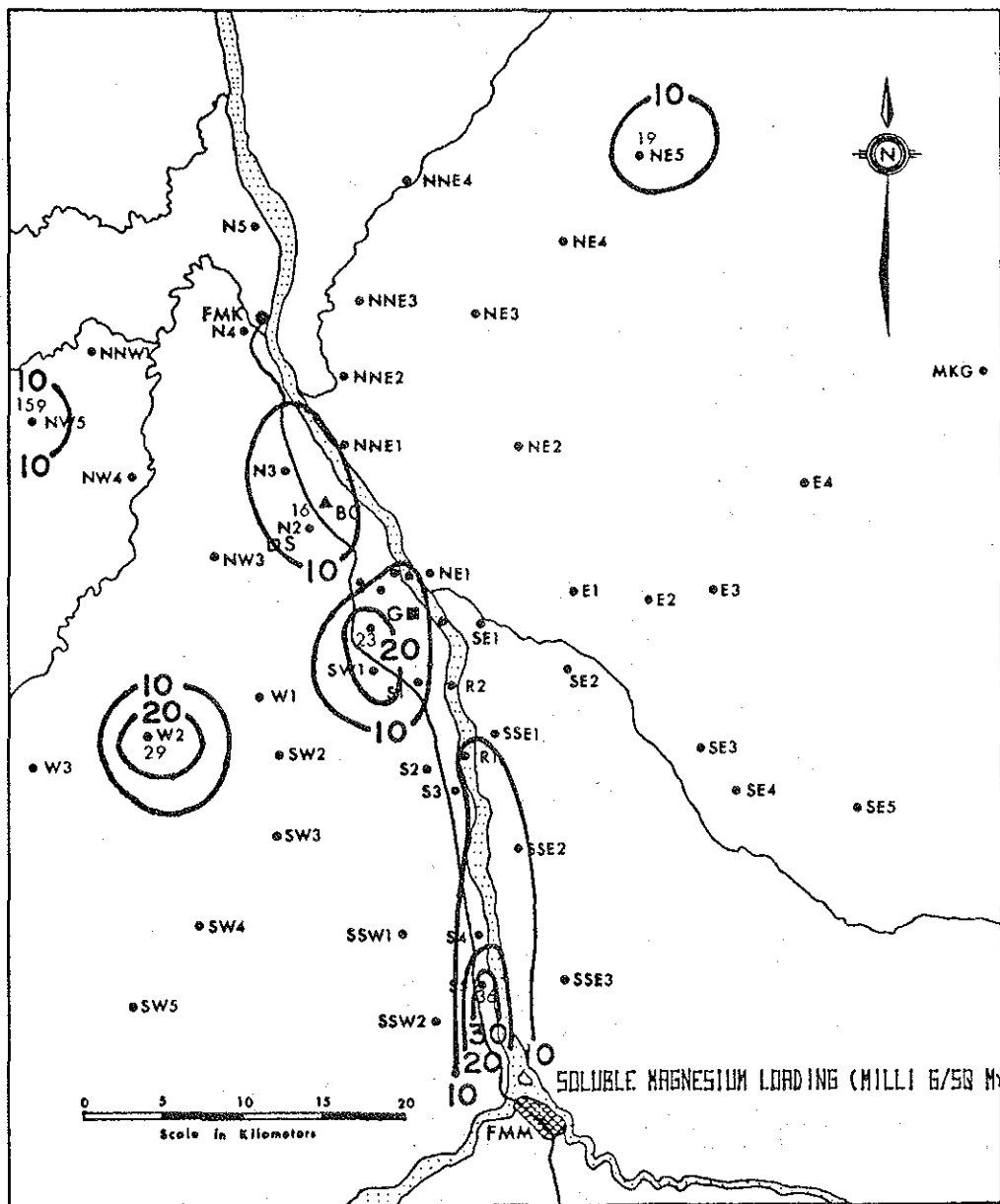


Figure 57. Spatial distribution of Mg^{++} snowpack loading.

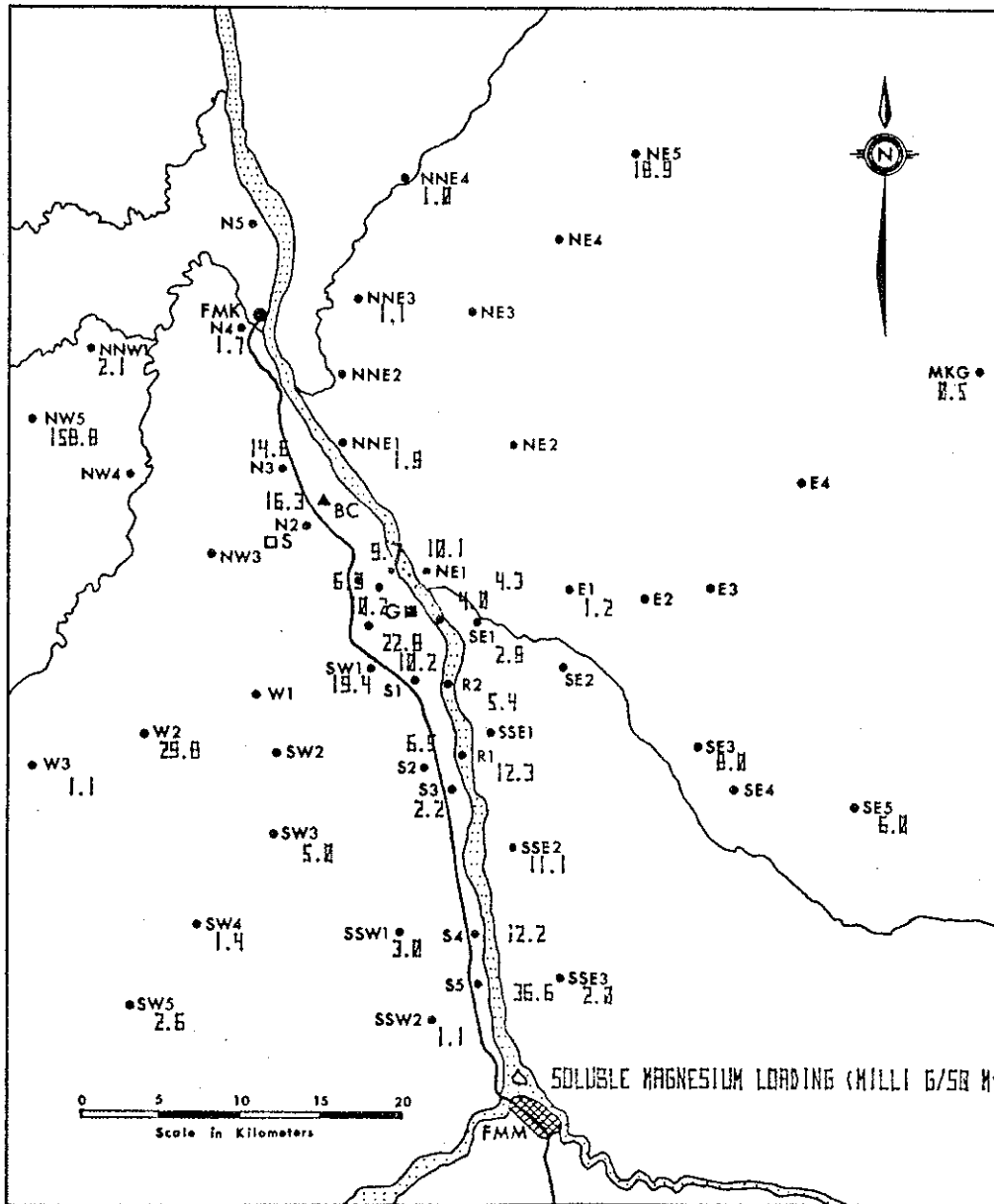


Figure 58. Plotted values of Mg⁺⁺ snowpack loading at sampling sites.

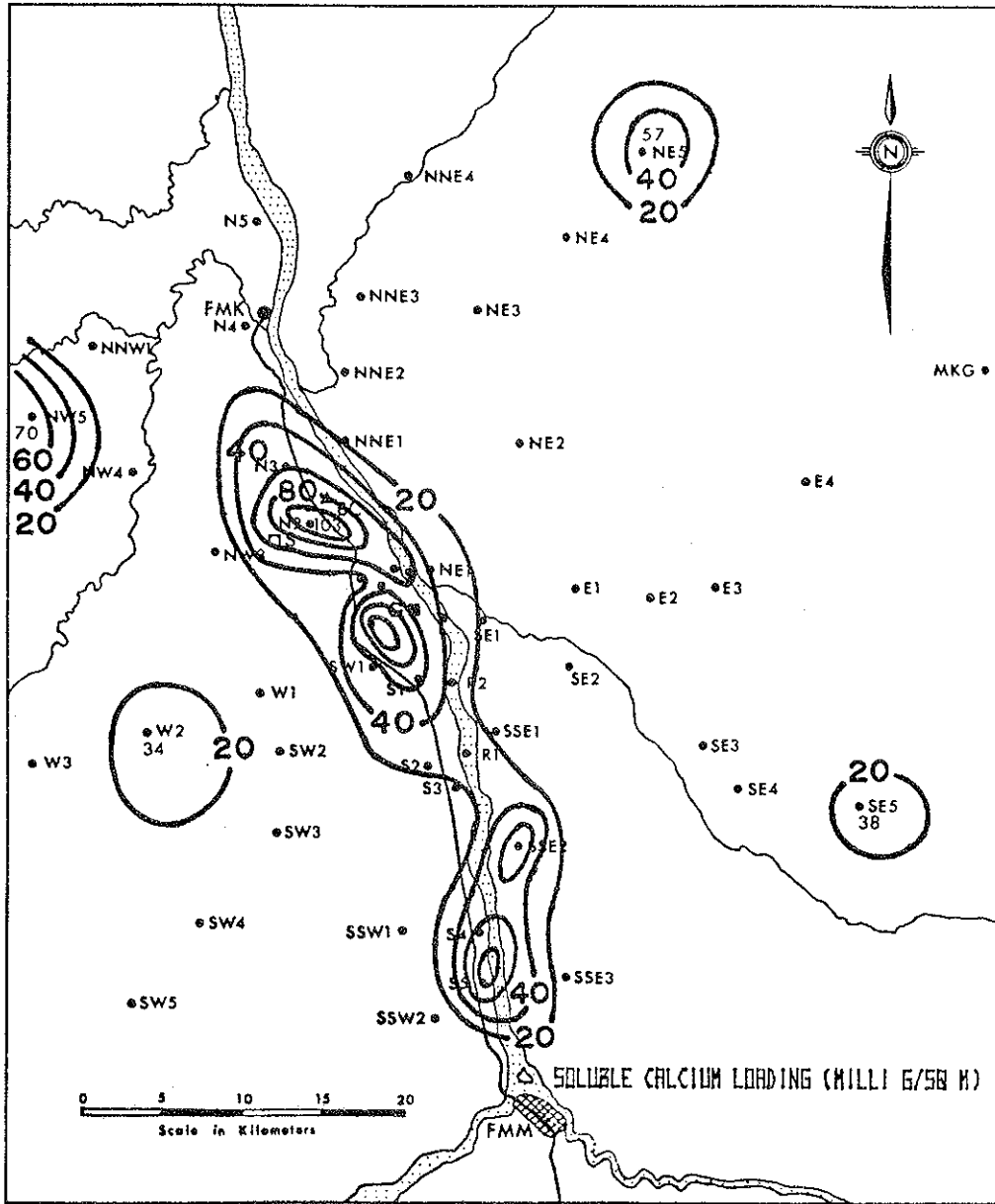


Figure 59. Spatial distribution of Ca^{++} snowpack loading.

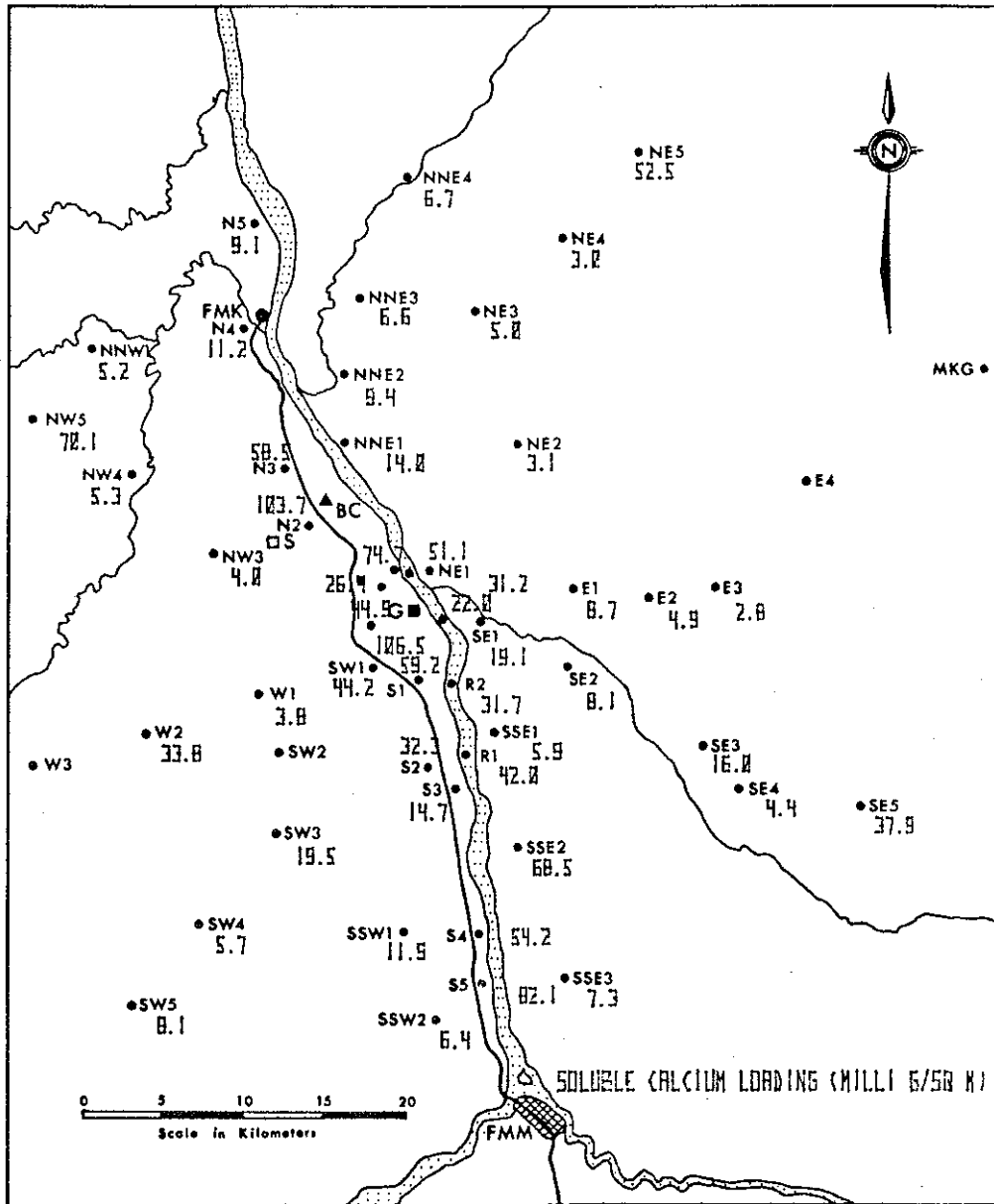


Figure 60. Plotted values of Ca^{++} snowpack loading at sampling sites.

8.3 THE SPATIAL DISTRIBUTION OF MEASURED SNOWPACK LOADINGS OF
INSOLUBLE PARTICULATE MASS AND OF Al, V, Mn, Ti, Fe, AND Ni

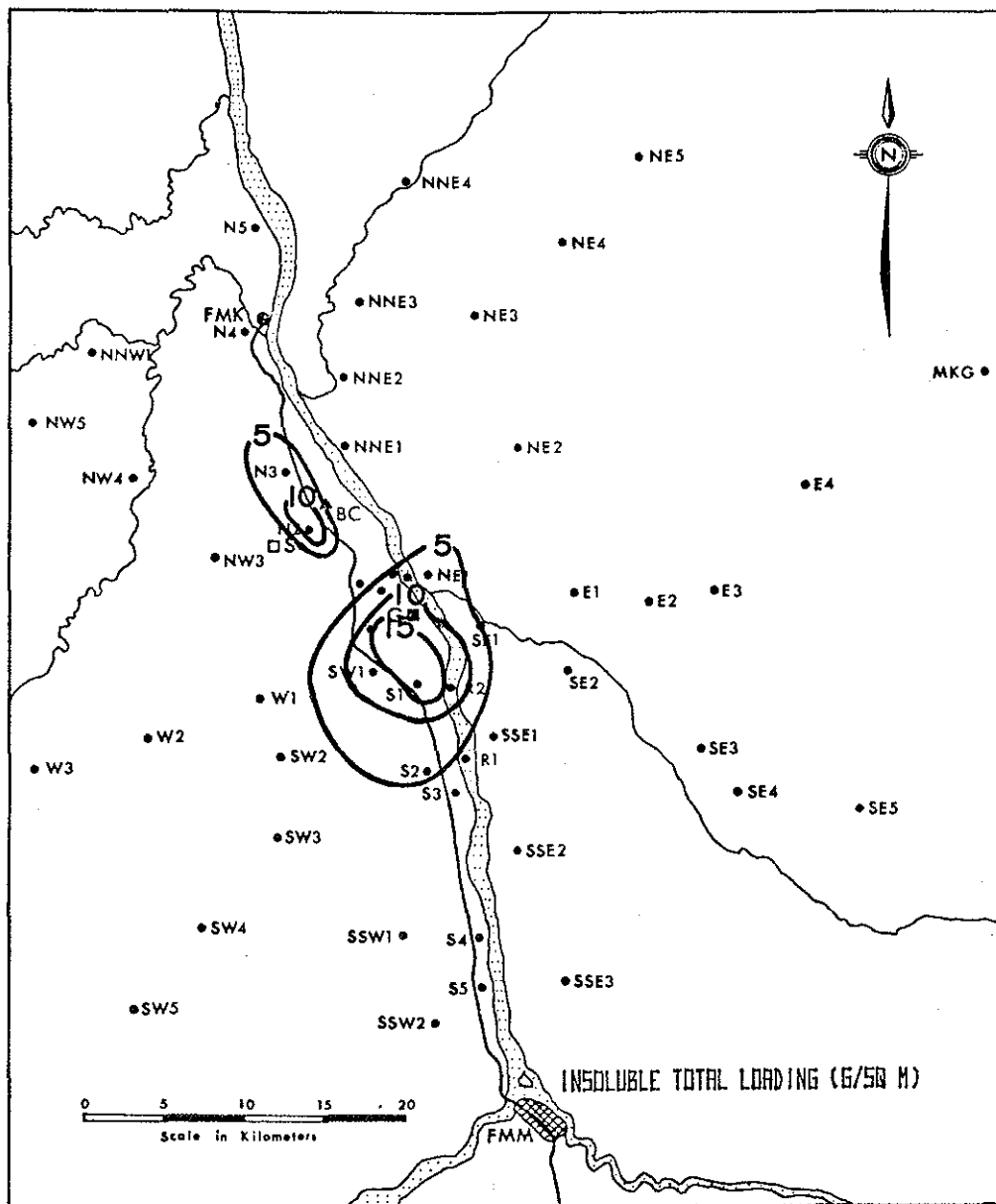


Figure 61. Spatial distribution of total insoluble metal loading.

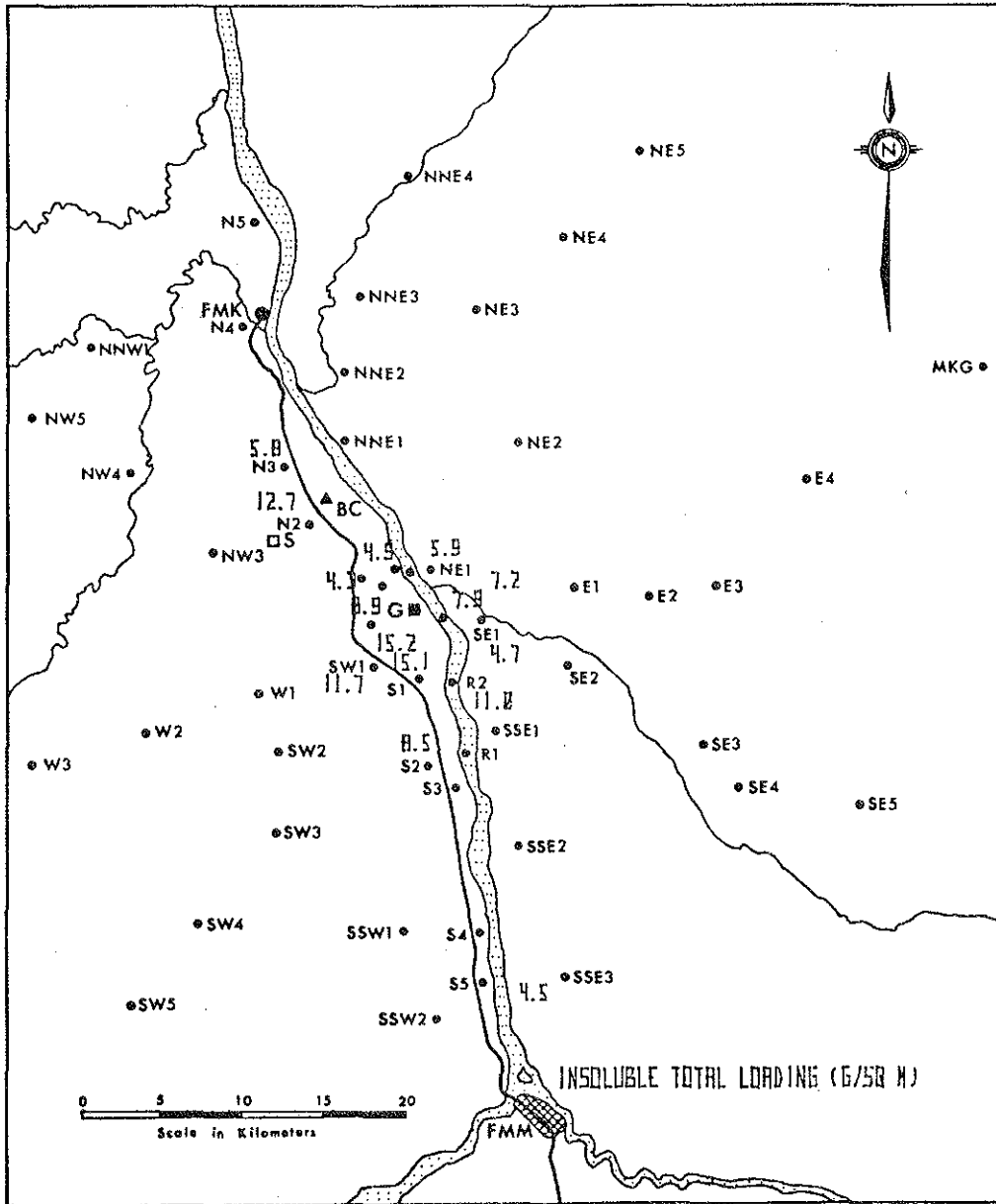


Figure 62. Plotted values of total insoluble metal loading at sampling sites.

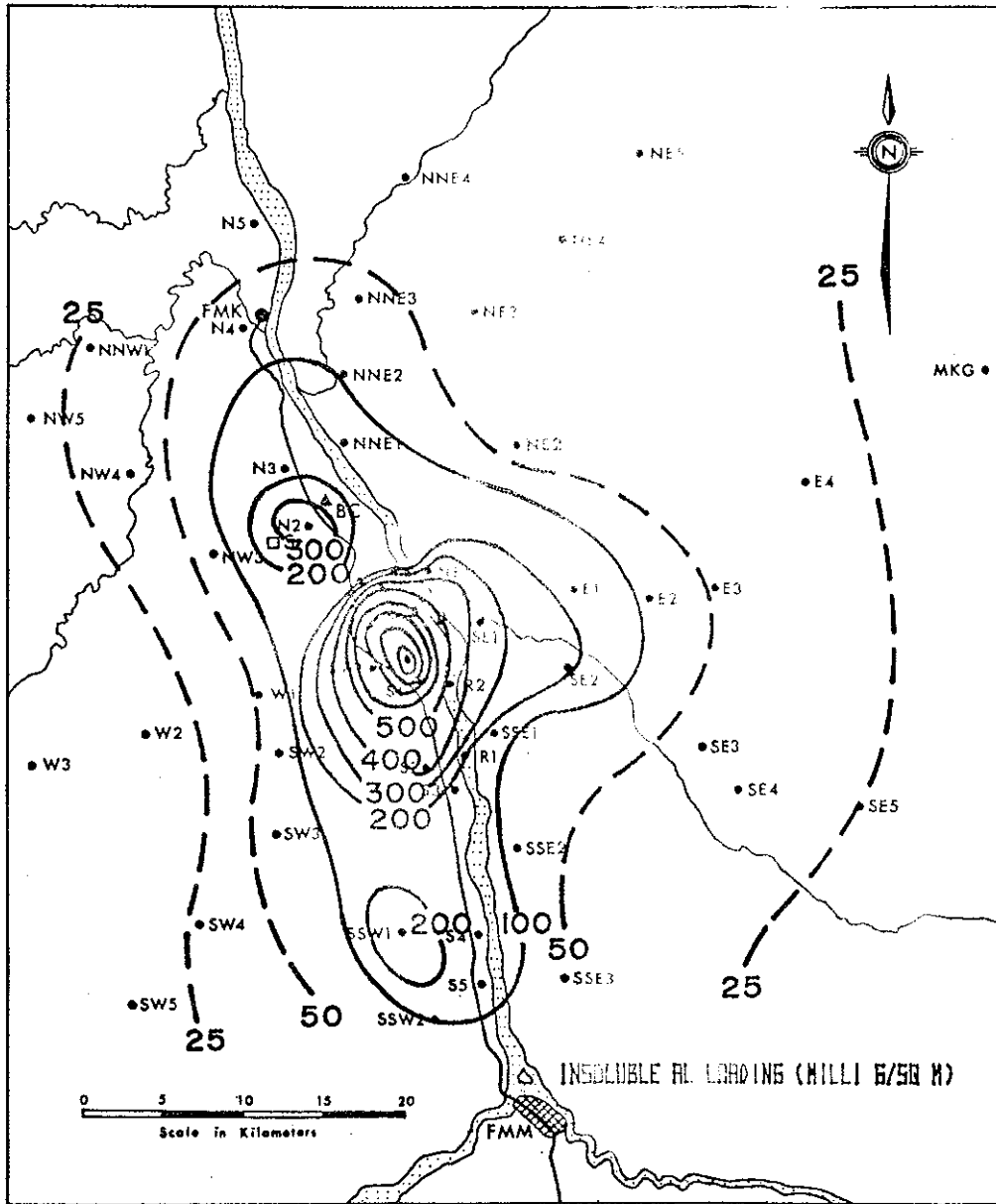


Figure 63. Spatial distribution of insoluble aluminum loading.

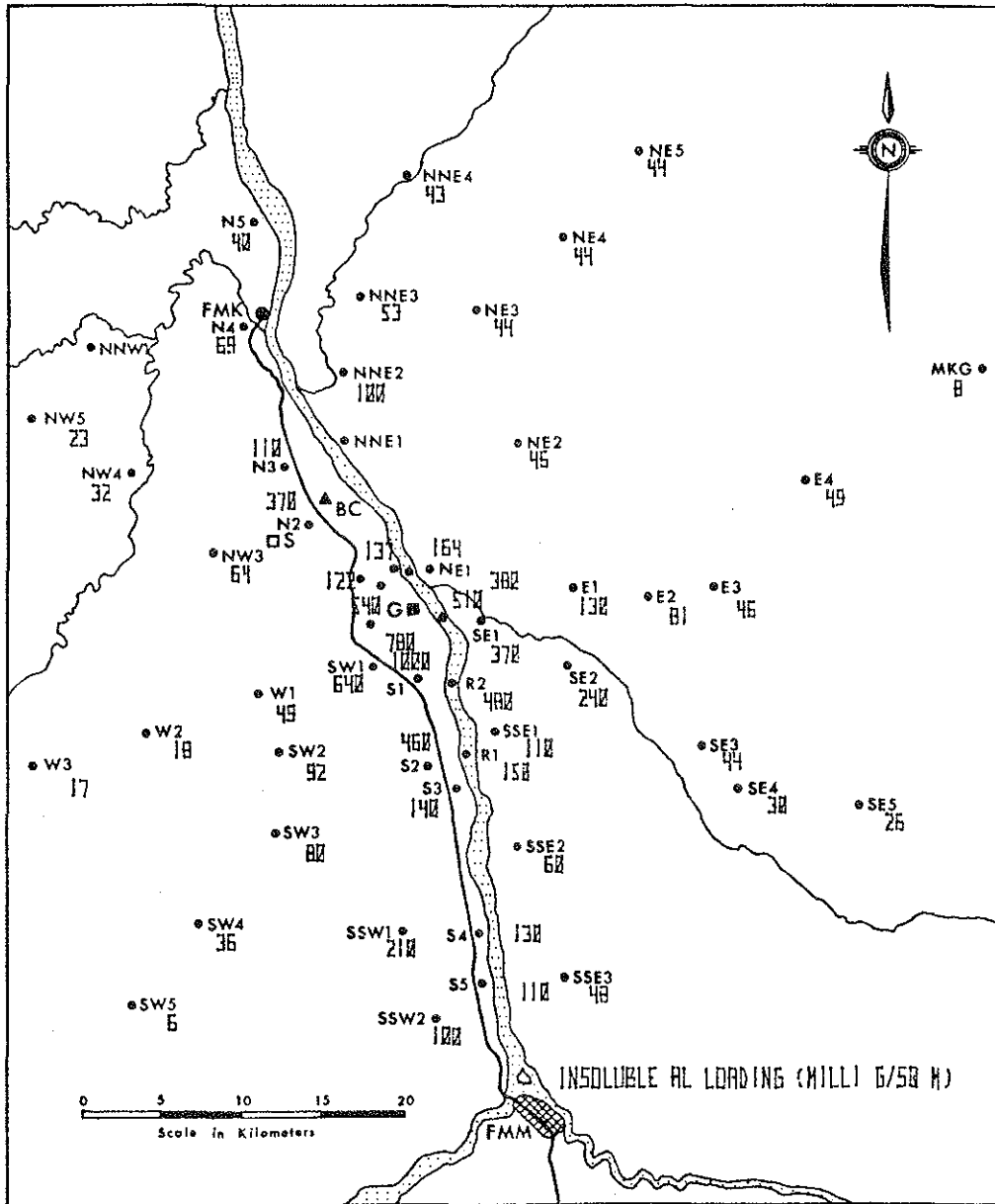


Figure 64. Plotted values of insoluble aluminum at sampling sites.

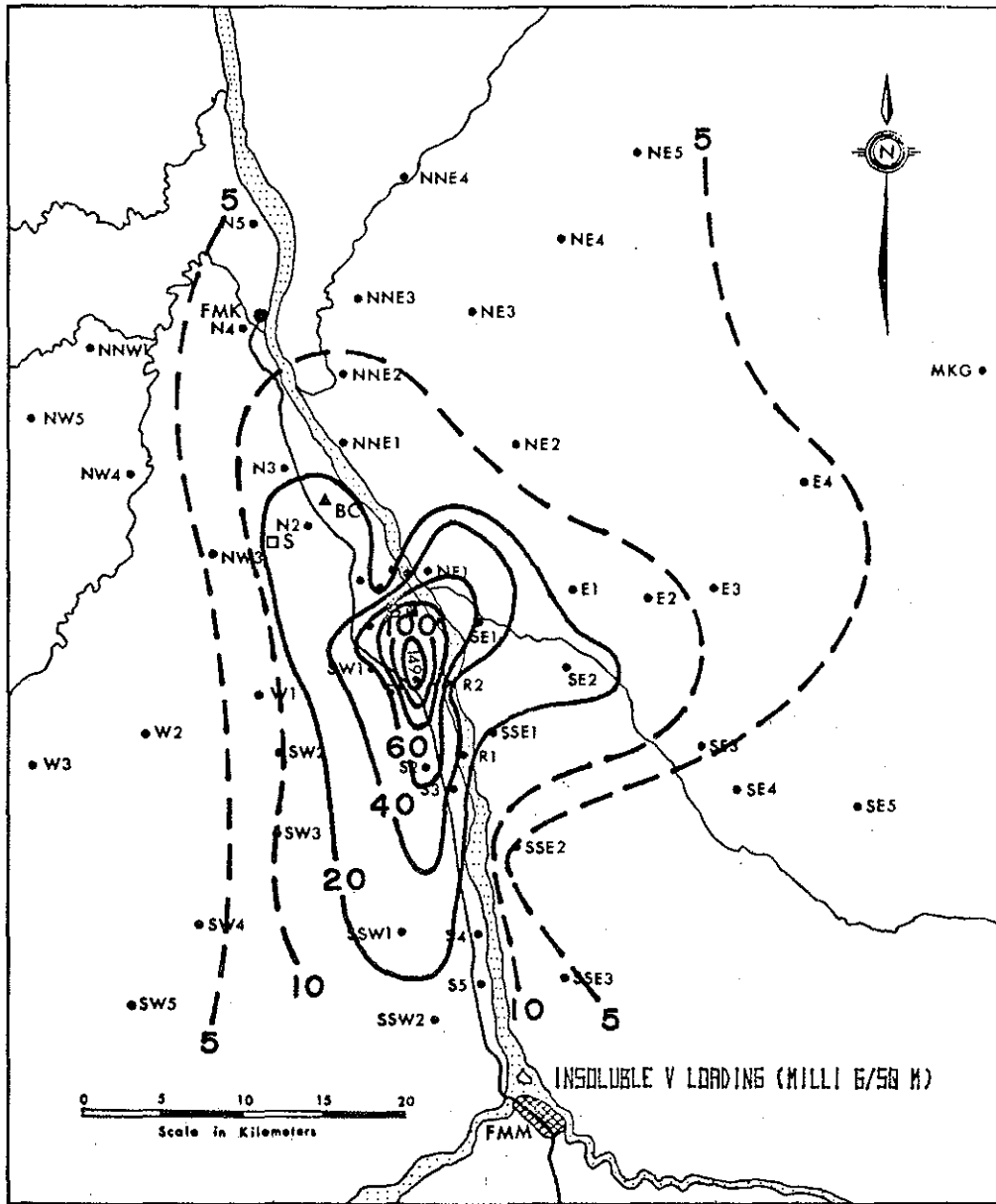


Figure 65. Spatial distribution of insoluble vanadium loading.

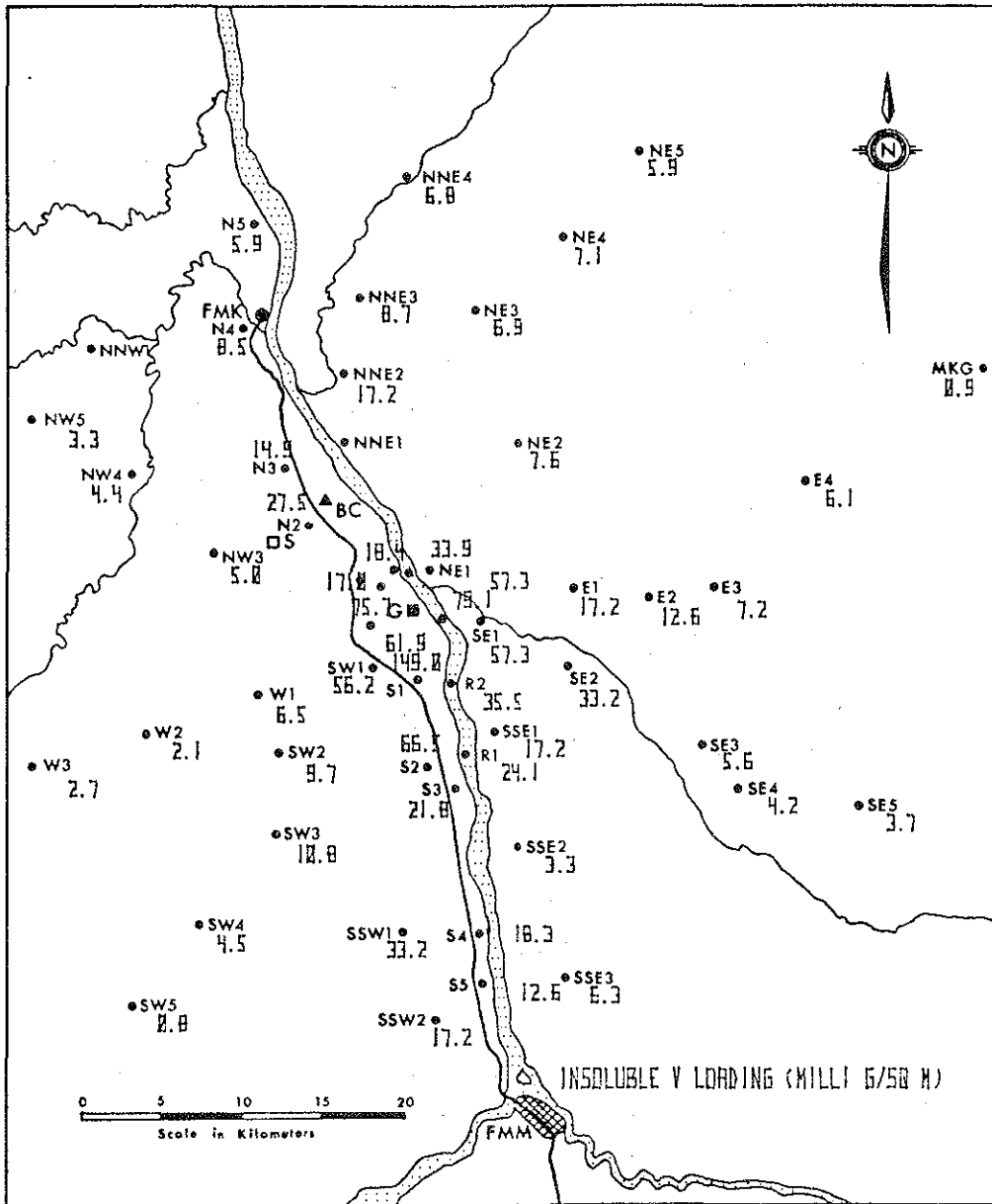


Figure 66. Plotted values of insoluble vanadium at sampling sites.

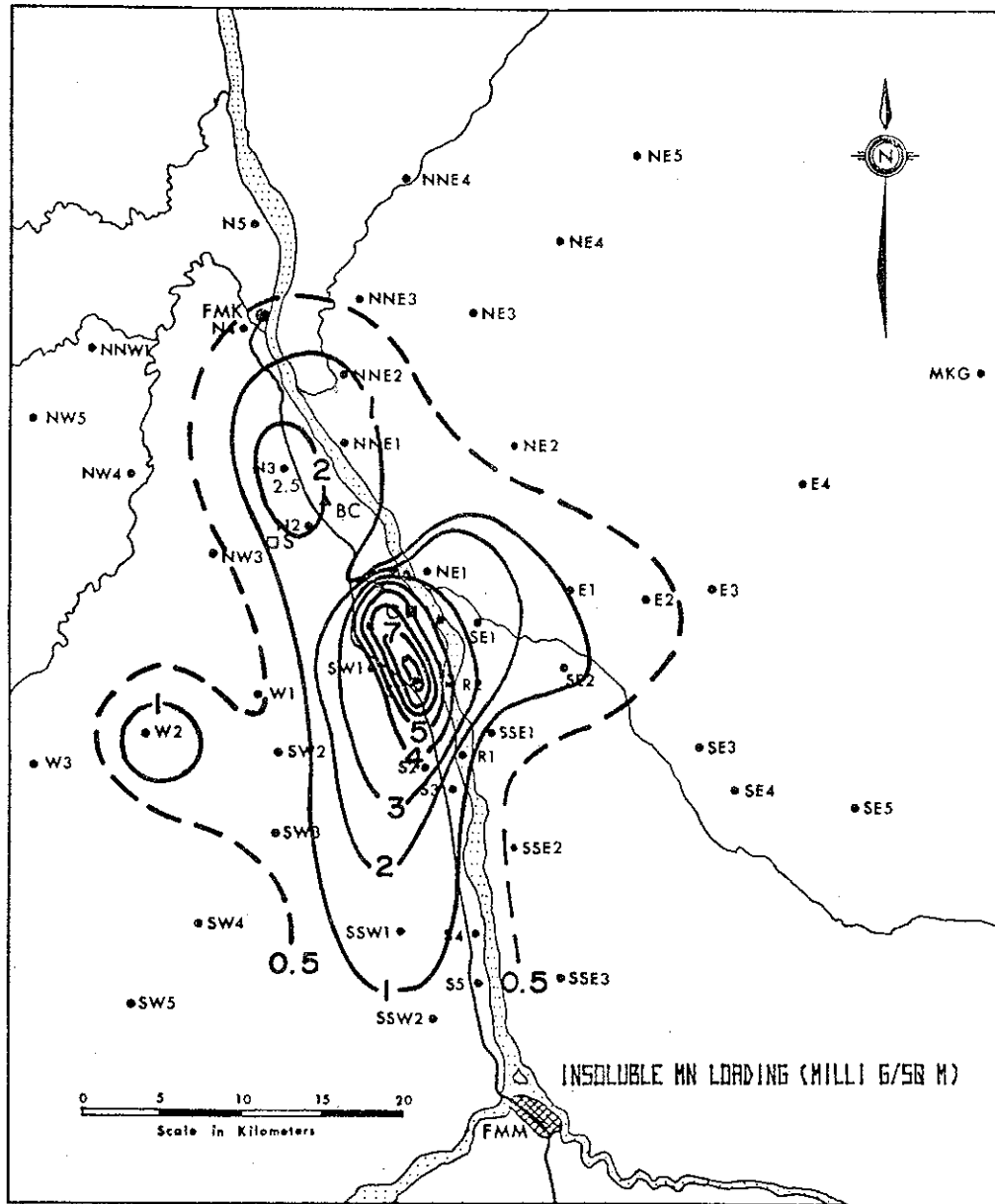


Figure 67. Spatial distribution of insoluble manganese loading.

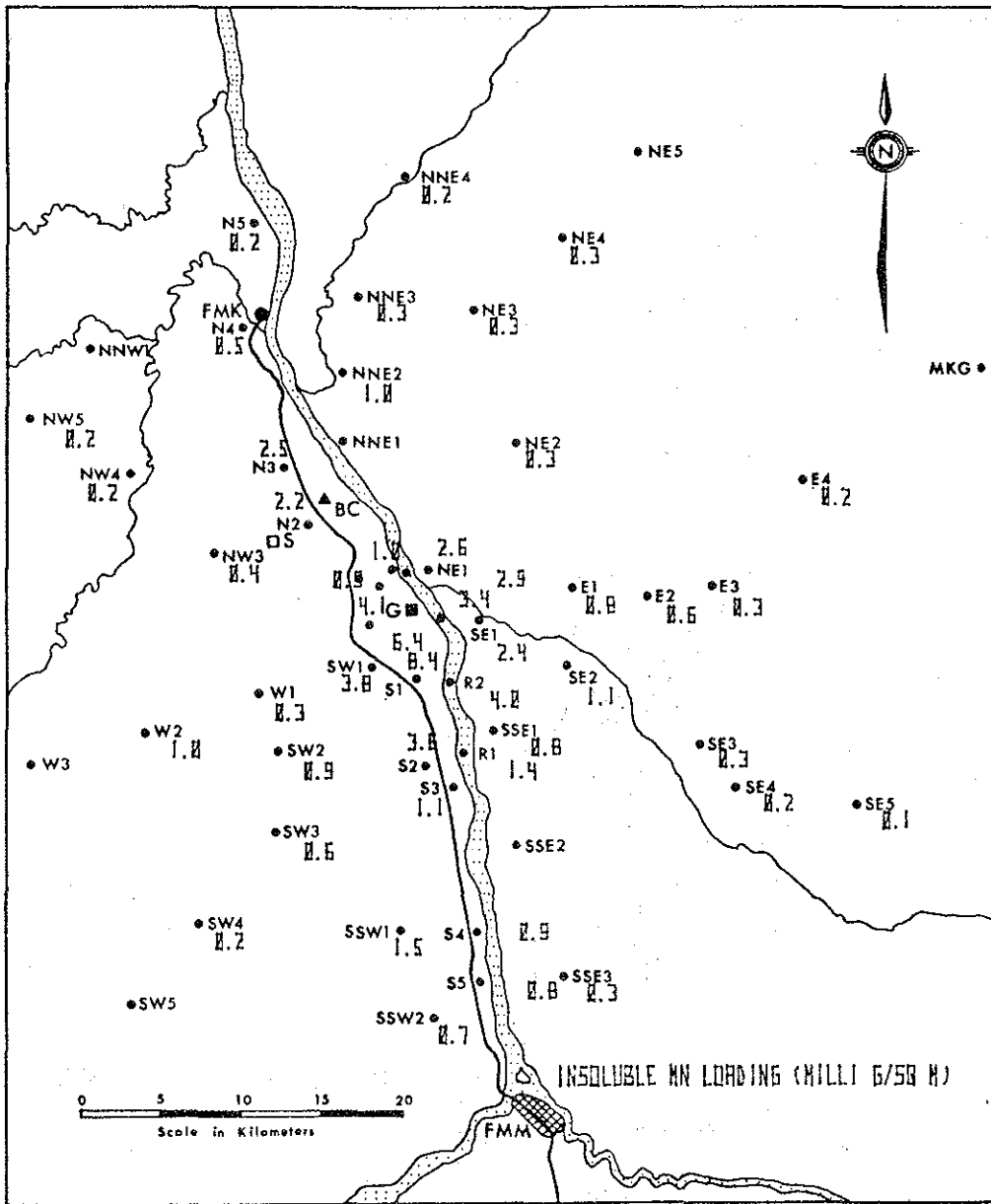


Figure 68. Plotted values of insoluble manganese at sampling sites.

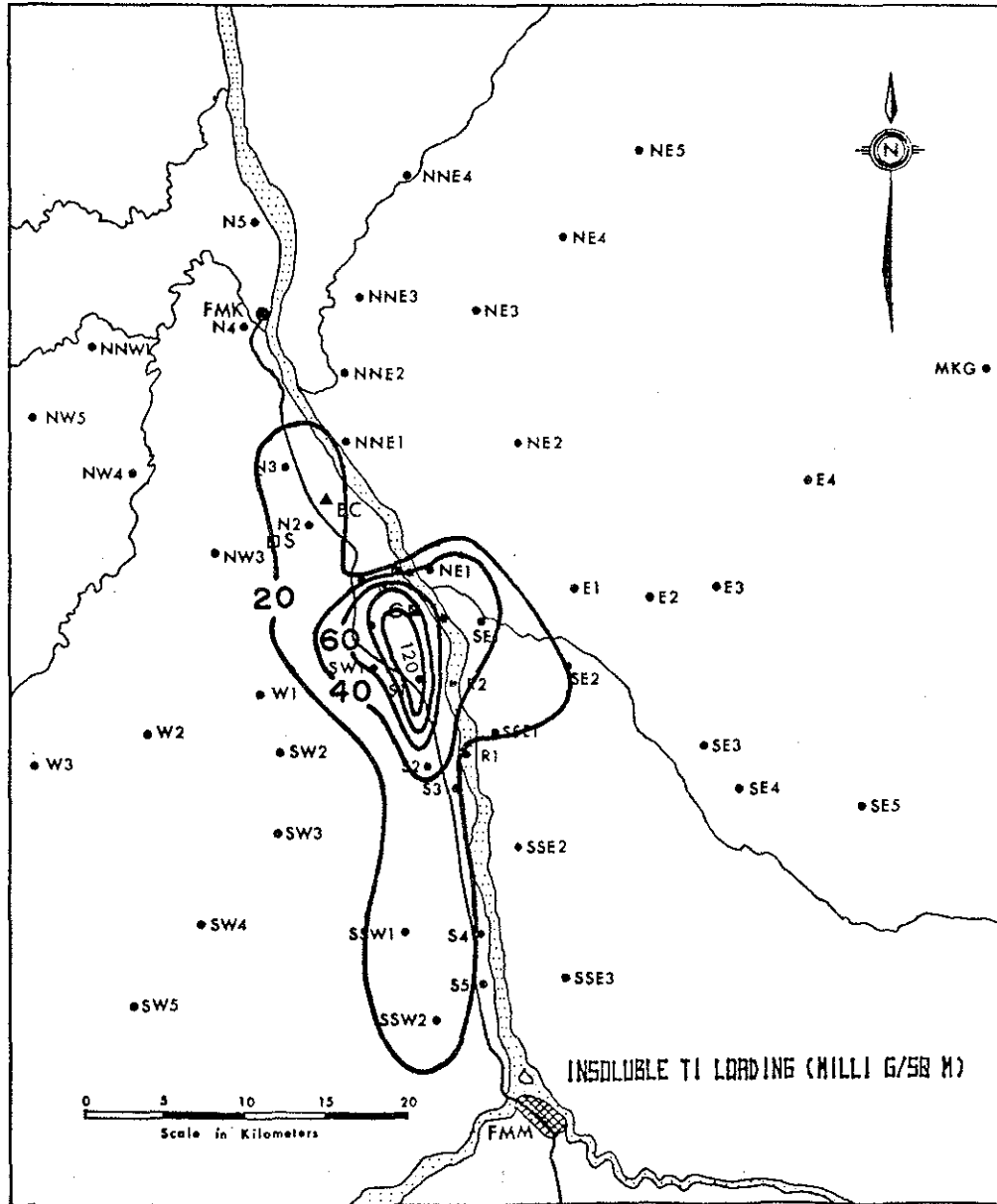


Figure 69. Spatial distribution of insoluble titanium loading.

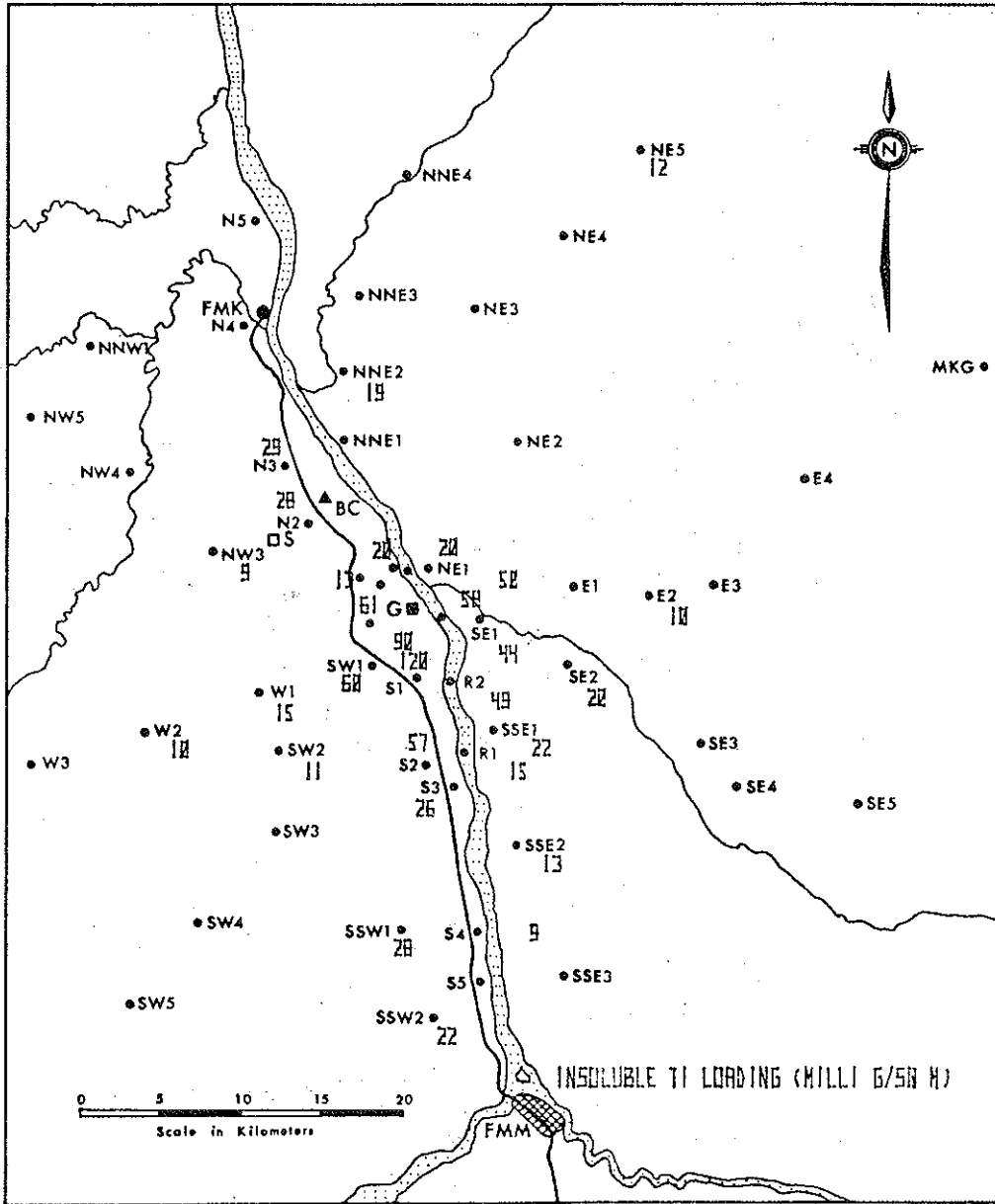


Figure 70. Plotted values of insoluble titanium at sampling sites.

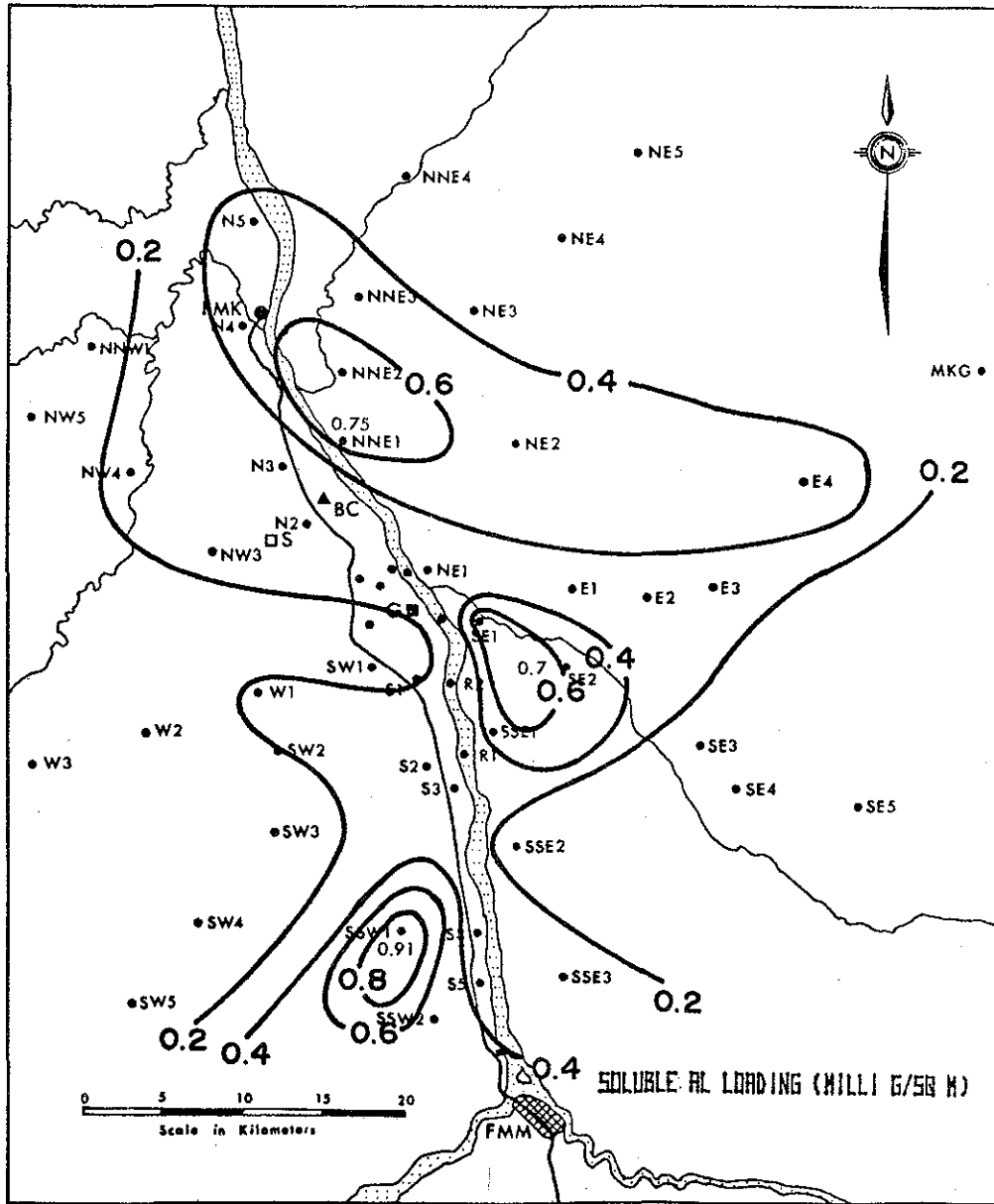


Figure 71. Spatial distribution of soluble aluminum loading.

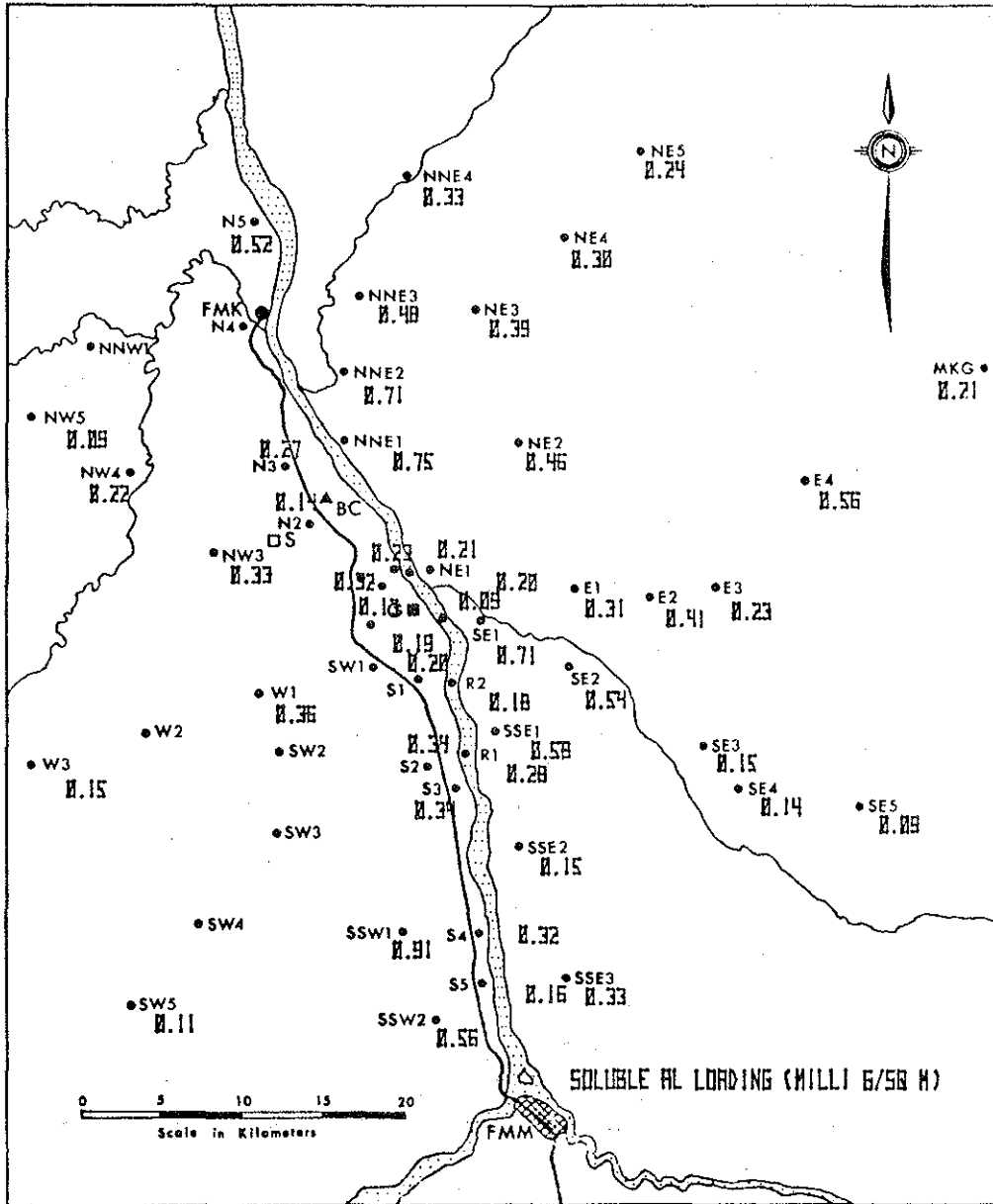


Figure 72. Plotted values of soluble aluminum loading at sampling sites.

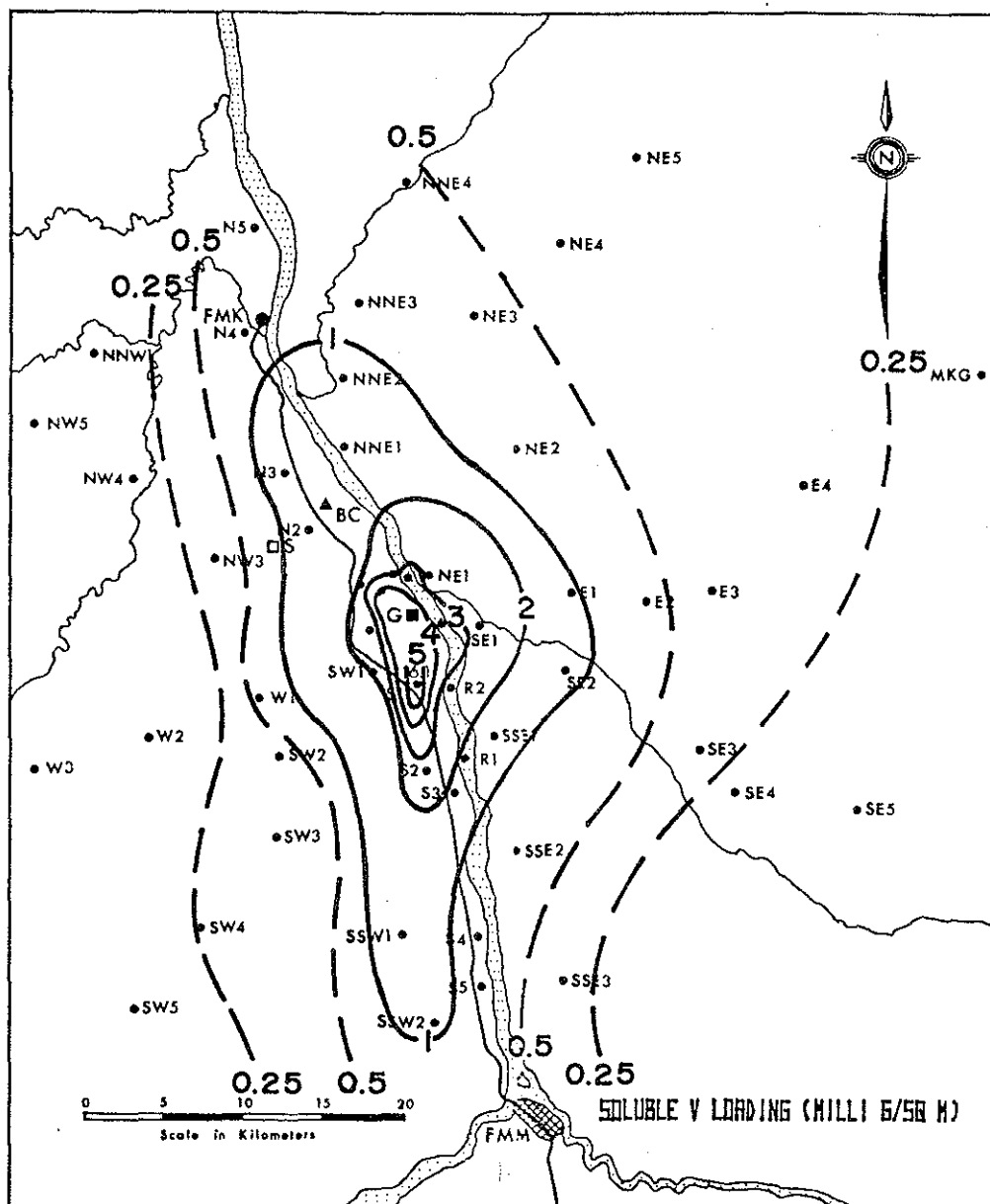


Figure 73. Spatial distribution of soluble vanadium loading.

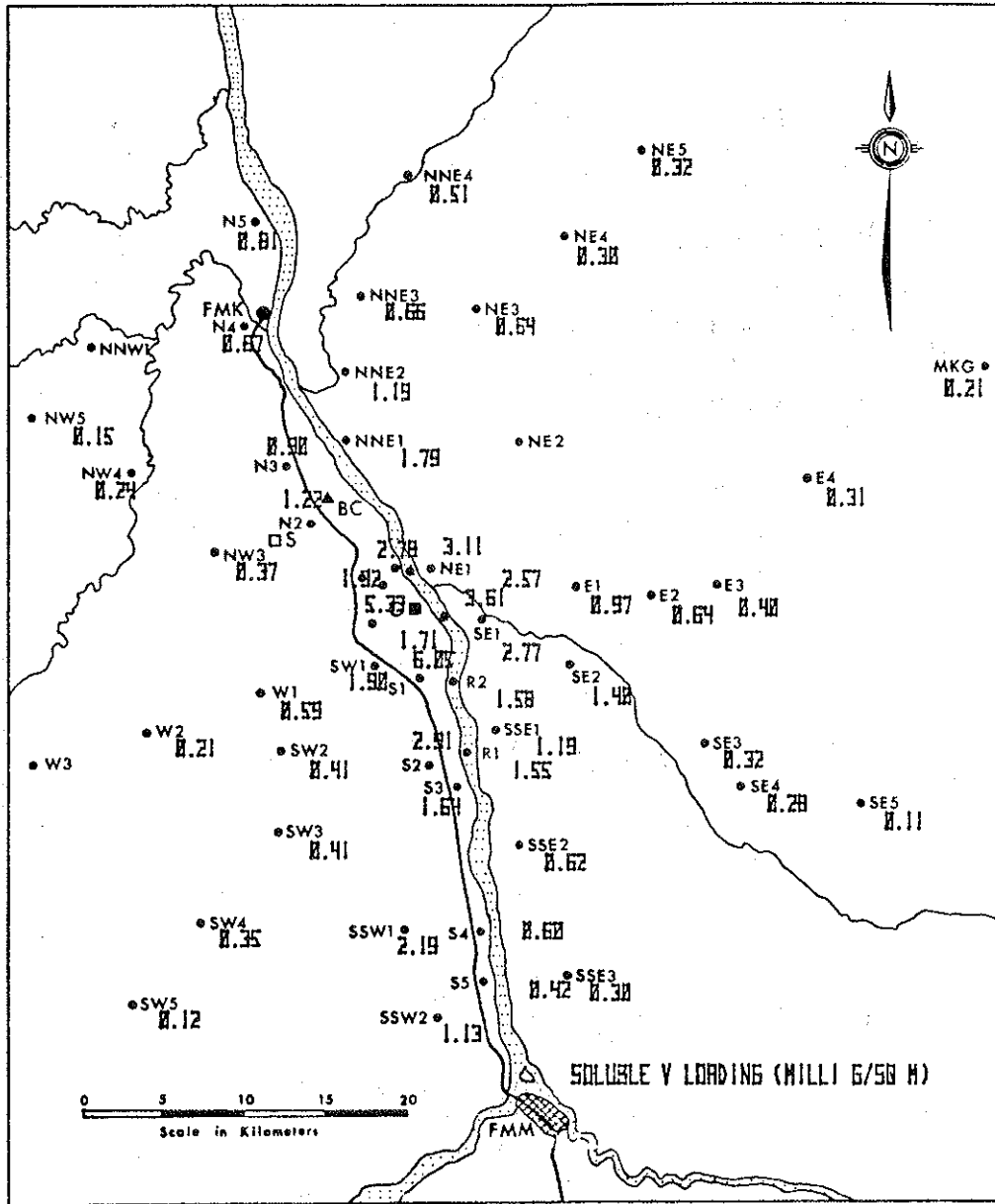


Figure 74. Plotted values of soluble vanadium loading at sampling sites.

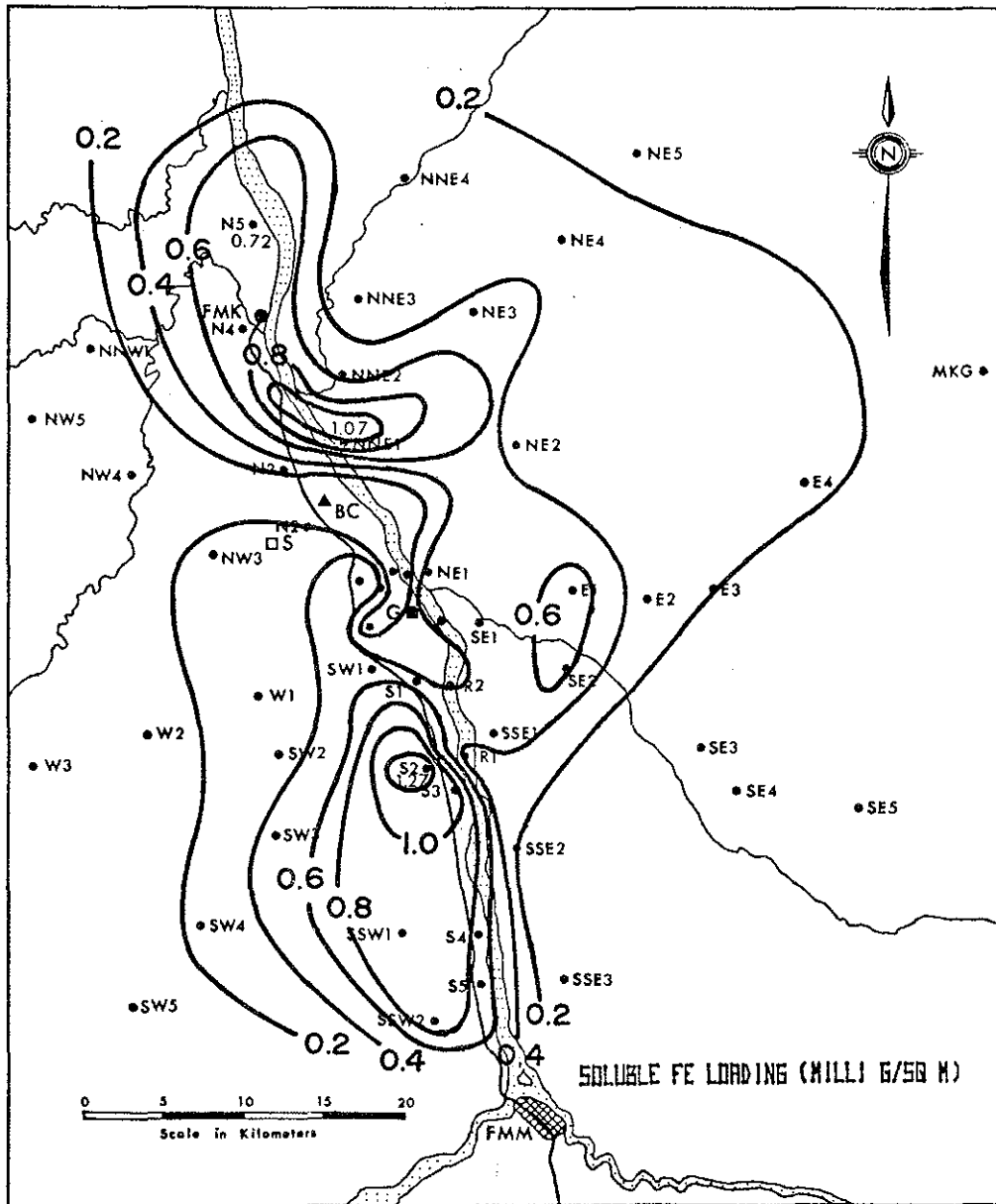


Figure 75. Spatial distribution of soluble iron loading.

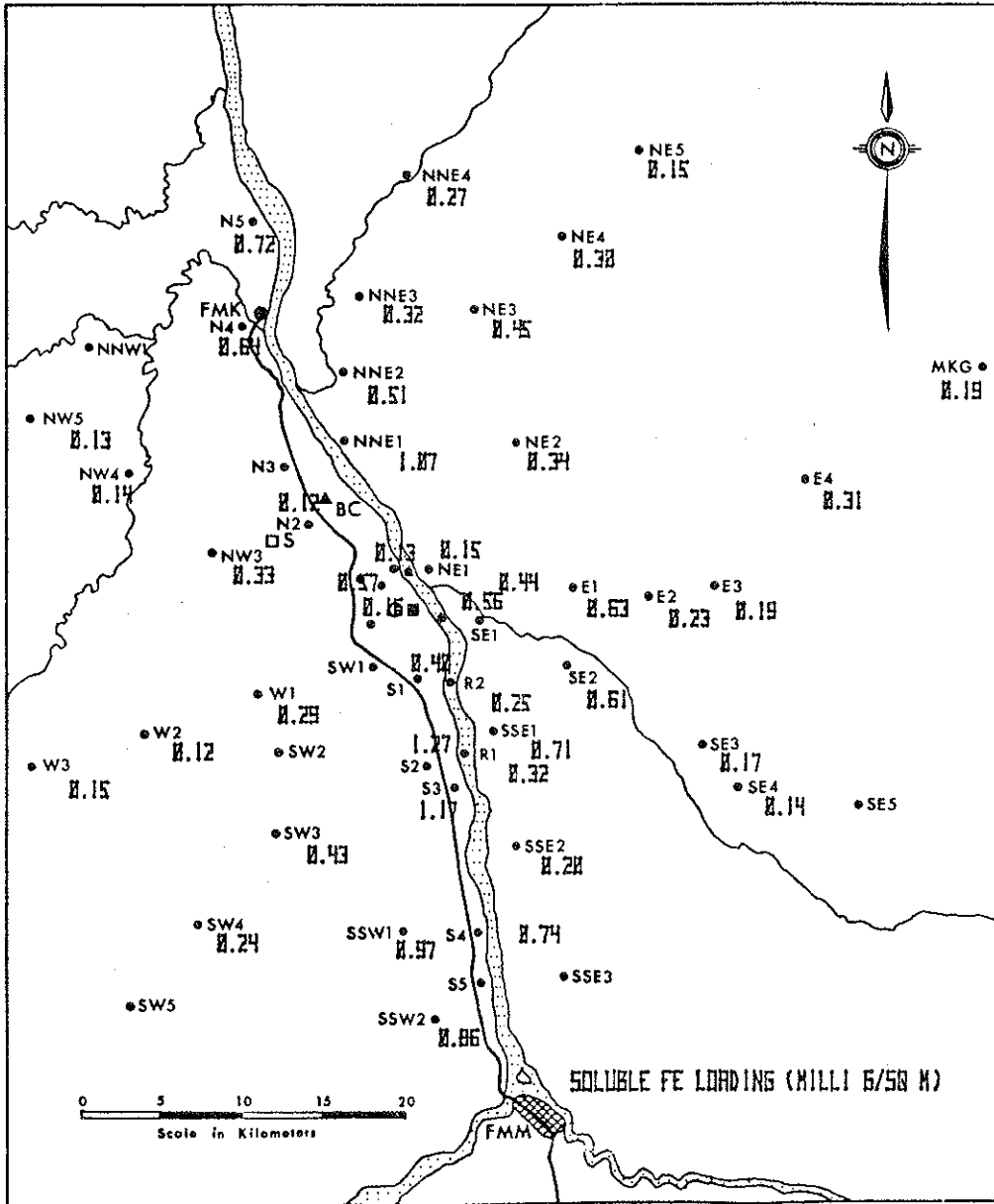


Figure 76. Plotted values of soluble iron loading at sampling sites.

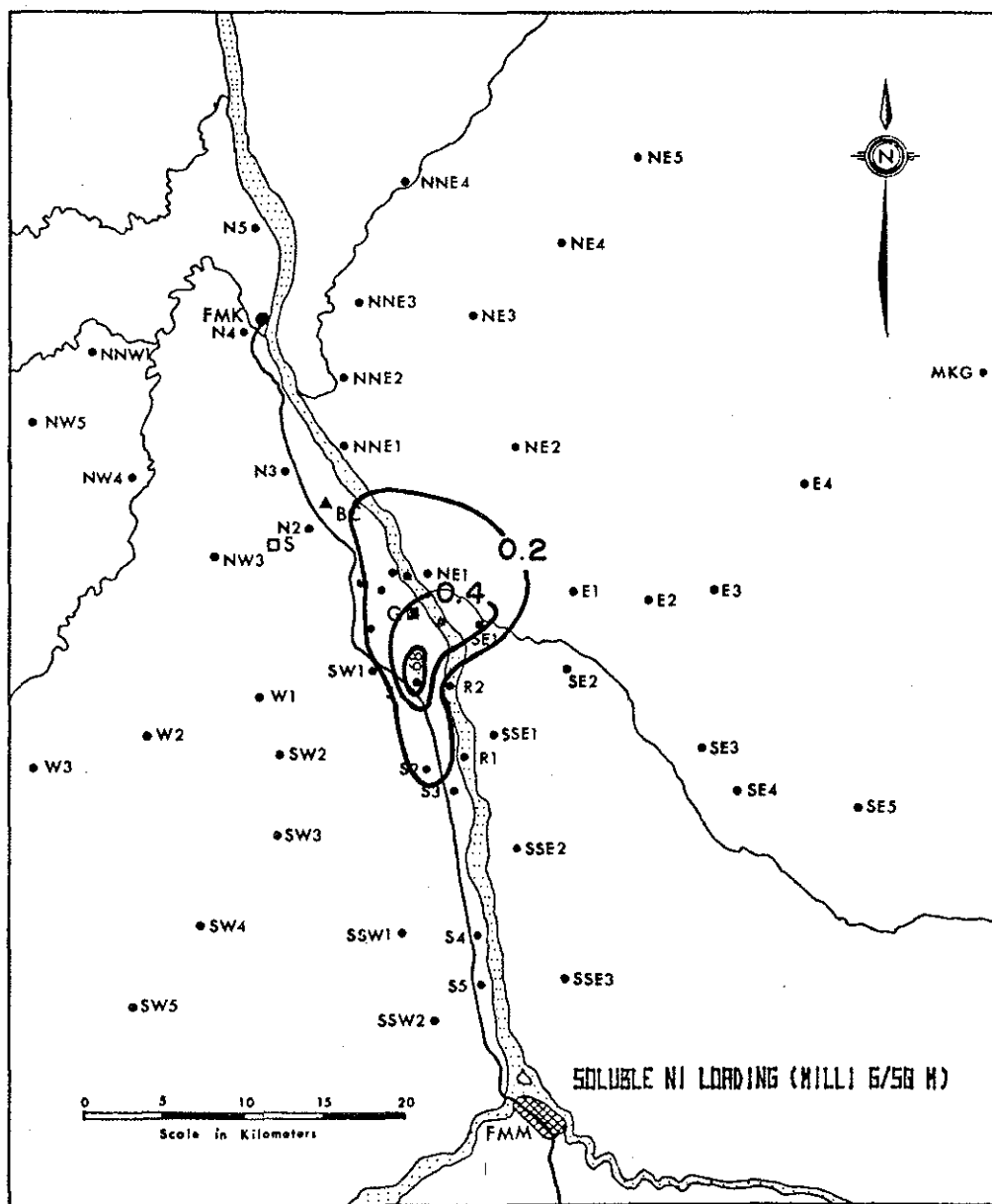


Figure 77. Spatial distribution of soluble nickel loading.

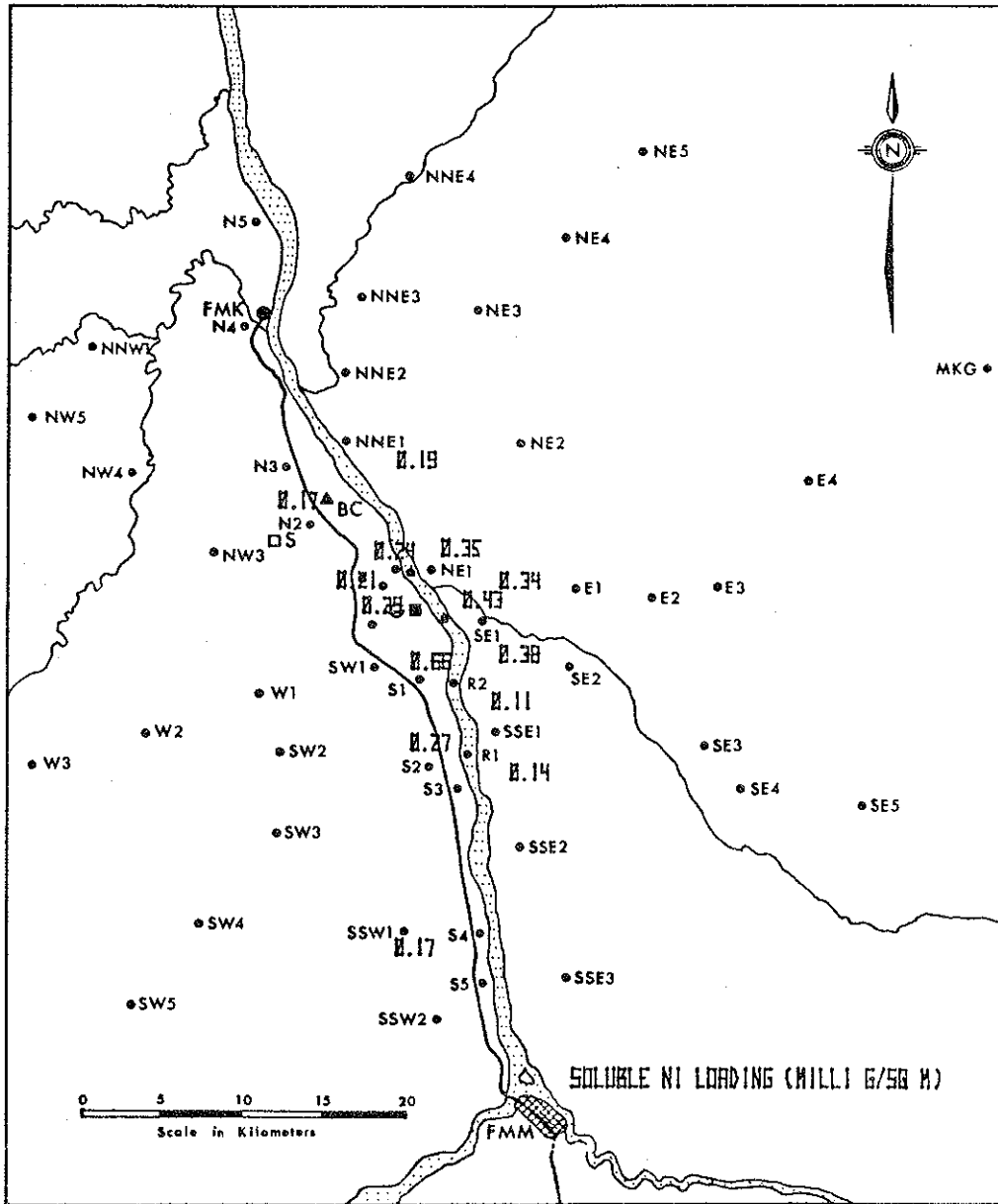


Figure 78. Plotted values of soluble nickel loading at sampling sites.

9. AO SERP RESEARCH REPORTS

1. AO SERP First Annual Report, 1975
2. AF 4.1.1 Walleye and Goldeye Fisheries Investigations in the Peace-Athabasca Delta--1975
3. HE 1.1.1 Structure of a Traditional Baseline Data System
4. VE 2.2 A Preliminary Vegetation Survey of the Alberta Oil Sands Environmental Research Program Study Area
5. HY 3.1 The Evaluation of Wastewaters from an Oil Sand Extraction Plant
6. Housing for the North--The Stackwall System
7. AF 3.1.1 A Synopsis of the Physical and Biological Limnology and Fisheries Programs within the Alberta Oil Sands Area
8. AF 1.2.1 The Impact of Saline Waters upon Freshwater Biota (A Literature Review and Bibliography)
9. ME 3.3 Preliminary Investigations into the Magnitude of Fog Occurrence and Associated Problems in the Oil Sands Area
10. HE 2.1 Development of a Research Design Related to Archaeological Studies in the Athabasca Oil Sands Area
11. AF 2.2.1 Life Cycles of Some Common Aquatic Insects of the Athabasca River, Alberta
12. ME 1.7 Very High Resolution Meteorological Satellite Study of Oil Sands Weather: "A Feasibility Study"
13. ME 2.3.1 Plume Dispersion Measurements from an Oil Sands Extraction Plant, March 1976
- 14.
15. ME 3.4 A Climatology of Low Level Air Trajectories in the Alberta Oil Sands Area
16. ME 1.6 The Feasibility of a Weather Radar near Fort McMurray, Alberta
17. AF 2.1.1 A Survey of Baseline Levels of Contaminants in Aquatic Biota of the AO SERP Study Area
18. HY 1.1 Interim Compilation of Stream Gauging Data to December 1976 for the Alberta Oil Sands Environmental Research Program
19. ME 4.1 Calculations of Annual Averaged Sulphur Dioxide Concentrations at Ground Level in the AO SERP Study Area
20. HY 3.1.1 Characterization of Organic Constituents in Waters and Wastewaters of the Athabasca Oil Sands Mining Area
21. AO SERP Second Annual Report, 1976-77
22. Alberta Oil Sands Environmental Research Program Interim Report to 1978 covering the period April 1975 to November 1978
23. AF 1.1.2 Acute Lethality of Mine Depressurization Water on Trout Perch and Rainbow Trout
24. ME 1.5.2 Air System Winter Field Study in the AO SERP Study Area, February 1977.
25. ME 3.5.1 Review of Pollutant Transformation Processes Relevant to the Alberta Oil Sands Area

26. AF 4.5.1 Interim Report on an Intensive Study of the Fish Fauna of the Muskeg River Watershed of Northeastern Alberta
27. ME 1.5.1 Meteorology and Air Quality Winter Field Study in the AOSERP Study Area, March 1976
28. VE 2.1 Interim Report on a Soils Inventory in the Athabasca Oil Sands Area
29. ME 2.2 An Inventory System for Atmospheric Emissions in the AOSERP Study Area
30. ME 2.1 Ambient Air Quality in the AOSERP Study Area, 1977
31. VE 2.3 Ecological Habitat Mapping of the AOSERP Study Area: Phase I
32. AOSERP Third Annual Report, 1977-78
33. TF 1.2 Relationships Between Habitats, Forages, and Carrying Capacity of Moose Range in northern Alberta. Part I: Moose Preferences for Habitat Strata and Forages.
34. HY 2.4 Heavy Metals in Bottom Sediments of the Mainstem Athabasca River System in the AOSERP Study Area
35. AF 4.9.1 The Effects of Sedimentation on the Aquatic Biota
36. AF 4.8.1 Fall Fisheries Investigations in the Athabasca and Clearwater Rivers Upstream of Fort McMurray: Volume I
37. HE 2.2.2 Community Studies: Fort McMurray, Anzac, Fort MacKay
38. VE 7.1.1 Techniques for the Control of Small Mammals: A Review
39. ME 1.0 The Climatology of the Alberta Oil Sands Environmental Research Program Study Area
40. WS 3.3 Mixing Characteristics of the Athabasca River below Fort McMurray - Winter Conditions
41. AF 3.5.1 Acute and Chronic Toxicity of Vanadium to Fish
42. TF 1.1.4 Analysis of Fur Production Records for Registered Traplines in the AOSERP Study Area, 1970-75
43. TF 6.1 A Socioeconomic Evaluation of the Recreational Fish and Wildlife Resources in Alberta, with Particular Reference to the AOSERP Study Area. Volume I: Summary and Conclusions
44. VE 3.1 Interim Report on Symptomology and Threshold Levels of Air Pollutant Injury to Vegetation, 1975 to 1978
45. VE 3.3 Interim Report on Physiology and Mechanisms of Air-Borne Pollutant Injury to Vegetation, 1975 to 1978
46. VE 3.4 Interim Report on Ecological Benchmarking and Biomonitoring for Detection of Air-Borne Pollutant Effects on Vegetation and Soils, 1975 to 1978.
47. TF 1.1.1 A Visibility Bias Model for Aerial Surveys for Moose on the AOSERP Study Area
48. HG 1.1 Interim Report on a Hydrogeological Investigation of the Muskeg River Basin, Alberta
49. WS 1.3.3 The Ecology of Macrobenthic Invertebrate Communities in Hartley Creek, Northeastern Alberta
50. ME 3.6 Literature Review on Pollution Deposition Processes
51. HY 1.3 Interim Compilation of 1976 Suspended Sediment Data in the AOSERP Study Area
52. ME 2.3.2 Plume Dispersion Measurements from an Oil Sands Extraction Plan, June 1977

53. HY 3.1.2 Baseline States of Organic Constituents in the Athabasca River System Upstream of Fort McMurray
54. WS 2.3 A Preliminary Study of Chemical and Microbial Characteristics of the Athabasca River in the Athabasca Oil Sands Area of Northeastern Alberta
55. HY 2.6 Microbial Populations in the Athabasca River
56. AF 3.2.1 The Acute Toxicity of Saline Groundwater and of Vanadium to Fish and Aquatic Invertebrates
57. LS 2.3.1 Ecological Habitat Mapping of the AOSERP Study Area (Supplement): Phase I
58. AF 2.0.2 Interim Report on Ecological Studies on the Lower Trophic Levels of Muskeg Rivers Within the Alberta Oil Sands Environmental Research Program Study Area
59. TF 3.1 Semi-Aquatic Mammals: Annotated Bibliography
60. WS 1.1.1 Synthesis of Surface Water Hydrology
61. AF 4.5.2 An Intensive Study of the Fish Fauna of the Steepbank River Watershed of Northeastern Alberta
62. TF 5.1 Amphibians and Reptiles in the AOSERP Study Area
63. ME 3.8.3 Analysis of AOSERP Plume Sigma Data
64. LS 21.6.1 A Review and Assessment of the Baseline Data Relevant to the Impacts of Oil Sands Development on Large Mammals in the AOSERP Study Area
65. LS 21.6.2 A Review and Assessment of the Baseline Data Relevant to the Impacts of Oil Sands Development on Black Bears in the AOSERP Study Area
66. AS 4.3.2 An Assessment of the Models LIRAQ and ADPIC for Application to the Athabasca Oil Sands Area
67. WS 1.3.2 Aquatic Biological Investigations of the Muskeg River Watershed
68. AS 1.5.3 Air System Summer Field Study in the AOSERP Study Area, June 1977
69. HS 40.1 Native Employment Patterns in Alberta's Athabasca Oil Sands Region
70. LS 28.1.2 An Interim Report on the Insectivorous Animals in the AOSERP Study Area
71. HY 2.2 Lake Acidification Potential in the Alberta Oil Sands Environmental Research Program Study Area
72. LS 7.1.2 The Ecology of Five Major Species of Small Mammals in the AOSERP Study Area: A Review
73. LS 23.2 Distribution, Abundance and Habitat Associations of Beavers, Muskrats, Mink and River Otters in the AOSERP Study Area, Northeastern Alberta
74. AS 4.5 Air Quality Modelling and User Needs
75. WS 1.3.4 Interim Report on a Comparative Study of Benthic Algal Primary Productivity in the AOSERP Study Area
76. AF 4.5.1 An Intensive Study of the Fish Fauna of the Muskeg River Watershed of Northeastern Alberta
77. HS 20.1 Overview of Local Economic Development in the Athabasca Oil Sands Region Since 1961.
78. LS 22.1.1 Habitat Relationships and Management of Terrestrial Birds in Northeastern Alberta

- 79. AF 3.6.1 The Multiple Toxicity of Vanadium, Nickel, and Phenol to Fish.
- 80. HS 10.2 & History of the Athabasca Oil Sands Region, 1980 to
HS 10.1 1960's. Volumes I and II.
- 81. LS 22.1.2 Species Distribution and Habitat Relationships of Waterfowl in Northeastern Alberta.
- 82. LS 22.2 Breeding Distribution and Behaviour of the White Pelican in the Athabasca Oil Sands Area.
- 83. LS 22.2 The Distribution, Foraging Behaviour, and Allied Activities of the White Pelican in the Athabasca Oil Sands Area.
- 84. WS 1.6.1 Investigations of the Spring Spawning Fish Populations in the Athabasca and Clearwater Rivers Upstream from Fort McMurray; Volume I.
- 85. HY 2.5 An intensive Surface Water Quality Study of the Muskeg River Watershed. Volume I: Water Chemistry.
- 86. AS 3.7 An Observational Study of Fog in the AOSERP Study Area.
- 87. WS 2.2 Hydrogeological Investigation of Muskeg River Basin, Alberta
- 88. AF 2.0.1 Ecological Studies of the Aquatic Invertebrates of the Alberta Oil Sands Environmental Research Program Study Area of Northeastern Alberta
- 89. AF 4.3.2 Fishery Resources of the Athabasca River Downstream of Fort McMurray, Alberta. Volume I
- 90. AS 3.2 A Wintertime Investigation of the Deposition of Pollutants around an Isolated Power Plant in Northern Alberta

These reports are not available upon request. For further information about availability and location of depositories, please contact:

Alberta Oil Sands Environmental Research Program
 15th Floor, Oxbridge Place
 9820 - 106 Street
 Edmonton, Alberta
 T5K 2J6

This material is provided under educational reproduction permissions included in Alberta Environment's Copyright and Disclosure Statement, see terms at <http://www.environment.alberta.ca/copyright.html>. This Statement requires the following identification:

"The source of the materials is Alberta Environment <http://www.environment.gov.ab.ca/>. The use of these materials by the end user is done without any affiliation with or endorsement by the Government of Alberta. Reliance upon the end user's use of these materials is at the risk of the end user.